NPS ARCHIVE
1965
HARRIS, J.

STUDIES OF PERIODICALLY QUENCHED REGENERATIVE SYSTEMS

JACK REDVER HARRIS

Library
Naval Postgraduate School
Monterey, California

DUDLEY KNOX LIBRARY
NAVAL POSTGRADUATE SCHOOL
MONTEREY CA 93943-5101

This document has been approved for public release and sale; its distribution is unlimited.

Mont 115 A



STUDIES OF PERIODICALLY QUENCHED REGENERATIVE SYSTEMS

* * * * *

Jack Redver Harris

STUDIES OF PERIODICALLY QUENCHED REGENERATIVE SYSTEMS

by

Jack Redver Harris

Lieutenant Commander, United States Navy

Submitted in partial fulfillment of
the requirements for the degree of

DOCTOR OF PHILOSOPHY

IN

ELECTRICAL ENGINEERING

United States Naval Postgraduate School
Monterey, California

1 9 6 5

NFS Archive
1905
Harris, J

U. S. Naval Postgraduate School
Monterey, California

DUDLEY KNOX LIBRARY
NAVAL POSTGRADUATE SCHOOL
MONTEREY CA 93943-5101

STUDIES OF PERIODICALLY QUENCHED REGENERATIVE SYSTEMS

by

JACK REDVER HARRIS

This work is accepted as fulfilling
the dissertation requirements for the degree of

DOCTOR OF PHILOSPHY

IN

ELECTRICAL ENGINEERING

from the

United States Naval Postgraduate School

ABSTRACT

The general method of amplification by periodically quenching an unstable system under the influence of an input signal is investigated by the use of mathematical calculation, digital computation and experimental verification. This type of amplification, of which superregeneration is just one specialized form, is specifically analyzed for electrical systems which can be made unstable with time invarient elements. Specific results from the investigation of a system described by a first order differential equation reveals the physical realizability of an amplificatory mode of operation having unusual selectivity responses. The experimental realizability of this system was accomplished by the development of a special form of dynatron using characteristics heretofore not exploited. Specific results from the investigation of the system described by a second order differential equation revealed fundamental selectivity/gain limitations for the linear system, a limitation which can be overcome by the use of a time varying regenerative cycle. Both systems demonstrated the capability of having a very high voltage and power gain throughout the audio and radio frequency spectrum. Finally a theoretical and experimental study of the characteristics of the superregenerative hiss (noise) is done in sufficient detail permitting two realizable systems to be developed, both which overcome the objectionable features of the superregenerative hiss.

ACKNOWLEDGEMENTS

The author wishes to express his sincere indebtedness to his research advisor, Dr. G.D. Ewing, Associate Professor of Electrical Engineering at the United States Naval Postgraduate School, for his invaluable direction, advice and patience. In addition he would like to thank Professors P.E. Cooper, and C.F. Klamm for their encouragement and advice during the early phases of development of the thesis area, along with Associate Professor R.P. Murray who was a co-worker on many phases of the experimental work done in this study. Finally, thanks are due to the readers for their help given during the final stages of manuscript preparation.

TABLE OF CONTENTS

Chapter	Title	Page
1.	Introduction	1
2.	First Order System	5
3.	First Order System Experimental Verification	45
4.	Basic Second Order Considerations	61
5.	Superregeneration	74
6.	Second Order System Experimental Verification	91
7.	Superregenerative Noise	99
8.	Experimental Verification of Noise Behavior	105
Appendix		
A.	Digital Computer Solutions	115
B.	Dynatron Investigation	148
C.	A Second Method of Squelch Control	154
Bibliography		157

LIST OF ILLUSTRATIONS

Figure		Page
2.1	Electrical Circuit Equivalent for the First Order Differential Equation	6
2.2	Voltage Gain vs Alpha * Time	8
2.3	Power Received vs Alpha * Time	11
2.4	Power Gain vs Alpha * Time	12
2.5	Typical Operation of a Sampling First Order System With a Slowly Varying Input	14
2.6	Normalized Output vs Omega	20
2.7	Output Voltage vs Input Phase Angle	21
2.8	Normalized Output vs Omega (Phase Varied)	22
2.9	Model of the First Order System for Periodic Varying Elements	25
2.10	Model of the First Order System for Sinusoidal Varying Elements	28
2.11	Output Voltage of a First Order System for a Nonlinear (A) and Linear Negative Resistance Device (B)	32
2.12	Output Voltage vs Time	39
2.13	Output Voltage vs Time (Incoherent)	41
2.14	Output Voltage vs Time (Coherent)	42
2.15	Output Voltage vs Input Phase	44
3.1	Current Controlled Resistive Device	46
3.2	Voltage Controlled Resistive Device	47
3.3	Negative Resistive Devices Characteristics	48
3.4	Analytical and Experimental Circuits for Verification of First Order Regenerative Sampling System	50
3.5	Representative Oscilloscope Photographs of Selected Modes of Operation of the First Order System	52
3.6	Experimental Results Reflecting Linear and Nonlinear Operation of the Sampling Dynatron, First Order System	54

3.7	Output vs Time (Nonlinear System)	56
3.8	Experimental Results Reflecting the Form of Output for Different Types of Input Sources, First Order System	58
3.9	Output vs Time (Modulated Resistance)	60
4.1	Electrical Circuit Equivalent for the Second Order Differential Equation	62
4.2	Output vs Time (Overdamped System)	66
4.3	Output vs Time (Critically Damped)	67
4.4	Output vs Time (Underdamped System)	68
4.5	Normalized Output vs Omega (Underdamped)	70
4.6	Output vs Time (Underdamped System)	72
4.7	Normalized Output vs Omega	73
5.1	Selectivity vs Linearity for Second Order System	79
5.2	Second Order System Equivalents	81
5.3	Alpha vs Time (Nonlinear)	89
5.4	Voltage vs Time (Nonlinear)	90
6.1	Second Order System Circuitry	92
6.2	Typical Envelope Waveforms for Linear and Nonlinear Modes, Second Order System	93
6.3	Grid and Plate Waveforms Observed During Selectivity Measurements	95
6.4	Frequency Response Curves for Linear and Time Varying Regenerative Cycle, Second Order System	97
6.5a	Resistance Modulated Second Order System	98
6.5b	Randomness of Output for Linear Superregenerator	98
7.1	Probability Distribution and Frequency Spectrum of Noise for the Superregenerative Amplifier	101
8.1	Distribution of the Pulse Waveforms of a Superregenerator)	107
8.2	Schematic of Audio Frequency Spectrum Analyzer	108

8.3 Representation of the Output of the Spectrum Analyzer 110

8.4 Bandpass Filter for Squelch Control Signal 113

B.1 Static and Dynamic Characteristics of the Dynatron Mode of Operation 150

B.2 Schematic for Testing Dynamic and Static Dynatron Characteristics 152

B.3 Plate Characteristics for the Dynatron with Various and Bias 153

C.1 Circuit of Superregenerative Receive with Squelch Control 156

CHAPTER ONE

Introduction

The method of electrical amplification by periodically quenching an unstable system that is under the influence of an input signal was first recognized by Armstrong in 1922 (1), and is known as superregeneration. Since then it has not enjoyed any great popularity except during World War II where it was exploited to a degree (2), and with radio amateurs where it afforded a simple means of obtaining a high degree of receiver sensitivity at the very high radio frequencies. The purpose of this study is two-fold: first, to investigate the general type of amplification of which superregeneration is just one form; and second, to analyze in depth certain characteristics of these amplifiers which are of particular interest in the real world.

The first foremention study area recognizes the fact that conventional radio frequency superregeneration is actually the result of having an unstable electrical system that is periodically sampling an input signal and being reset to a rest condition where it again can resample a new input signal. By appreciating the behavior of the general differential equation

$$a_m \frac{d^m q}{dt^m} \cdots a_1 \frac{dq}{dt} + a_0 q = e(t), \qquad (1\text{-}1)$$

under certain coefficient constraints that tend to make the system described by this differential equation unstable, an understanding of the sampled unstable amplificatory mechanism can be had. The second study area analyzes the characteristics of the random noise and the gain versus selectivity characteristics of conventional superregeneration in a linear

mode of operation. In addition, possible solutions to the objectionable noise and poor selectivity features of the conventional superregenerator are discussed, these features being the principal deterrents to its commercial exploitation. One solution to the noise problem has resulted in an issuance of a United States patent (3). In addition to the two main areas of investigation, other minor areas are reported on which resulted as an outgrowth from the experimental work. These areas are the characteristics of a special form of dynatron and the exploitation of the change of quench frequency in a superregenerative detector.

The areas of investigation are segmented as follows:

a. Chapter Two discusses in detail the degenerative mode of superregeneration, defined here as a system that can be described by a first order differential equation. Both linear and non-linear parameters are analyzed, augmented by the extensive use of the digital computer for computation and graphical presentation.

b. Chapter Three discusses the circuitry and the results of the experimental verification of many of the modes of operation analytically investigated in Chapter Two. Use of a special form of dynatron was necessary for this verification, which with its associated circuitry allowed an oscillographic pictorial presentation of the performance of the degenerative superregenerative amplifier.

c. Chapter Four is an extension of Chapter Two where now the second order differential equation is investigated. The regenerative underdamped, critically damped, and overdamped cases are analyzed for gain and selectivity features. Again both analytical and digital computer computation methods are used for presentation.

d. Chapter Five is an extension of the results of Chapter Four for

those parameters which are associated with conventional superregeneration. The selectivity vs. gain features for the linear mode are analyzed along with the resultant changes that take place if a time-varying resistive element is used. The possibility of increased selectivity vs. gain for a given sampling period under this time varying mode of operation is analyzed and pictorially presented. Finally the nonlinear resistive system is investigated with mathematical and pictorial presentations.

e. Chapter Six, similar to Chapter Three, is the discussion of the circuitry and the results of the experimental verification of many of the modes of operation analytically investigated in Chapters Four and Five.

f. Chapter Seven investigates the nature of the random noise or characteristic hiss of the conventional superregenerative amplifier. After an analytical speculation of its envelope distribution, the resultant noise spectrum is analyzed.

g. Chapter Eight describes the experimental verification of the speculations of Chapter Seven along with the development of an operational circuit that allows for the feature of squelch operation of a superregenerative circuit.

h. Appendix A is a brief description of the particular computer programs used in this dissertation along with a listing of the essential features of the various subroutines.

i. Appendix B discusses the behavior of the special form of dynatron used for the experimental work of this dissertation. Experimental comparison between a conventional dynatron and the special form is performed and pictorially presented.

j. Appendix C describes another possible form of squelch operation for superregeneration that takes advantage of the change in quench frequency of a self quenching superregenerative detector/amplifier with a

change of incoming signal level.

Finally it is appropriate to mention that throughout this dissertation the possible influence of microscopic nonlinearity on the basic macroscopic behavior of a system is ignored. One such example of this microscopic nonlinearity would be the current versus voltage behavior of a carbon composition resistor where this nonlinearity is often associated with noise.

CHAPTER TWO

First Order System

2.1 Basic First Order Considerations

The fundamental behavior of a periodic sampling system that is electrically unstable during part of its cycle of operation can be conceptually appreciated by studying the linear first order differental equation

$$e(t) = a(t)q + b(t)\frac{dq}{dt}, \tag{2-1}$$

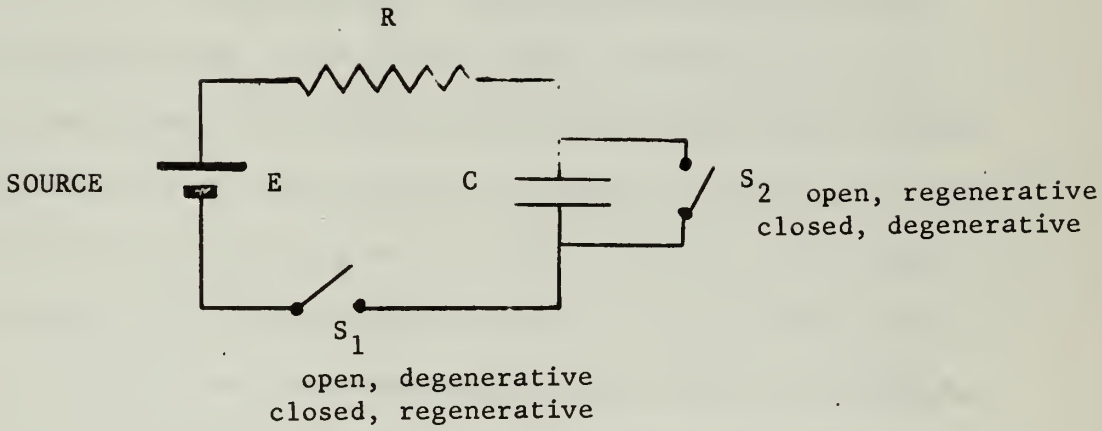
where its general solution can be extracted by a well known method (4) resulting in

$$q(t) = e^{-\int \frac{a(t)}{b(t)}dt} \int e^{+\int \frac{a(t)}{b(t)}dt} \frac{e(t)}{b(t)}dt + De^{-\int \frac{a(t)}{b(t)}dt}, \tag{2-2}$$

where D is determined by the initial conditions of a given system. If e(t) is a step function, zero before time (t) = 0, and E afterwards and if a(t) and b(t) are constant after t = 0, a particular solution to equation (2-2) can be had that lends itself to a physical interpretation, whereby associating the term q(t) with electrical charge, E with voltage, a(t) with inverse capacitance in farad^{-1} (C^{-1}), and b(t) with electrical resistance in ohms (R), Figure 2-1 becomes the physical reality. When the initial conditions are such that at t = 0, q = 0 then the solution to equation (2-2) becomes

$$q(t) = \frac{E}{a}\left(1 - e^{-\frac{at}{b}}\right), \tag{2-3}$$

demonstrating the possibility of the charge being very large, dependent on the sign and magnitude of at/b, and at the same time, linearily dependent on E.



ELECTRICAL CIRCUIT EQUIVALENT FOR THE FIRST
ORDER DIFFERENTIAL EQUATION

FIGURE 2-1

It will be of interest to study the circuit of Figure 2-1 as to the ratio of the output voltage across the capacitor (E_c) to the input voltage. This ratio, which is the voltage amplificatory factor (K_v), can be realized by noting that q is E_c times the capacitance of C. Utilizing equation (2-3), K_v can be written as

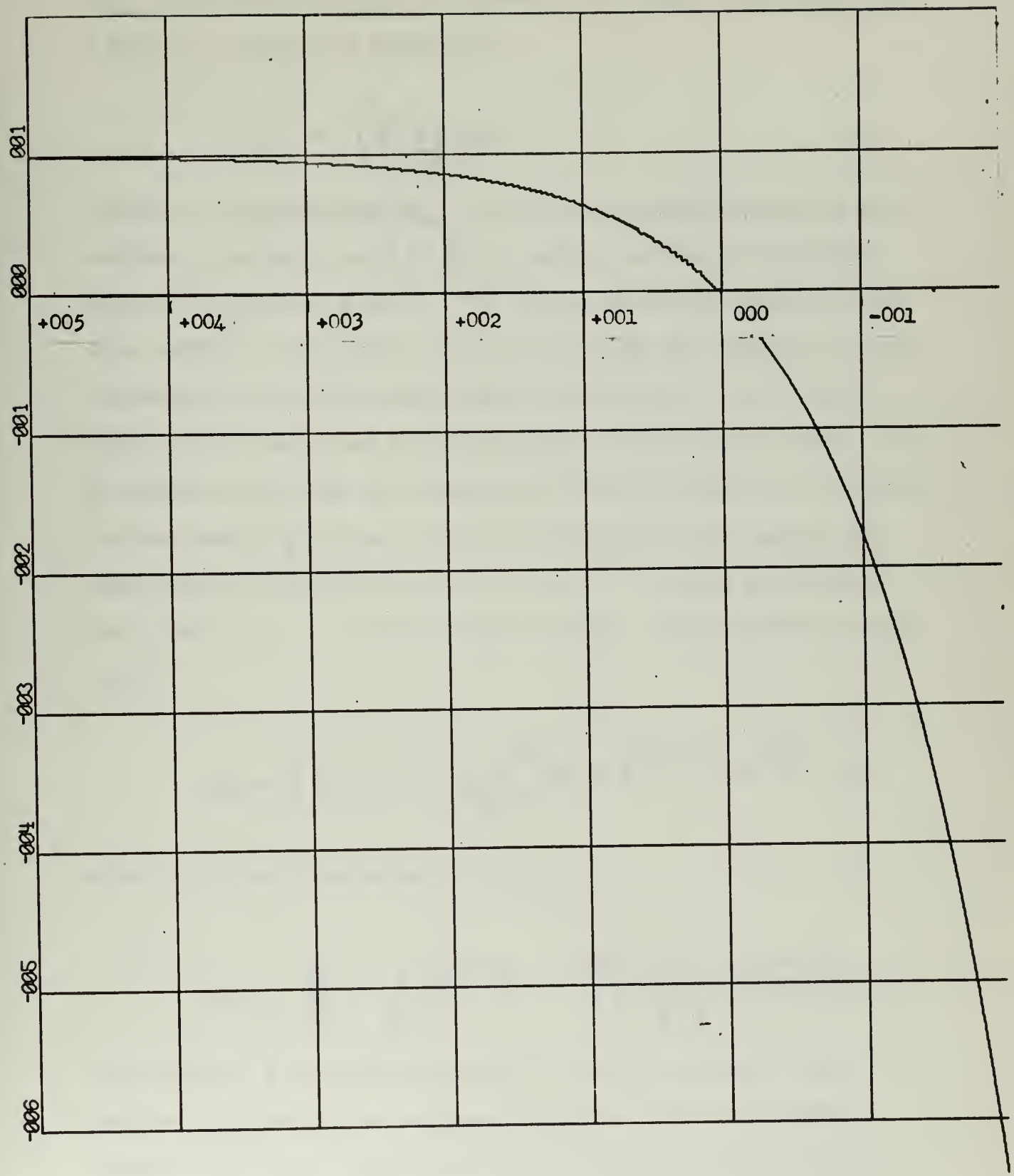
$$1 - e^{-\frac{at}{b}}, \tag{2-4a}$$

and by letting α equal to a/b,

$$1 - e^{-\alpha t}. \tag{2-4b}$$

Figure 2-2 graphically represents this ratio or gain factor for both positive and negative αt, where time is always considered positive. Both positive and negative gains are possible, the negative gain meaning a polarity reversal in the output voltage as compared to the input voltage. It is noticed that for increasing negative αt, the gain of the system can become very large. It is this possibility of a very large gain, which is still under the control of system parameters such as the input voltage, that is the basic motivation for this study of unstable amplifiers. Although the forementioned behavior is very elementary in nature, its system behavior will well characterize the theoretical and operational behavior of the common second order system counterpart, the r-f superregenerative amplifier, along with having unique features of its own.

To complete the understanding of the potential operational capabilities of the previously described system, here to fore to be called the first order system since it can be described by a first order differential equation, another measure of performance can be introduced, that is, power gain. The power gain of the system (K_p) for the forementioned system can be analyzed by recognizing that its input energy



X-SCALE = 1.00E+00 UNITS/INCH.
Y-SCALE = 1.00E+00 UNITS/INCH.

VOLTAGE GAIN VS ALPHA*TIME

RUN 1

FIGURE 2-2



(W_{in}) supplied by the source is E times the net charge discharged during a period t. This can be expressed as

$$W_{in} = \int_0^t E \frac{dq}{dt} dt. \tag{2-5}$$

Likewise the output energy (W_{out}) stored in C, energy which can be made available to do work, would be $\frac{1}{2}q^2/C$, where q would be the net charge added to C during the period t. The energy supplied or absorbed by the other element in the circuit, that is R, would be the difference between the energy in C and the energy supplied by the source. As it will be seen, both the source and R can be suppliers or absorbers of energy, and as was done in the case of voltage gain, it will be beneficial to evaluate the power gain (K_p) of the circuit for both positive and negative $\alpha\tau$. Again using the initial conditions of t = 0, q = 0 and E switched into the circuit at t = 0, the input energy becomes, using equations (2-3) and (2-5),

$$W_{in} = \int_0^t E\, dq = \int_0^t \frac{E^2 e^{-\alpha\tau}}{R} dt = E^2 C\left(1 - e^{-\alpha\tau}\right), \tag{2-6}$$

while the output energy becomes

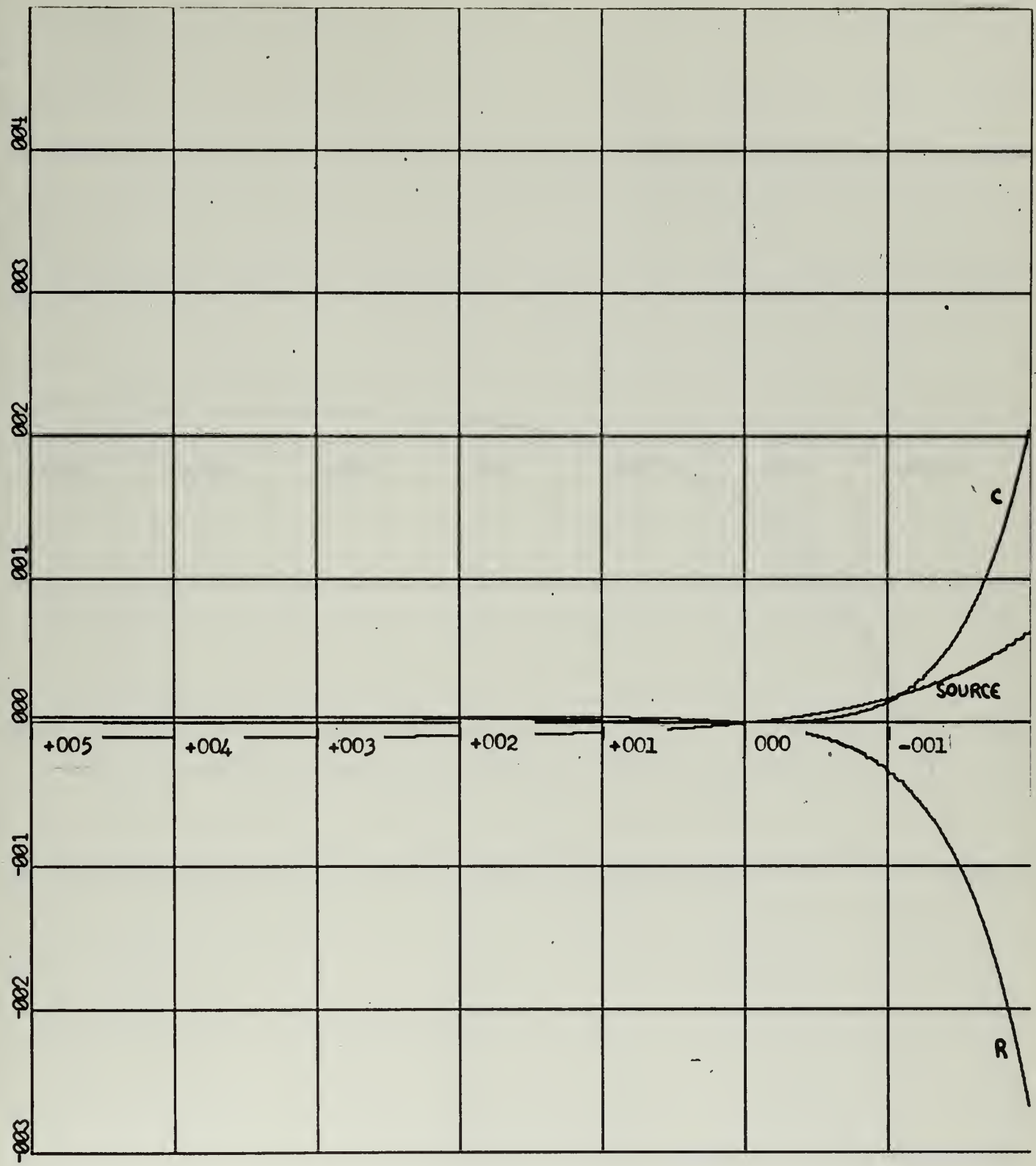
$$W_{out} = \frac{q^2}{2C} = \frac{1}{2C}\left\{E^2C^2\left(1 - e^{-\alpha t}\right)^2\right\} = \frac{E^2C}{2}\left\{1 - 2e^{-\alpha\tau - 2\alpha t}\right\}. \tag{2-7}$$

Since there is a common time involved for both the input and output energies, the ratio of the energies is also the ratio of the powers involved, that is K_p. Equating the ratio of equations (2-6) and (2-7) will give

$$\frac{W_{out}}{W_{in}} = K_p = \frac{(1-2e^{-\alpha t}+e^{-2\alpha t})}{2(1-e^{-\alpha t})}. \qquad (2\text{-}8)$$

Figure 2-3 is a graph of the power supplied or received by the three elements of the basic circuit, while Figure 2-4 is a plot of the K_p of the system both as a function of positive and negative αt . From Figure 2-3 can be observed the peculiar behavior of both the source and R as αt becomes negative, where now R becomes a source, and the source becomes a sink for the energy. Figure 2-4 shows the relationship between the value of αt and K_p, where for negative αt the power gain can become very large but negative, the negativeness reflecting the fact that the input source has now become an absorber of energy, that is, it is being charged. It is important to appreciate that even though the source eventually absorbs power, it can still control the power output capability of C. In this particular system of constant parameters, the amplification factor is also independent of the input voltage or power.

With this basic understanding of the behavior of the first order system it is desirable to evaluate how the system could be utilized in an engineering application. This can be accomplished by having the system periodically reset to an initial condition of no charge in C and letting the cycle of unstable operation start again under the influence of a given input voltage. If power amplification is desired, such as having the charge perform work as part of a servo system or driving an acoustic transducer, this requires the energy stored in C at the time t to be transferred to the load and the cycle repeated. This should be done



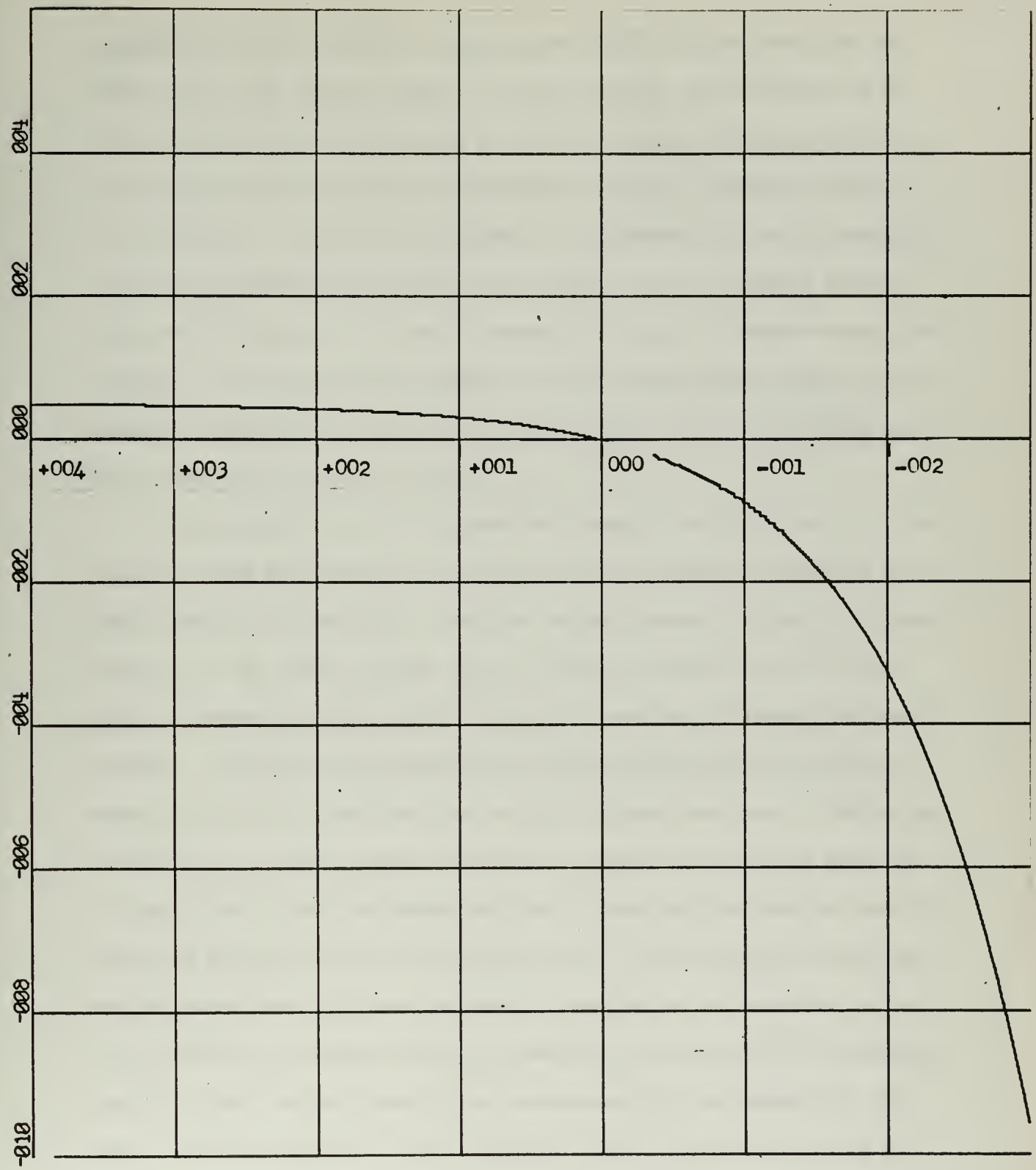
X-SCALE = 1.00E+00 UNITS/INCH.
Y-SCALE = 1.00E+01 UNITS/INCH.

POWER RECEIVED VS. ALPHA*TIME

RUN 1

FIGURE 2-3





X-SCALE = 1.00E+00 UNITS/INCH.
Y-SCALE = 2.00E+00 UNITS/INCH.

POWER GAIN VS ALPHA*TIME

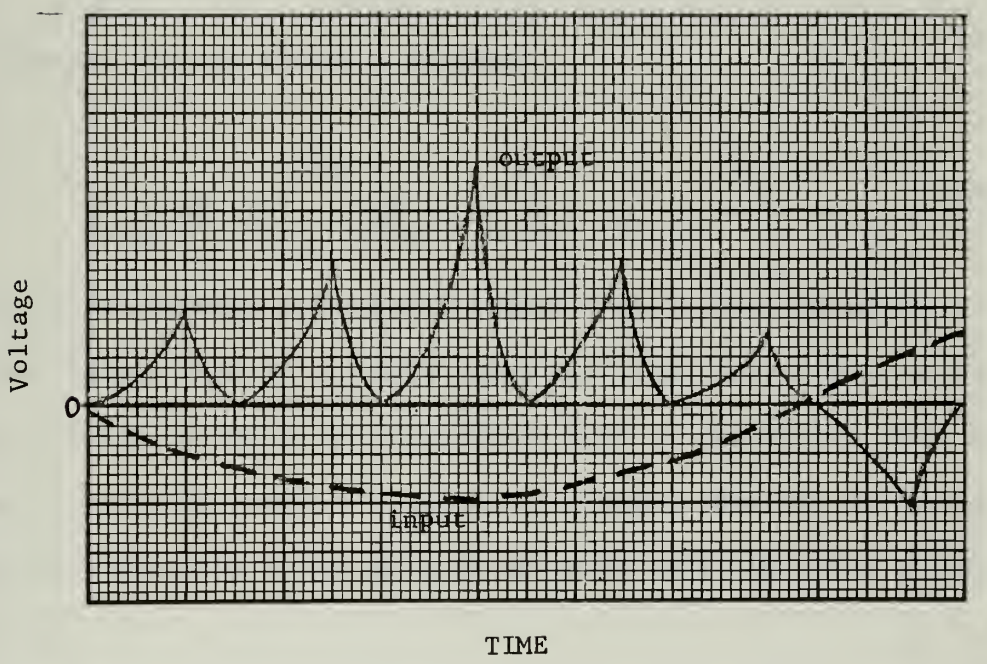
RUN 1

FIGURE 2-4



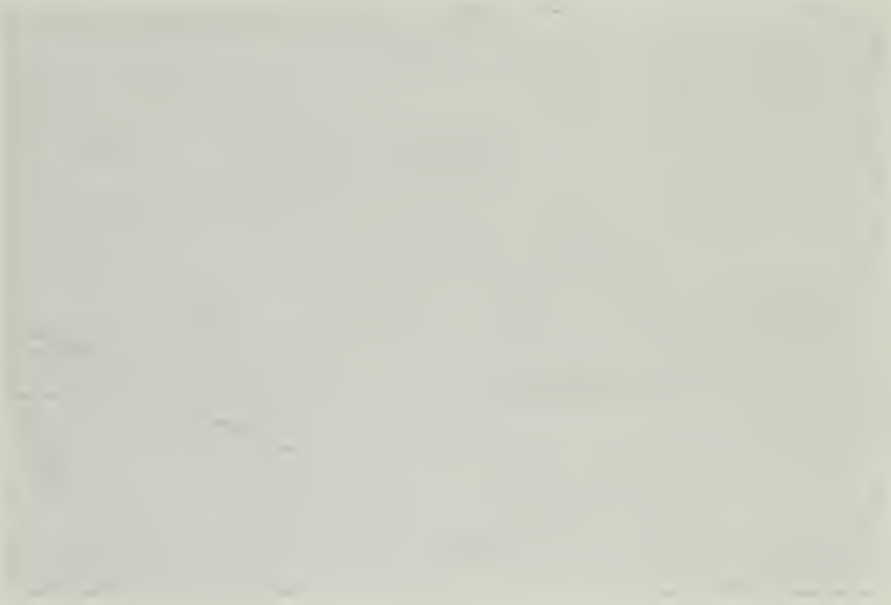
preferably without resistive losses which would distract from the net power gain of the entire system. If only voltage amplification is desired, then all that is required is that the charge, therefore the voltage across C, be periodically discharged through a shunting resistive device across C. After this discharge is performed and the discharging device is disconnected allowing the voltage to build up again across C under the influence of the input source, the cycle of operation would be repeated. It is tactically assumed here for this argument that this repetitive operation is such that the input source can be considered constant during the unstable period.

If the input voltage is instead very slowly varying, that is, slow enough so that the impressed voltage is nearly constant during the unstable portion of operation, then the voltage across C is still a direct function of the input voltage and the system will have for a low frequency alternating input source the output envelope following the input envelope. Figure 2-5 represents a few cycles of operation of such an operation with both the input and output voltages portrayed. One method of having the circuit shown in Figure 2-1 behave as portrayed would be to repetitively have the connecting switch open and the shorting switch connected across C during the discharge time, then have the connecting switch closed with the shorting device open during the unstable period. It is necessary to assume that the remaining voltage on C be discharged down to a small enough value to be inconsequential as compared to the input. If this does not occur, there will be a coherency existing between envelope developments which will swamp out the effect of the input source. This can be mathematically appreciated by analyzing equation (2-2) with an initial q_o in the system; that is, a voltage is still



TYPICAL OPERATION OF A SAMPLING FIRST
ORDER SYSTEM WITH A SLOWLY VARYING INPUT

FIGURE 2-5



existing across C. Equation (2-2) now becomes

$$q(t) = EC\left\{1 - \left(1 - \frac{q_0}{EC}\right)e^{-\alpha t}\right\}, \tag{2-9}$$

and when αt is negative and large, the unstable case of interest where K_v and K_p can become large, this equation approaches

$$q(t) \doteq e^{-\alpha t}(q_0 - EC), \tag{2-10}$$

and the output voltage across C becomes

$$E_{out} \doteq e^{-\alpha t}(E_c - E), \tag{2-11}$$

where E_c is the voltage that exists across C at t = 0. Unless E is magnitudes larger than E_c, E_c will swamp the input source causing coherency to exist, normally an undesirable mode of operation. This effect is often observed in normal r-f superregeneration when the quenching, ie., discharging, operation is incomplete and leads to a condition of very poor sensitivity.

Another consideration of the basic circuit is the fact that if during an unstable period the input voltage is not constant, the output at the end of an unstable period is more dependent on the earlier presented voltages. A simple example of this can be had by considering a symmetric square wave of magnitude E and duration t as an input during the unstable portion of circuit operation. Assuming the positive voltage preceeds first and utilizing equation (2-11) the voltage across C at the end of the first half period becomes

$$E_c \doteq e^{-\frac{\alpha t}{2}}(-E), \tag{2-12}$$

and with $\frac{\alpha\tau}{2} \ll 0$ can allow the second portion of the input voltage to be subliminal. This type of behavior can be exploited to allow for increased selectivity in conventional superregeneration, and is discussed in Chapter Five.

Finally, all the considerations so far mentioned have assumed that α and t were constant. It is possible to have circuitry where α or t which are functions of some controlling source. If the frequency of variation of the parameters is low enough to allow it to be considered constant during an unstable period, and if a constant input voltage is maintained, the output voltage is exponentially dependent on $\alpha\tau$. It will be shown later that it is possible to make such a system operate in a manner that will have certain desirable characteristics. Even though the general problem of time varying parameters is not simple, there is one set of circumstances that can be physically realized and also adapts itself to easy interpretation. If the value of C is made dependent on an input source, such as a capacitor microphone under the influence of acoustical pressure, and if the changes of capacitance are linearly dependent on pressure then the total C of the circuit becomes

$$C = C_0 + kp, \tag{2-13}$$

where C_0 is the steady state capacity, p is acoustical overpressure and k is a proportionality constant. Defining $\alpha_0 = 1/RC_0$ and having the permutations of C small compared to C_0, α can be rewritten as

$$\alpha = \frac{1}{R(C_0+kp)} = \frac{1}{RC_0\left(1+\frac{kp}{C_0}\right)} = \alpha_0\left\{1-\frac{kp}{C_0}\right\}. \tag{2-14}$$

Now the gain of this system will be defined as the change of the output voltage as compared to a change of acoustical pressure. Assuming that αt is large and negative allows equation (2-11) to be used, and by defining E_1 as the steady state output voltage when no modulation occurs and E_2 the output when an input pressure occurs, then the change of output voltage becomes $E_2 - E_1$. This can be written for an input voltage of E as

$$E_1 = e^{-\alpha_0 t}(-E), \quad E_2 \doteq e^{-\alpha_0\left(1-\frac{kp}{C_0}\right)t}(-E), \tag{2-15a}$$

or

$$E_2 - E_1 \doteq -E e^{-\alpha_0 t}\left\{e^{+\frac{kp}{C_0}} - 1\right\}. \tag{2-15b}$$

With the condition given of small permutations of C, and with $\frac{kp}{C_0}$ small enough so that $e^{+\frac{kp}{C_0}}$ can be expanded to become approximately $1 + \frac{kp}{C_0}$ then $E_2 - E_1$ becomes

$$E_2 - E_1 \doteq -E e^{-\alpha_0 t}\left\{\frac{kp}{C_0}\right\}, \tag{2-16}$$

which states that for small enough permutations, a linear relation exists between the output and input sources. Finally the gain of such a system becomes

$$\frac{E_2 - E_1}{p} = \frac{-E e^{-\alpha_0 t} k}{C_0}, \tag{2-17}$$

and even with the restriction of $kp \ll C_o$, it is still possible to have a large gain by having negative $\alpha \cdot t$ large or E large. A similar result occurs if a modulated resistance such as a carbon microphone is placed in series with the negative resistance.

2.2 The Frequency Dependency Of The First Order System.

With this background on the behavior of the first order system in unstable operation it is desirable to develop its frequency response. Assuming now that the input source voltage is of the form $E \cos(\omega t + \theta)$ and that all the elements are still constant, at least piecewise, then equation (2-2) becomes

$$q(t) = e^{-\int \alpha\, dt} \int e^{+\int \alpha\, dt} \frac{E}{R} \cos(\omega\tau+\theta)\, dt + De^{-\int \alpha\, dt}, \quad (2\text{-}18)$$

which becomes

$$q(t) = \frac{E}{R}\left\{\frac{\alpha\cos(\omega t+\theta) + \omega \sin(\omega t+\theta)}{\alpha^2+\omega^2}\right\} + De^{-\alpha t} \quad (2\text{-}19a)$$

or

$$q(t) = \frac{E}{R}\left\{\frac{\sin(\omega t+\theta+\phi)}{(\alpha^2+\omega^2)^{1/2}}\right\}, \quad \phi = \tan^{-1}\frac{\alpha}{\omega}, \quad (2\text{-}19b)$$

where D is again determined by the initial conditions. Assuming that at $t = 0$, $q = 0$, then D has a value

$$D = -\frac{E}{R}\left\{\frac{\sin(\theta+\phi)}{(\alpha^2+\omega^2)^{1/2}}\right\}, \quad (2\text{-}20)$$

and the voltage across the capacitor becomes

$$E_c = \frac{E\alpha}{(\alpha^2+\omega^2)^{1/2}}\left\{\sin(\omega t+\phi+\theta) - e^{-\alpha t}\sin(\theta+\phi)\right\}, \qquad (2\text{-}21)$$

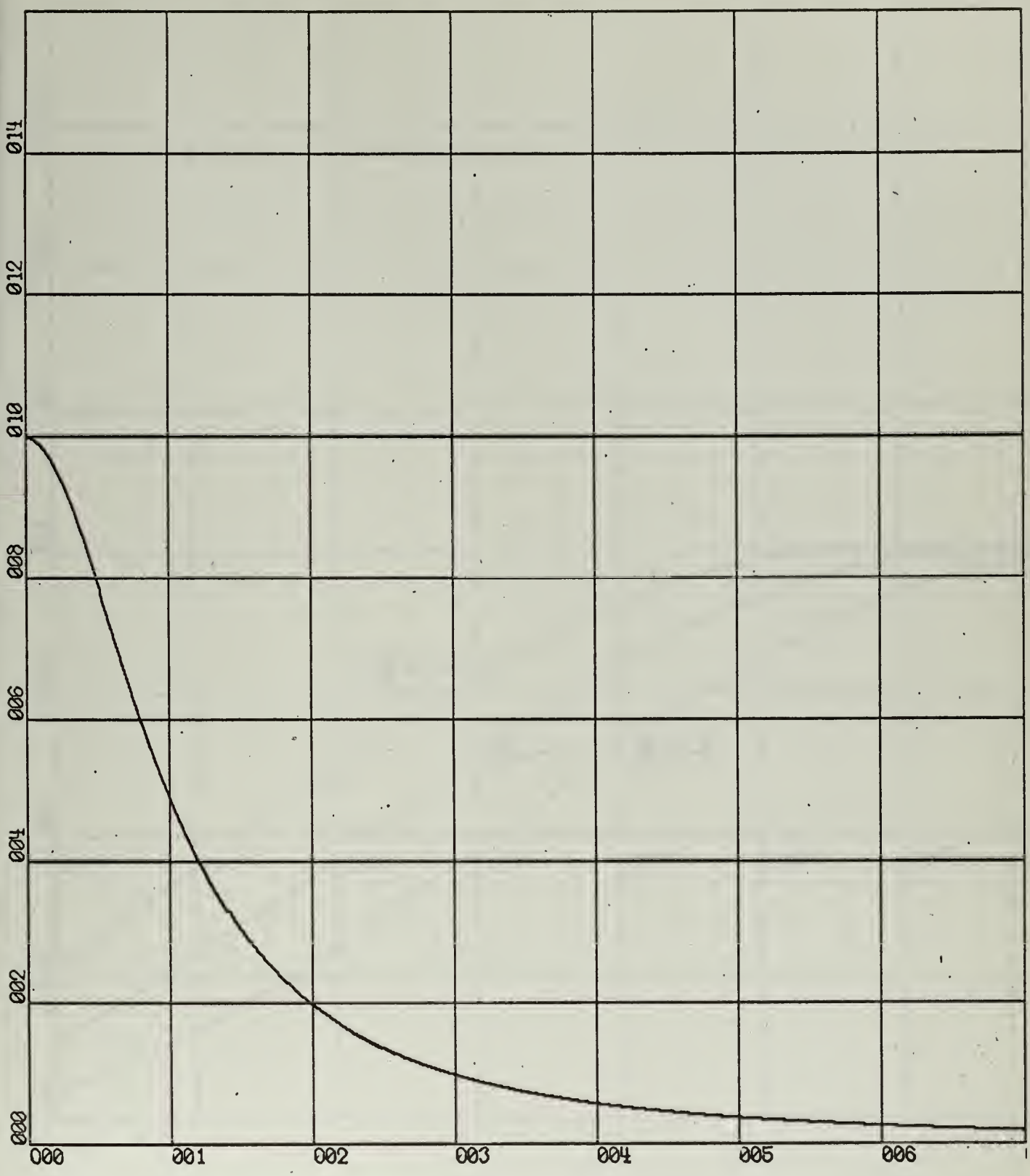
and when $\alpha t \ll 0$ can be written as

$$E_c \doteq \frac{-E\alpha e^{-\alpha\tau}}{(\alpha^2+\omega^2)^{1/2}}\sin(\theta+\phi), \qquad (2\text{-}22a)$$

which for $\omega = 0$, $\theta = 0$, becomes

$$E_c \doteq -Ee^{-\alpha t}, \qquad (2\text{-}22b)$$

agreeing with equation (2-11) for no initial charge. For a given α, t, and E, it is possible to plot E_c as a function of ω. Figure 2-6 is such a plot for $\theta = 0$ with all output voltages normalized to $\omega = 0$ or d-c. It is important to realize that while the output is not necessarily a replica of the input voltage, such as is the normal behavior of standard amplifiers, the output is still linearly sensitive to the magnitude of the driving source, its frequency and its initial phase. This phase sensitivity is unlike standard amplifiers and deserves further investigation. Figure 2-7 graphically demonstrates for three different ratios of $\frac{\alpha}{\omega}$ the normalized value of the output voltage as a function of the phase angle. This phase sensitivity of the system holds special interest since it could be used as a phase or f-m detector at low frequencies desirable in certain automatic frequency control systems and the like. In addition, this peculiar behavior results in selectivity curves which vary as a function of input phase. Figure 2-8 graphs this behavior for three phase angles,

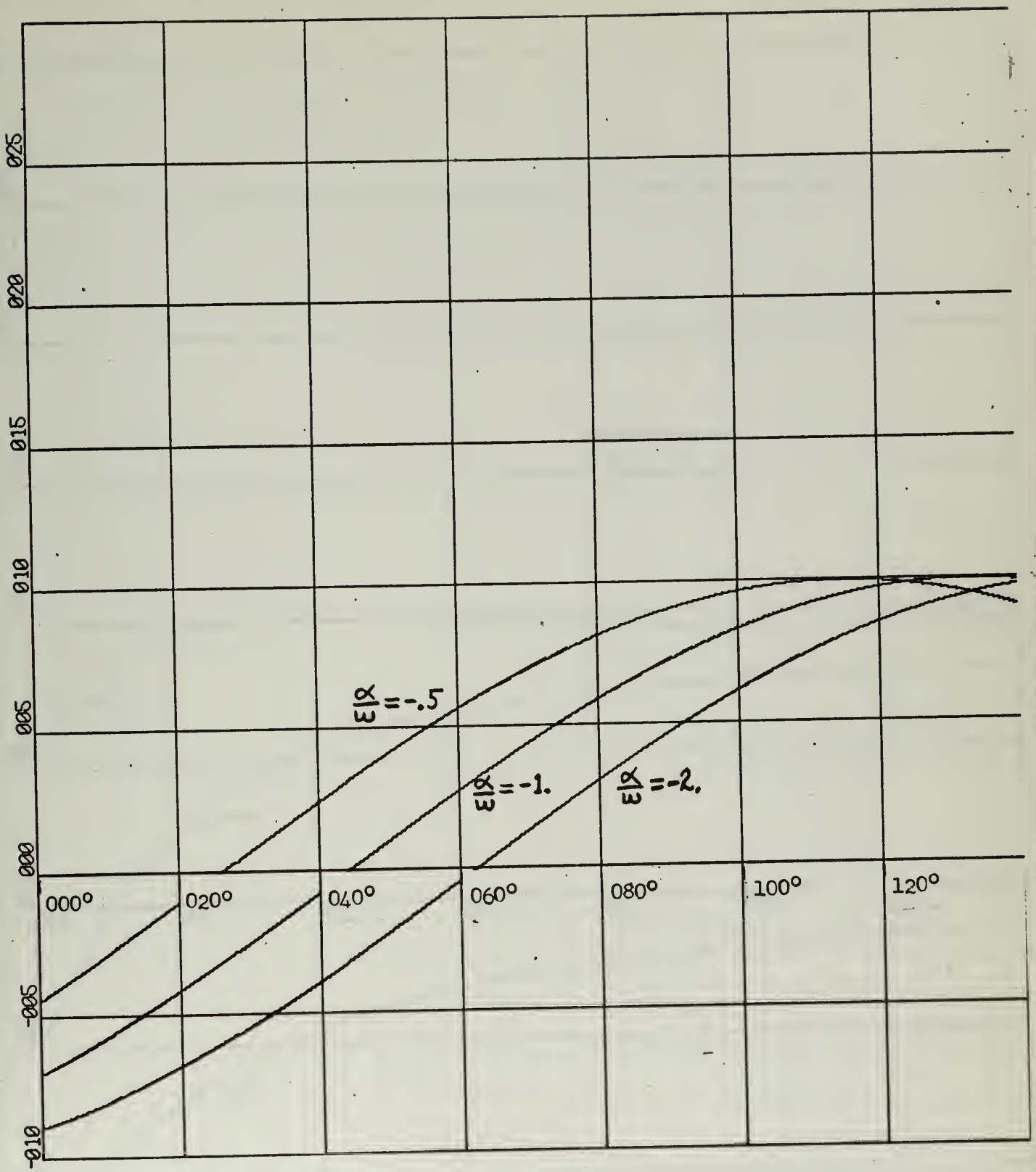


X-SCALE = 1.00E+00 UNITS/INCH.
Y-SCALE = 2.00E-01 UNITS/INCH.

NORMALIZED OUTPUT VS OMEGA

RUN 1

FIGURE 2-6

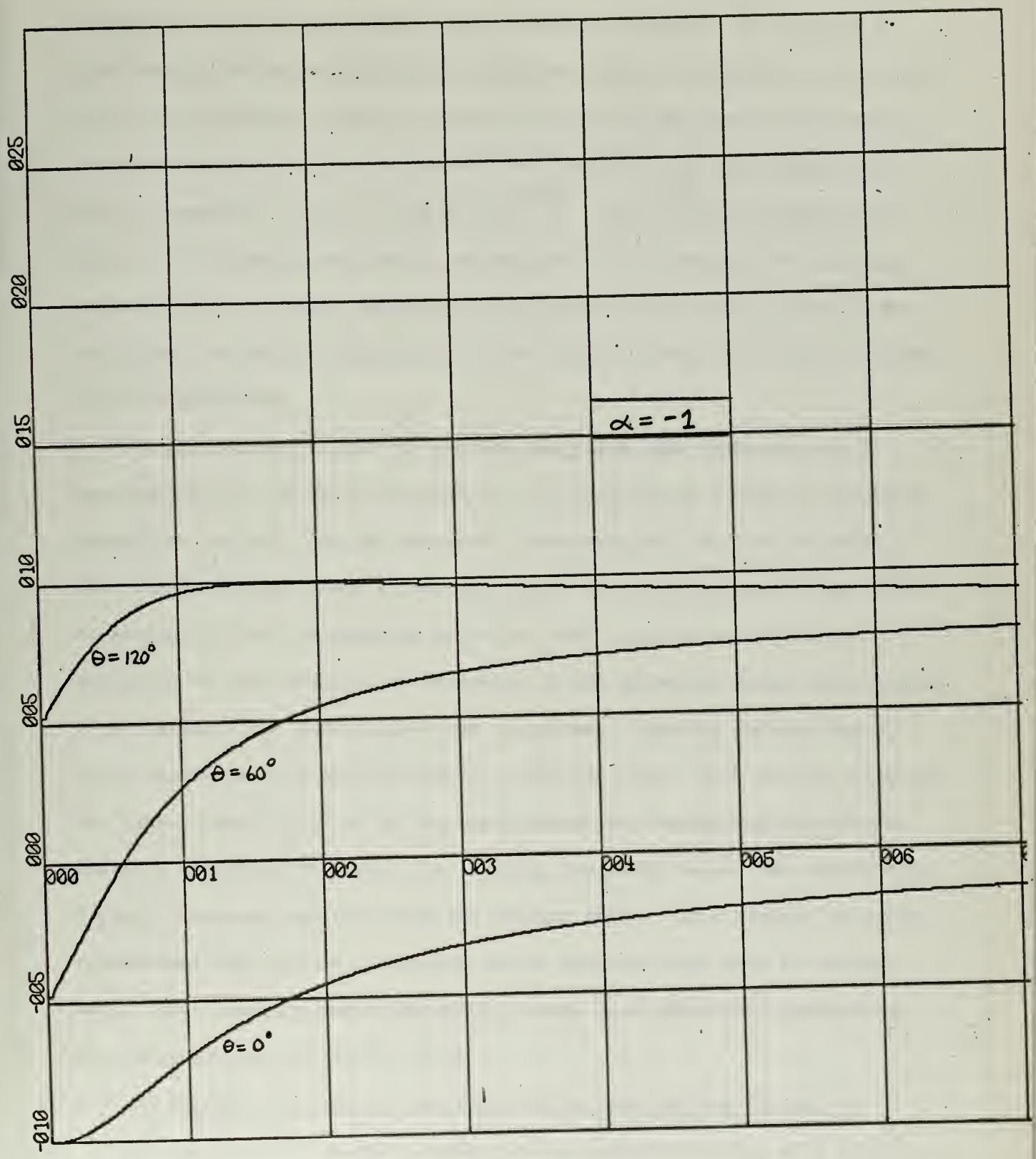


X-SCALE = 1.00E+00 UNITS/INCH.
Y-SCALE = 5.00E-01 UNITS/INCH.

OUTPUT VOLTAGE VS INPUT PHASE ANGLE

RUN 1

FIGURE 2-7



X-SCALE = 1.00E+00 UNITS/INCH.
Y-SCALE = 5.00E-01 UNITS/INCH.

NORMALIZED OUTPUT VS OMEGA (PHASE VARIED

RUN 1

FIGURE 2-8



equal to unity, where it is readily apparent that the system can have the properties of a low pass, high pass, or even a frequency null system by just having the cycle of unstable operation begin at different phase angles, though the response curves in Figure 2-8 are only one part of the overall frequency sensitivity of the system, and the basic low pass behavior as seen in equation (2-21) as $\alpha\left(\alpha^2+\omega^2\right)^{-1/2}$ must still be considered. Since it it possible to develop systems which will trigger the unstable portion of the unstable amplifier for different phase angles, such as by using axis crossing information, such an unusual frequency response system could be developed.

It is appropriate here to mention the place that sampling theory does pertain in the above discussion (5). Sensitivity to input parameter changes is evident from the previous discussions but it does not imply that the system will have a coherent output for varying inputs from period to period, unless the sampling period is such to allow a complete description of the frequency of variation of the parameter being investigated. If for example the input source has a constant frequency and amplitude, but a slowly varying phase parameter, then the output will reflect uniquely the phase characteristics of the input source as transferred through the unstable amplifier only when the sampling frequency is at least twice the highest frequency involved with the varying phase. This concept is quite fundamental and will be a limiting factor whenever high gain is desired but a short sampling period demanded because high modulating frequencies are involved with the input source.

2.3 The Regenerative First Order System With Time Varying Parameters.

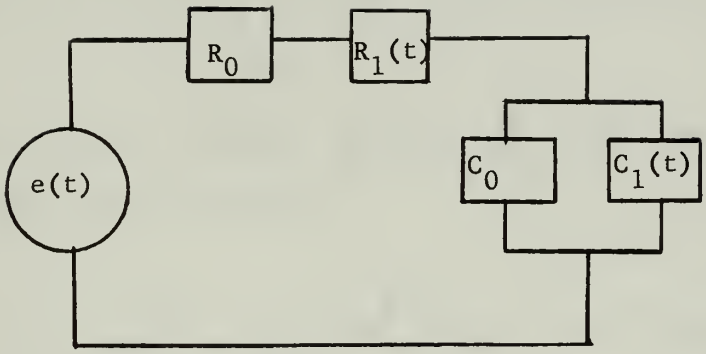
The next order of sophistication in the analytical study of a first order system would be to allow R and C to vary periodically with time,

both with a frequency and phase which could be independent of each other and the input source. It is reasonable and desirable to eventually assume an equation model of the form

$$e(t) = q\left(C_0 + C_1(t)\right)^{-1} + \left(R_0 + R_1(t)\right)\frac{dq}{dt}, \qquad (2\text{-}23)$$

where within the original premise of this dissertation, the particular conditions of interest will be where R is periodically sampling between a positive and negative value.

With this basic appreciation of circuit behavior, a mathematical model will be developed which will allow for a more exact evaluation of circuit behavior. Figure 2-9 is the equivalent circuit which has equation (2-23) as its describing function. It is noticed that an additive capacity variance term $C_1(t)$ was chosen for it represents the additional capacitance which would have been added if an original circuit capacity is shunted by an external capacitive, such as a reactance tube under the influence of a variational voltage. Normally these devices can be made with a linear relationship between the variational voltage and the permutation in the capacity if the permutations are small compared to the static capacity of the variational device and a sinusoidal voltage input results in a sinusoidal capacitive change. As before, the capacitance of the system will always be considered positive. The modulation of the resistive term will likewise be considered to be a small fraction of the constant term R_o in equation (2-23) where R_o is to be studied when negative, though again if the system is to be operational it must be periodically sampled and reset as previously mentioned.



MODEL OF THE FIRST ORDER SYSTEM
FOR PERIODIC VARYING ELEMENTS

FIGURE 2-9



The particular method of solution to be used is one that has been described in Pipes (6) and augmented by transformational calculus. Referring to equation (2-23) it can be rewritten as

$$e(t) = \frac{\int i(t)\,dt}{C_o + C_1(t)} + R_o\, i(t) + R_1(t)\, \dot{i}(t), \qquad (2\text{-}24a)$$

and approximated when C_1 is reasonably less than C_o by

$$e(t) = \left(S_o + S_1(t)\right)\int i(t)\,dt + \left(R_o + R_1(t)\right) i(t), \qquad (2\text{-}24b)$$

where $S_o = 1/C_o$, and $S_1 = C_1/C_o^2$. Letting $\mathcal{L}$ f(t) = the Laplace of f(t) = F(s), this equation becomes

$$E(s) = I(s)\left\{R_o + \frac{S_o}{s}\right\} + \mathcal{L}\left\{R_1(t)\, i(t) + S_1(t)\int i(t)\,dt\right\}. \qquad (2\text{-}25)$$

By defining $Z(s) = R_o + S_o/s$, $\mathcal{L}\left(R_1(t)\, i(t) + S_1(t)\int i(t)dt\right) = G(s)$ then

$$I(s) = \frac{E(s)}{Z(s)} - \frac{G(s)}{Z(s)}, \qquad (2\text{-}26a)$$

which with $(sR_o + S_o)^{-1}$ defined as H(s) becomes

$$I(s) = \frac{H(s)E(s)}{s} - \frac{H(s)G(s)}{s}. \qquad (2\text{-}26b)$$

By use of the Convolution Integral, the inverse transform of the equation becomes

$$i(t) = \int_o^t h(t-u)\,e(u)\,du - \int_o^t h(t-u)\left\{R_1(u)\, i(u) + S_1(u)\int i(u)\,du\right\} du, \qquad (2\text{-}27)$$

but $i_o(t) = \int_o^t h(t-u)e(u)du$ is the current that would flow if $R_1 = 0$ and $S_1 = 0$, therefore equation (2-27) becomes

$$i(t) = i_o(t) - \int_o^t h(t-u)\left\{R_1(u)\,i(u) + S_1(u)\int i(u)du\right\}du. \qquad (2\text{-}28)$$

Volterra (7) has shown that a solution to equation (2-28) is of the form

$$i(t) = i_o(t) - i_1(t) + i_2(t) \cdots \qquad (2\text{-}29a)$$

where

$$i_m(t) = \int_o^t h(t-u)\left\{R_1(u)\,i_{m-1}(u) + S_1(u)\int i_{m-1}du\right\}du, \qquad (2\text{-}29b)$$

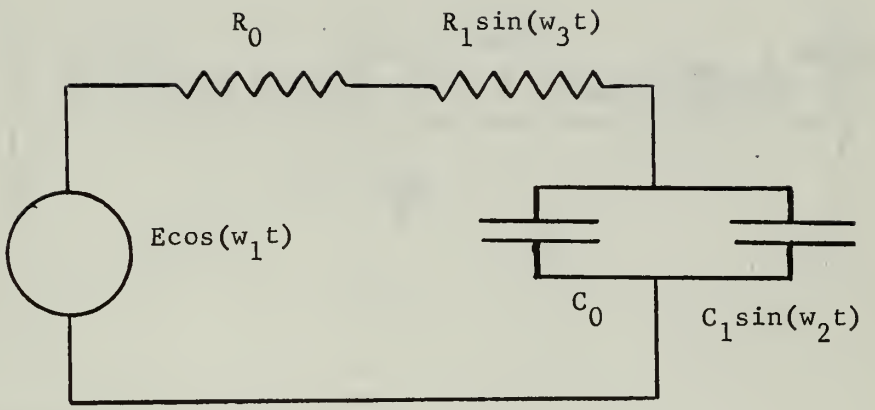
and in transform notation can be written as

$$i_o(t) = \mathcal{L}^{-1}\left\{\frac{E(s)}{Z(s)}\right\}, \qquad (2\text{-}29c)$$

$$i_m(t) = \mathcal{L}^{-1}\frac{1}{Z(s)}\left\{\mathcal{L}\left(R_1(t)i_{m-1}(t) + S_1(t)\int i_{m-1}(t)dt\right)\right\}. \qquad (2\text{-}29d)$$

To give an example of this form of solution, the first two terms for the system described in Figure 2-10 will be calculated under the conditions where unstable operation exists due to negative resistance. With these operating conditions the steady state current becomes

$$i_o(\tau) = \mathcal{L}^{-1}\left\{\frac{E(s)}{Z(s)}\right\} = E\,\mathcal{L}^{-1}\left\{\frac{S}{s^2+\omega_1^2} \otimes \frac{S}{SR_o + S_o}\right\} = \frac{E}{R_o}\mathcal{L}^{-1}\left\{\frac{s^2}{(s^2+\omega_1^2)(s+\alpha)}\right\} \qquad (2\text{-}29e)$$



MODEL OF THE FIRST ORDER SYSTEM
FOR SINUSOIDAL VARYING ELEMENTS

FIGURE 2-10



where $\alpha_o = S_o/R_o$. The inverse transform of this becomes

$$\frac{E}{R_o}\left\{\left\{\frac{\alpha_o^2}{\alpha_o^2+\omega_1^2}\right\}e^{-\alpha_o t}+\frac{1}{\omega_1}\left\{\frac{(-\omega_1^2)^2}{\alpha_o^2+\omega_1^2}\right\}^{1/2}\sin(\omega_1 t+\psi)\right\}, \qquad (2\text{-}29f)$$

$$\psi = -\tan^{-1}\frac{\omega_1}{\alpha_o}$$

which $\doteq \frac{E}{R_o}\left\{\frac{\alpha_o^2 e^{-\alpha_o t}}{\alpha_o^2+\omega_1^2}\right\}$ for $\alpha_o t \ll 0$. Likewise $i_i(t)$ becomes

$$\frac{E}{R_o}\mathcal{L}^{-1}\left\{\frac{\mathcal{L}\left[R_1 \sin\omega_3 t\left(\frac{\alpha_o^2}{\alpha_o^2+\omega_1^2}\right)e^{-\alpha_o t}+S_1\sin\omega_2 t\left(\frac{-\alpha_o}{\alpha_o^2+\omega_1^2}\right)e^{-\alpha_o t}\right]}{R_o+\frac{S_o}{S}}\right\}. \qquad (2\text{-}29g)$$

By parts this yields

$$\mathcal{L}\left\{R_1\sin\omega_3 t\left(\frac{\alpha_o^2}{\alpha_o^2+\omega_1^2}\right)e^{-\alpha_o t}\right\} = \frac{R_1\alpha_o^2}{\alpha_o^2+\omega_1^2}\left\{\frac{\omega_3}{(S+\alpha_o)^2+\omega_3^2}\right\}, \qquad (2\text{-}29h)$$

$$\mathcal{L}\left\{S_1\sin\omega_2 t\left(\frac{-\alpha_o}{\alpha_o^2+\omega_1^2}\right)e^{-\alpha_o t}\right\} = \frac{-S_1\alpha_o^2}{\alpha_o^2+\omega_1^2}\left\{\frac{\omega_2}{(S+\alpha_o)^2+\omega_2}\right\}, \qquad (2\text{-}29i)$$

and now equation (2-29g) inverse becomes

$$\dot{i}_1(t) = \frac{E\alpha_o^2 e^{-\alpha_o t}}{R_o^2(\alpha_o^2+\omega_1^2)}\left[\frac{R_1}{R_o}\left\{\frac{-\alpha_o}{\omega_3}+\left(\frac{\alpha_o^2+\omega_3^2}{\omega_3^2}\right)^{1/2}\sin(\omega_3 t+\psi_1)\right\}+\frac{S_1}{R_o}\left\{\frac{1}{\omega_2}-\frac{1}{\alpha_o}\left(\frac{\alpha_o^2+\omega_2^2}{\omega_2^2}\right)^{1/2}\sin(\omega_2 t+\psi_2)\right\}\right], \quad (2\text{-}29j)$$

$$\psi_1 = \tan^{-1}\frac{\omega_3}{-\alpha_o} - \frac{\pi}{2}$$

$$\psi_2 = \tan^{-1}\frac{\omega_2}{-\alpha_o} - \frac{\pi}{2}$$

Therefore i(t) becomes for the combined first two terms

$$\dot{i}(t) \doteq \dot{i}_o(t) - \dot{i}_1(t) \doteq \frac{Ee^{-\alpha_o t}}{R_o}\left\{\frac{\alpha_o^2}{\alpha_o^2+\omega_1^2}\right\}\left[1-\left(\frac{R_1}{R_o}\left\{\frac{-\alpha_o}{\omega_3}+\left(\frac{\alpha_o^2+\omega_3^2}{\omega_3^2}\right)^{1/2}\sin(\omega_3 t+\psi_1)\right\}+\frac{S_1}{R_o}\left\{\frac{1}{\omega_2}-\frac{1}{\alpha_o}\left(\frac{\alpha_o^2+\omega_2^2}{\omega_2^2}\right)^{1/2}\otimes\right.\right.\right. \quad (2\text{-}30)$$

$$\left.\left.\left.\sin(\omega_2 t+\psi_2)\right\}\right)\right], \quad \psi_1 = \tan^{-1}\frac{\omega_3}{-\alpha_o} - \frac{\pi}{2}, \quad \psi_2 = \tan^{-1}\frac{\omega_2}{-\alpha_o} - \frac{\pi}{2}.$$

An integration of this expression would give the q(t) of the system with the integration constants being determined by the initial conditions. The presence of the exponential term and the modulating quantities reveal the potential of having high amplification. It is appropriate to mention here that the system could have its output taken across some resistive load instead of the capacitor. If in Figure 2-10, part of R_o was an external load resistor, the output of the system could be considered across this resistance, and equation (2-30) describes directly the influence the varying parameters would have on the output.

2.4 Behavior Of The First Order System With Nonlinear Elements.

As a final consideration of the behavior of the first order system, it is worthy to mention the effects of element nonlinearity on circuit behavior. Of particular interest will be the effects of a nonlinear negative resistance, for it is by nature a real life consideration, though the nonlinear capacitor is also of interest since it does occur in such devices as semiconductor junctions.

Figure 2-11a shows a typical development of the output voltage under such nonlinear operation where saturation occurs due to the negative resistance power limitations, though the knee can be quite sharp instead of a gradual saturation. This behavior is contrasted with Figure 2-11b which is representative of a linear system. To appreciate the basic behavior of a nonlinear system such as represented in Figure 2-11a, it will be assumed that a fixed αt exist until saturation occurs. Assuming the basic system's input voltage has a value of E_1, then the average voltage across C during a regenerative phase of operation of period t is

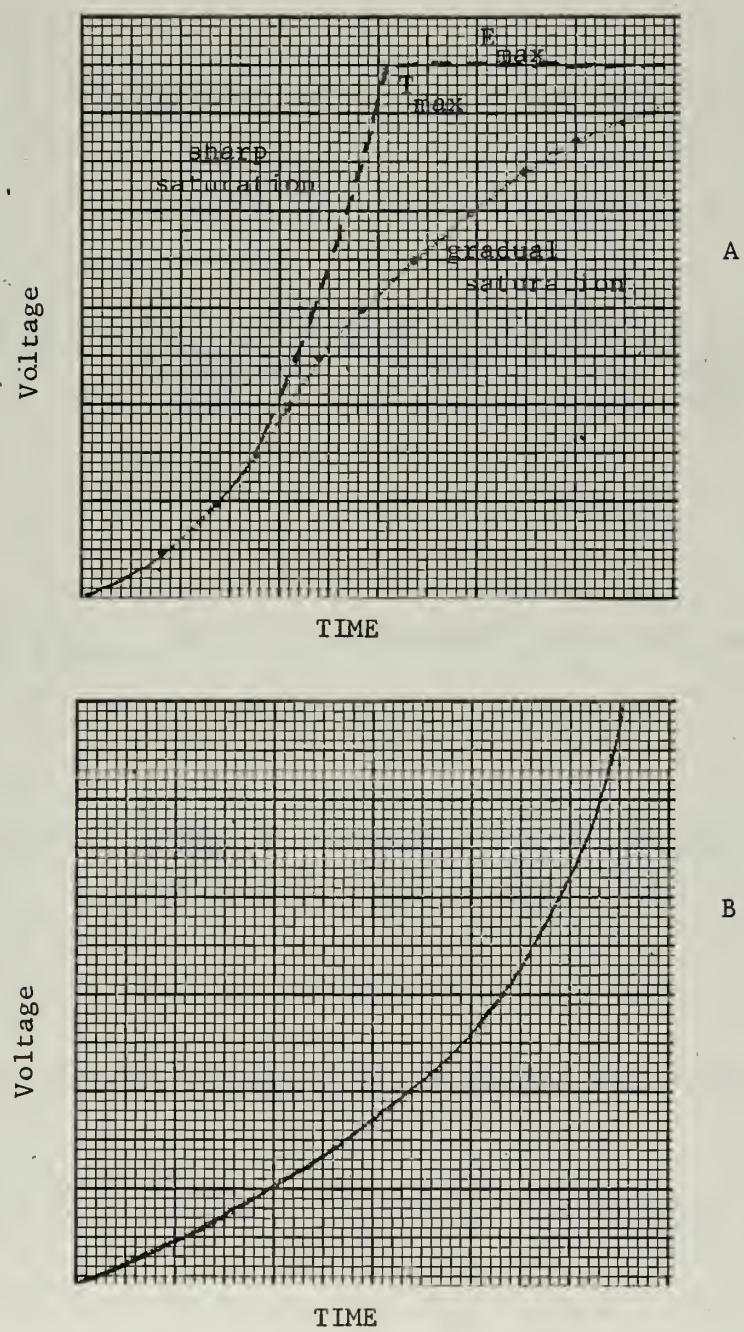
$$\langle E_{C1} \rangle \doteq \frac{1}{t} \left\{ \int_0^{t_{max}} - E_1 e^{-\alpha \tau} \, dt + E_{max} (t - t_{max}) \right\}, \qquad (2\text{-}31)$$

where t_{max} is related by the expression

$$E_{max} \doteq - E_1 e^{-\alpha t_{max}} \qquad (2\text{-}32a)$$

or

$$-\frac{1}{\alpha} \ln \frac{E_{max}}{-E_1} \doteq t_{max} \quad , E_{max} \text{ the saturation voltage .} \qquad (2\text{-}32b)$$



OUTPUT VOLTAGE OF A FIRST ORDER SYSTEM FOR A NONLINEAR (A) AND LINEAR NEGATIVE RESISTANCE DEVICE (B)

FIGURE 2-11

If equation (2-31) is integrated with respect to t_{max} it becomes

$$\langle E_{c1} \rangle \doteq \frac{1}{t}\left\{ \frac{E_1}{\alpha}\left(e^{\ln \frac{E_{max}}{-E_1}} - 1 \right) + E_{max}\left(t + \frac{1}{\alpha} \ln \frac{E_{max}}{-E_1} \right) \right\} \qquad (2\text{-}33a)$$

or

$$\langle E_{c1} \rangle \doteq \left\{ -\frac{(E_{max} + E_1)}{\alpha t} + E_{max}\left(1 + \frac{1}{\alpha t} \ln \frac{E_{max}}{-E_1} \right) \right\}. \qquad (2\text{-}33b)$$

If $|E_1| << |E_{max}|$ which is operationally often the case then this becomes

$$\langle E_{c1} \rangle \doteq \left\{ \frac{-E_{max}}{\alpha t} + E_{max}\left(1 + \frac{1}{\alpha t} \ln \frac{E_{max}}{-E_1} \right) \right\}. \qquad (2\text{-}34)$$

Likewise for an input voltage of E_2, the output now becomes

$$\langle E_{c2} \rangle \doteq \left\{ \frac{-E_{max}}{\alpha t} + E_{max}\left(1 + \frac{1}{\alpha t} \ln \frac{E_{max}}{-E_1} \right) \right\}, \qquad (2\text{-}35)$$

where the change in average output voltage, $\langle E_{c2} \rangle - \langle E_{c1} \rangle$ is

$$\langle \Delta E_c \rangle \doteq -\frac{E_{max}}{\alpha t} \left(\ln E_1 - \ln E_2 \right). \qquad (2\text{-}36)$$

From equation (2-36), it can be seen that the dynamic change in average output voltage is a function of the change of the logarithms of the input voltage. This behavior gives rise to a logarithmic amplifier capability which has permitted the well-known automatic gain control (AGC) operation of the superregenerative detector and offers possibilities of a simple system of logarithmic response at audio frequencies.

The forementioned model of a sharp discontinuity in the power capability of the negative source can be expressed in another way, that is a resistive device whose response can be defined by some appropriate analytical expression. Following the reasoning of Herold (8) on negative resistance devices, and of such authors as Frink (9) on superregenerators, a nonlinear resistive element which approaches infinite resistance as the voltage across the negative resistance is increased will be assumed, a model appropriate for a voltage controlled device.

A particular model for the resistance to be evaluated will be of the form

$$R = \frac{-K}{1 - |JE|}, \qquad (2\text{-}37)$$

where the quantity E is the voltage across the resistor and J a constant. This model approximates the basic behavior of the negative voltage controlled resistive device such as a dynatron or tunnel diode. It has the basic feature of a voltage controlled device in that as the voltage across

the resistive device is increased, the resistance increases to infinity until a voltage is reached where R becomes positive. If the regenerative first order system is considered and J of equation (2-37) is considerably smaller than one, then the quantity E can be replaced by -q/c or $-E_c$. Now equation (2-37) becomes

$$R \doteq \frac{-K}{1-|Mq|}, \quad M = \frac{J}{C}. \tag{2-38}$$

This approximation demands that the basic resistance at turn-on time does not allow an instantaneous value of voltage across R to change its initial value from the static value, a reasonable condition with the type of linearity dynamic range and input voltages that are normally encountered. Now realizing that with no initial charge on C and a positive d-c input voltage, an increasing negative charge is developed by the resistor, then equation (2-38) can be safely written as

$$R \doteq \frac{-K}{1-Mq}, \qquad \text{M is negative}, \tag{2-39}$$

and the first order system differential equation can now be written as

$$\left\{\frac{-K}{1-Mq}\right\}\frac{dq}{dt} + \frac{q}{C} = e(t), \; e(t) \text{ positive}. \tag{2-40}$$

A specific example of a solution to the equation for real values would be to consider the case of all quantities being unity except for $|M|$, which can be considered a floating variable smaller than unity. Equation (2-40) now becomes

$$K\frac{dq}{dt} + (Mq-1)q = Mq - 1 \qquad (2\text{-}41a)$$

or

$$K\frac{dq}{dt} = -Mq^2 + (M+1)q - 1 \ . \qquad (2\text{-}41b)$$

This is directly integrable when put in the form

$$\frac{dq}{-Mq^2+(M+1)q-1} = \frac{dt}{K} \ , \qquad (2\text{-}42)$$

and becomes

$$\text{constant} + \frac{K}{\sqrt{(M+1)^2-4M}} \ln\left\{\frac{-2Mq+M+1-\sqrt{(M+1)^2-4M}}{-2Mq+M+1+\sqrt{(M+1)^2-4M}}\right\} = t \qquad (2\text{-}43)$$

which if $|M| << 1$ allows equation 2-43 to become

$$\text{constant} + K \ln\left\{\frac{-2Mq+2M}{-2Mq+2}\right\} \doteq t \qquad (2\text{-}44a)$$

or

$$\frac{-2Mq+2M}{-2Mq+2} \doteq k' e^{t/K} \ , \qquad (2\text{-}44b)$$

where with the initial condition q = 0 when t = 0 requires k' = M and finally equation (2-44b) becomes

$$\frac{-2Mq+2M}{-2Mq+2} \doteq Me^{t/K} . \qquad (2\text{-}45)$$

With the original restriction that q is zero or negative only, it can be seen that as $t \rightarrow \infty$, $q \longrightarrow (M)^{-1}$ and the boundness of q and an E_c is apparent. Figure 2-11a (solid curve) is actually a graphical presentation of this function and the exponential form becoming asymptotically stable with time is apparent. This basic behavior of a boundness of the system's response is characteristic of not only the first order system but of many higher order systems where nonlinearity occurs, a common example being a conventional LCR oscillator where the nonlinearity of the active device limits the envelope of the oscillations in a similar manner. In Chapter Three, it will be seen that this can be experimentally verified by the dual of this circuit by taking advantage of the curvature in the resistive effects of a dynatron.

2.5 Ditigal Computer Solutions For Selected Modes Of Operation Of The First Order System.

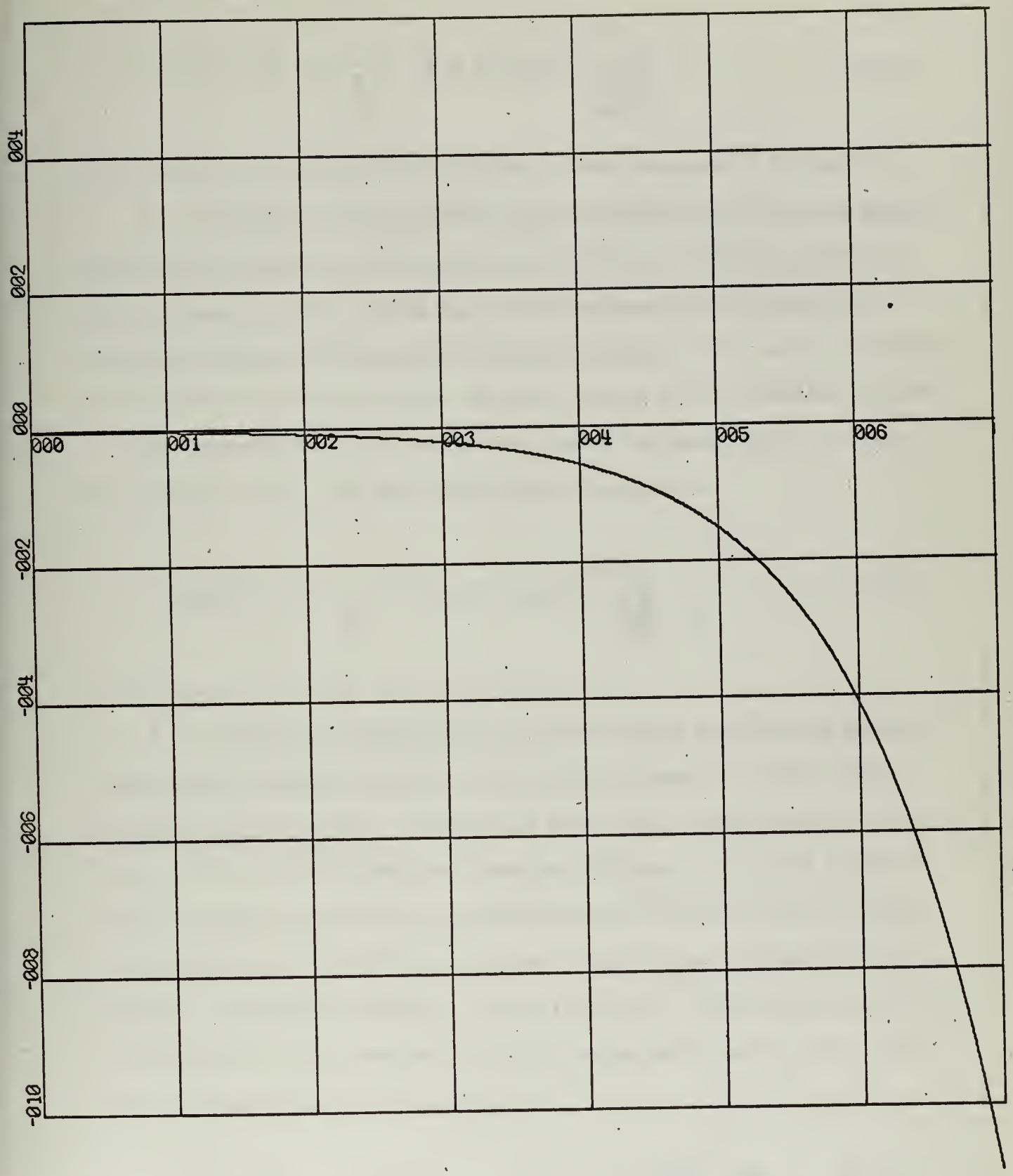
The numerical analysis and conceptual verification of much of the purely mathematical study of this chapter and succeeding chapters was accomplished by the use of numerical calculus, with solutions performed on a CDC 1604 computer. The use of the fourth order Runge-Kutta method to solve a generalized differential equation with a library routine known as INTEG 1 was used. Appendix A contains a description of this program along with the subroutines used for all digital computations in this dissertation. As with any numerical method reasonable care had to be

taken to insure that the result truly represented the behavior of the differential equation under consideration. Normally a physical appreciation of the behavior of the system along with the evaluation of the numerical steps of sufficiently small value will insure the validity of the results obtained by numerical methods. The potential inaccuracy of numerical methods becomes of special concern in this dissertation where the equations studied are normally unstable though finite sampling does diminish this concern. In general, whenever the results remain essentially the same even though the step size was reduced, it is assumed that the results are valid.

Since the majority of the investigations of the dissertation involved more than one method of analysis the agreement of their results were used as a reasonable proof to their validity. Following are representive computer solutions to modes of operation previously described in sections one through four.

A. C constant and positive, R constant and negative with step voltage input. This case described by equation (2-3) and shown as a circuit in Figure 2-1, is represented by Figure 2-12. The parameters chosen here were R = one ohm, C = one farad, E = one volt, time in seconds and an initial charge of zero. The negative exponential output voltage as anticipated by equation (2-3) is verified.

B. C constant, R sinusoidally varying between positive and negative values with a positive average value of resistance (incoherent operation) and the input a slowly varying sinusoidal function with a period substantially larger than the period of the resistive variations. Here the degenerative versus regenerative phases are such to insure incoherency between cycles of operation. The output voltage versus time is shown in



X-SCALE = 1.00E+00 UNITS/INCH.
Y-SCALE = 2.00E+02 UNITS/INCH.

OUTPUT VOLTAGE VS TIME

RUN 1

FIGURE 2-12



Figure 2-13 for the differential equation

$$\cos(.1t) = q + (1 + 4\cos t)^{-1} \frac{dq}{dt}, \qquad (2\text{-}46a)$$

whose behavior conceptually corresponds to that represented in Figure 2-5.

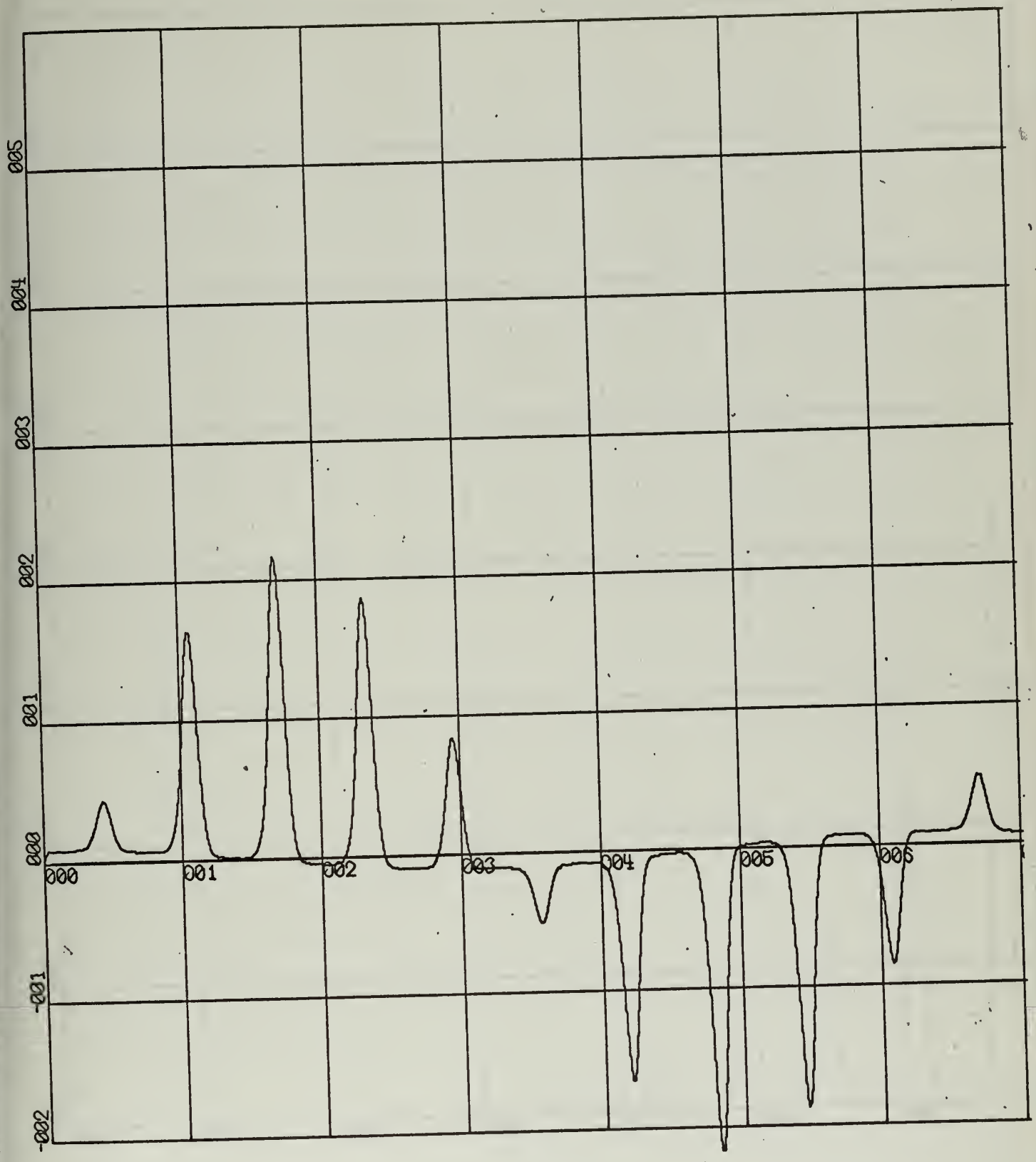
C. C constant, R sinusoidually varying between positive and negative values with a negative average value of resistance, (coherent operation) and the input a slowly varying sinusoidal function with a period substantially larger than the period of the resistance. This case corresponds to the previous case except that coherency exists between sampling periods and the subsequent loss of correlation between the input source and output voltage occurs. The particular equation solved is

$$\cos(.1t) = q + (-.1 + 4\cos t)^{-1} \frac{dq}{dt}, \qquad (2\text{-}46b)$$

and is graphically shown by Figure 2-14.

D. C constant, R sinusoidually varying between positive and negative values with incoherent operation, input source sinusoidal with a slowly varying phase (frequency). In order to graphically demonstrate the sensitivity of the output voltage as a function of phase for a given input frequency but with a periodically sampling system, the periodically sampling system similar to described in B was used only the input phase angle or frequency very slowly changing as time progressed, slow enough to allow the assumption it was constant during any regenerative period. The particular differential equation solved was

$$-\cos(\tau + .034t) = q + (1 + 4\cos t)^{-1} \frac{dq}{dt}, \qquad (2\text{-}47)$$

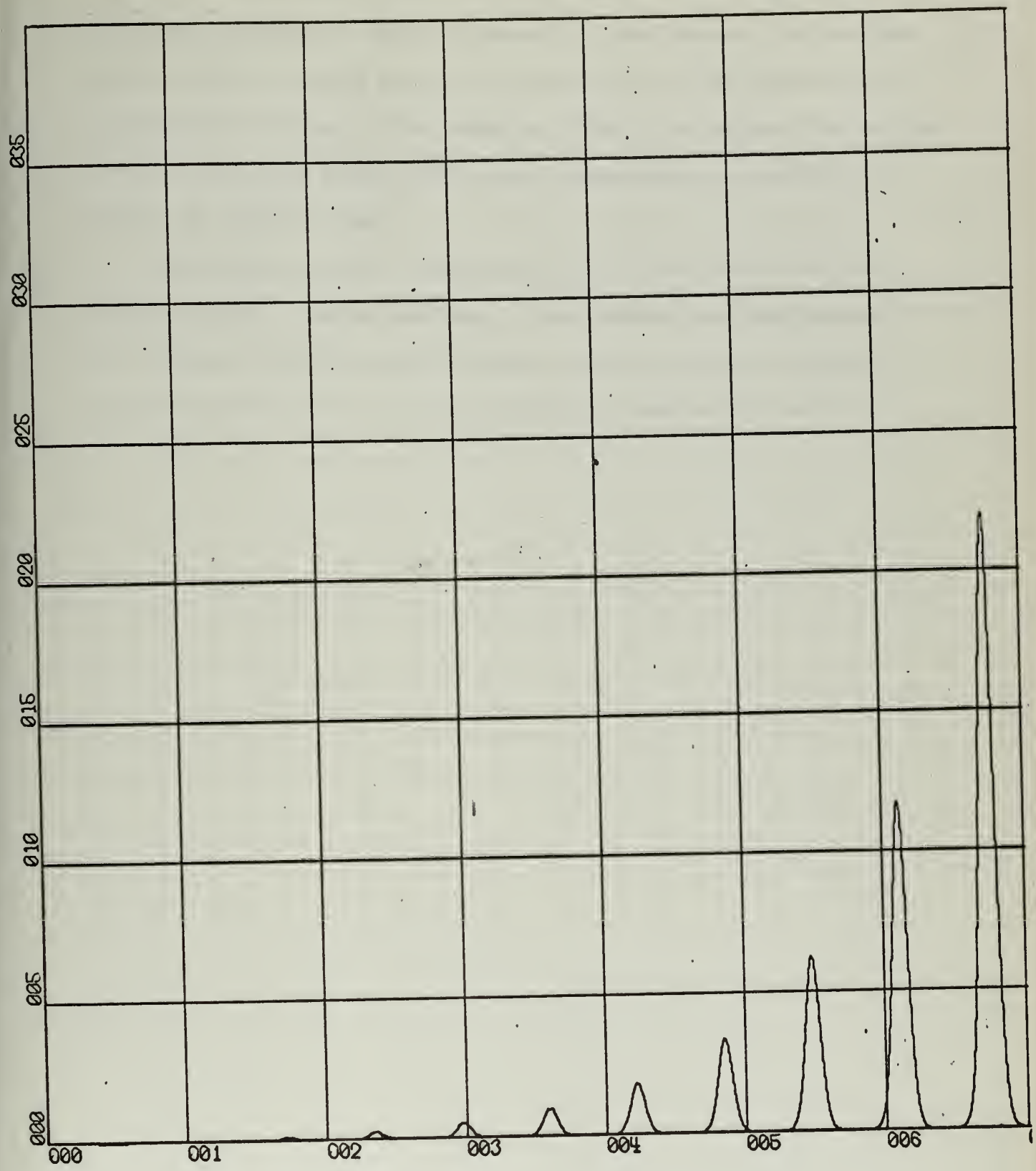


X-SCALE = 1.00E+01 UNITS/INCH.
Y-SCALE = 1.00E+01 UNITS/INCH.

OUTPUT VOLTAGE VS TIME (INCOHERENT)

RUN 1

FIGURE 2-13



X-SCALE = 1.00E+01 UNITS/INCH.
Y-SCALE = 5.00E+04 UNITS/INCH.

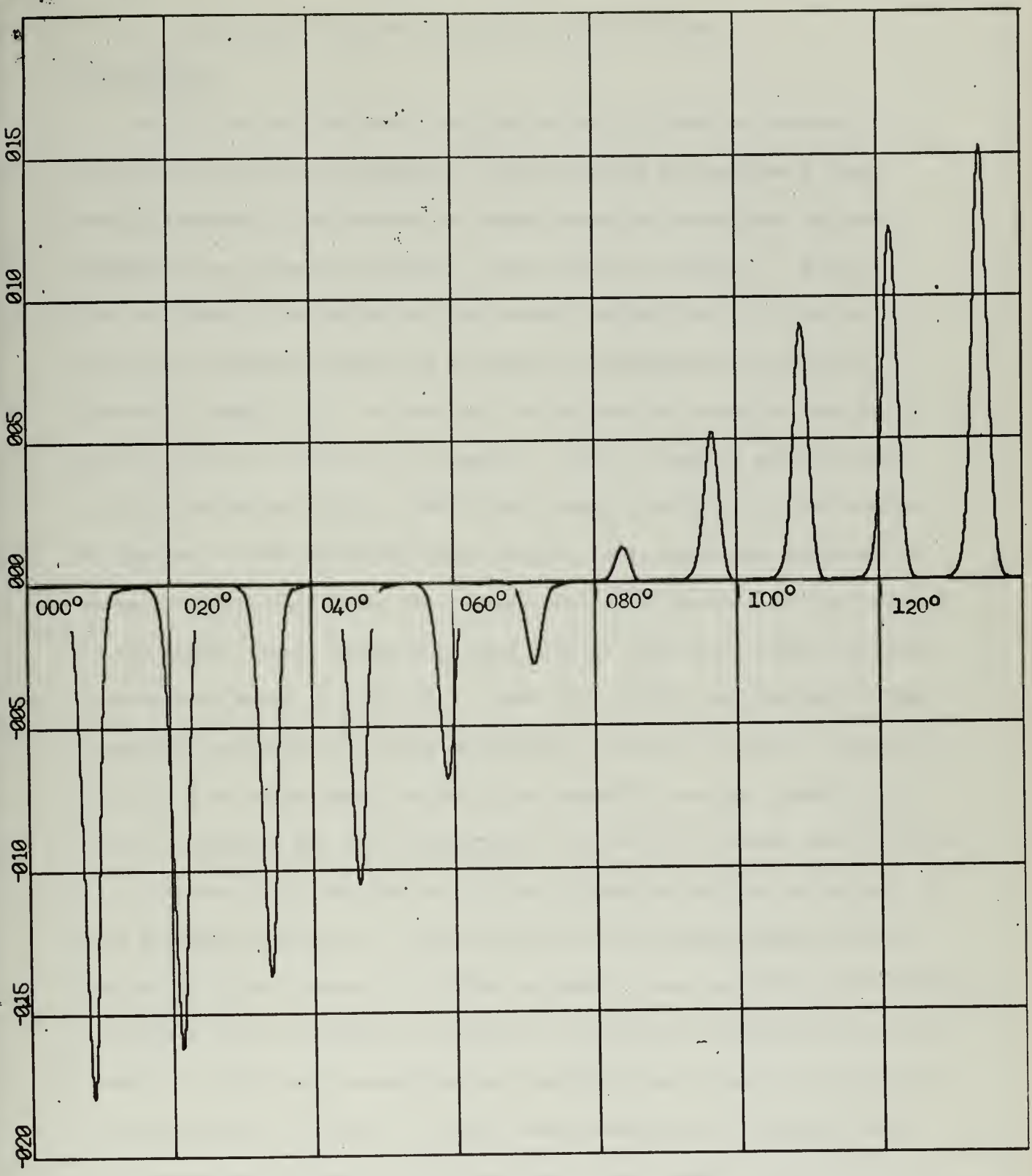
OUTPUT VOLTAGE VS TIME (COHERENT)

RUN 1

FIGURE 2-14

where E_c is portrayed graphically by Figure 2-15. Each major time division presenting 20 degree increments of input angle. The envelope of the peaks of sampled points shows the output voltage sensitivity as anticipated in Figure 2-7 and equation (2-22a). As obvious from equation (2-47), the slowly varying phase can be represented as a varying frequency but constant phase.

In addition to these computer solutions of the first order unstable systems, computer solutions to the unstable nonlinear system and variable resistive unstable linear system are covered in Chapter Three where they will be directly compared to experimental results.



X-SCALE = 1.00E+01 UNITS/INCH.
Y-SCALE = 5.00E+01 UNITS/INCH.

OUTPUT VOLTAGE VS INPUT PHASE

RUN 1

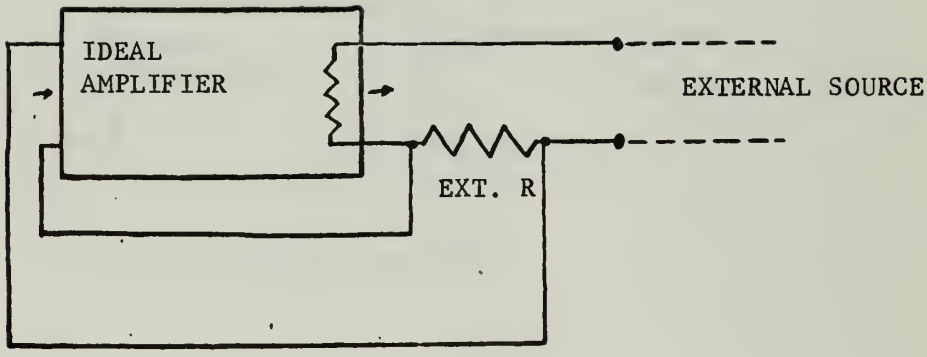
FIGURE 2-15

CHAPTER THREE

First Order System Experimental Verification

3.1 General

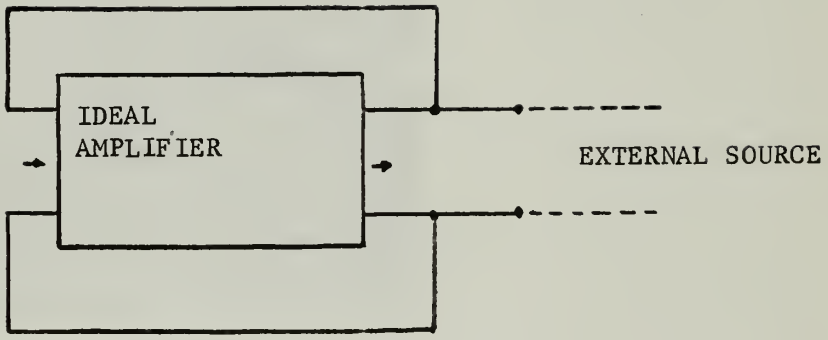
Before any experimental verification of the material covered in Chapter Two could be performed, it was necessary to overcome a fundamental limitation that existed in normal negative resistance devices, whether it be feedback amplifier, tunnel diode or dynatron. Except for the tunnel diode which has the general properties of a dynatron, the topic of devices operating as negative resistances is completely covered by Herold (8). In general, the behavior of negative resistance devices fall into two basic catagories, either a current controlled or voltage controlled device. The current control devices are represented by the arc or glow discharge tubes and the ideal amplifier connected as shown in Figure 3-1, while the voltage controlled devices are represented by the tunnel diode, dynatron and the voltage controlled ideal amplifier connected as shown in Figure 3-2. Both the standard current and voltage controlled resistive functions are shown in Figure 3-3a where a potential difficulty in using these devices in an unstable sampling system as portrayed in Chapter Two can be observed. For low input signal amplification it is necessary for the device, whether current or voltage controlled, to have a negative resistance characteristic at low input signals without having its effect swamped by another parameter, such as the initial voltage or current that is required for negative resistance operation in most devices. In addition, in sampling and resetting the system it is required that no transit or change in steady state parameters be obtained which could swamp the influence of the low level input signal, though later on when the second order system is studied it will be seen that there exists



CURRENT CONTROLLED RESISTIVE DEVICE

FIGURE 3-1

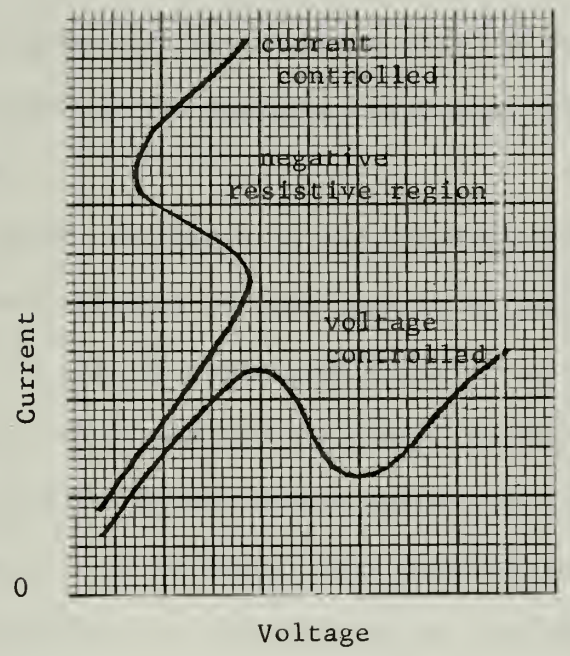




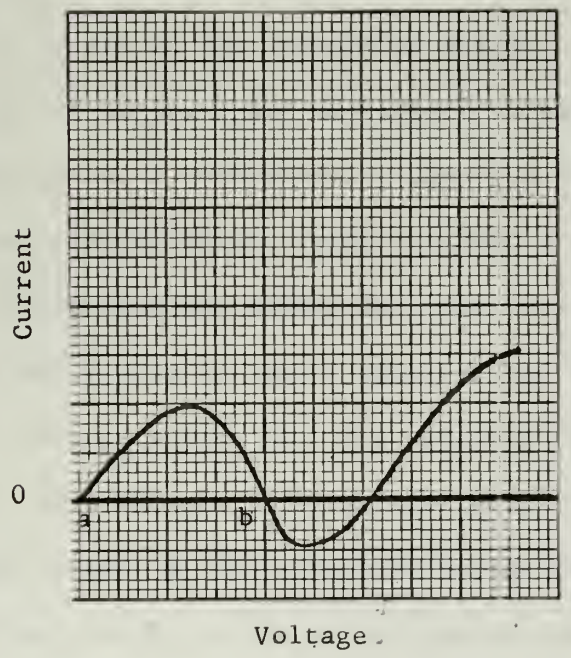
VOLTAGE CONTROLLED RESISTIVE DEVICE

FIGURE 3-2





A standard devices



B special dynatron

NEGATIVE RESISTIVE DEVICES CHARACTERISTICS

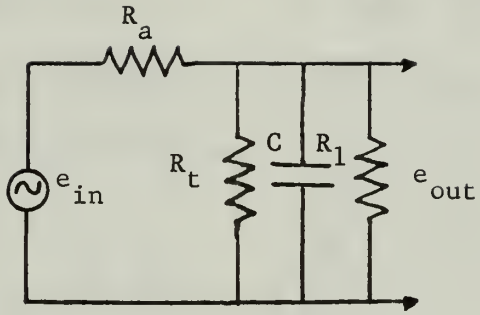
FIGURE 3-3



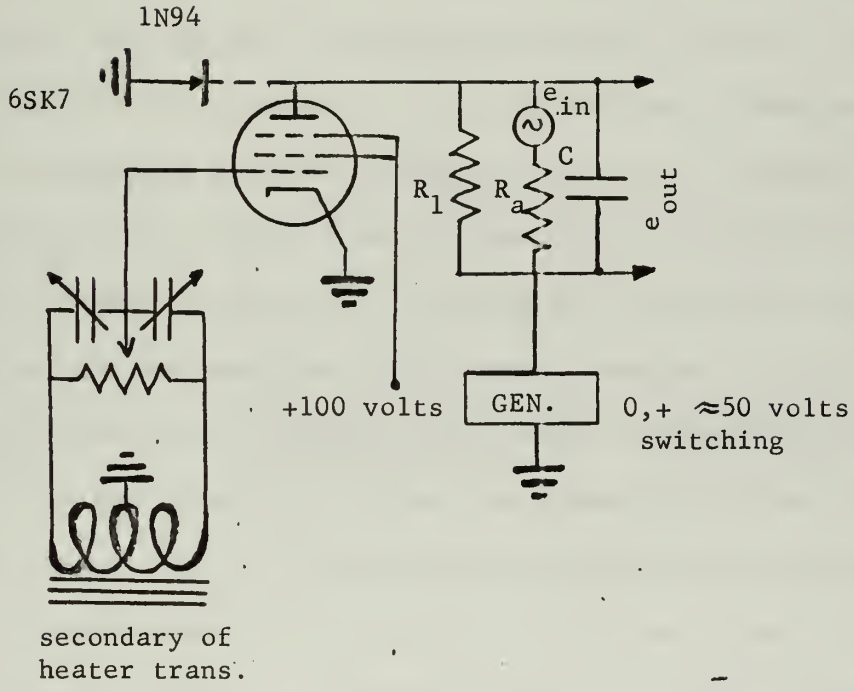
a way to overcome this constraint. There was found one device which overcame the forementioned objections and allowed for experimental verification of the concepts of Chapter Two. This device was obtained by using certain vacuum tubes in a special mode of dynatron operation. The detailed experimental study of this mode of operation is covered in Appendix B but it is sufficient here to say that a plate characteristic as such in Figure 3-3b was obtained with the additional capability of having the value of the negative resistance dependent on the control grid voltage.

It is often convenient to analytically translate the current vs. voltage characteristics of such devices as tunnel diodes, feedback amplifiers, so that the operating point of initial interest is centered at the origin, where now the resistance of such a system can be considered as voltage divided by the current as long as linearity is preserved. As it is to be shown, this translation is electrically performed in this dissertation by the addition of a voltage source in series with a device which has the behavior similar to that shown in Figure 3-3b where point b is now at the translated origin.

Referring to Figure 3-3b, if circuit voltages were made to switch between points a and b periodically, then the device would be portraying to an external circuit first a positive then a negative resistance without externally influencing the system ie., for both positive and negative resistance initial points (a and b) there is not current through the device therefore no voltage across it. One possible circuit configuration which could exploit this feature is shown in Figure 3-4a where e_{in} is the equivalent signal source, R_a its effective series resistance, R_1 and C constitute the load and R_t is the active resistance which can periodically



A



B

ANALYTICAL AND EXPERIMENTAL CIRCUITS FOR VERIFICATION OF FIRST ORDER REGENERATIVE SAMPLING SYSTEM

FIGURE 3-4



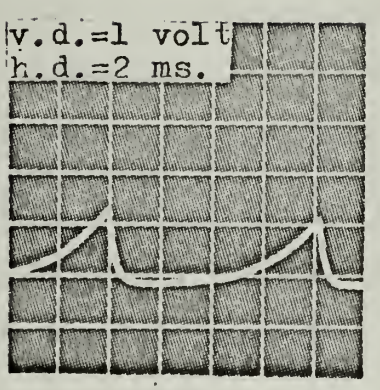
switch between a positive and negative value. If initially a quiescent condition exists in the circuit and at time zero an input is applied, then in transform notation there exist

$$E_c = \frac{e_{in}}{C(R_a)(s+\alpha)} \quad , \quad \alpha = \frac{1}{C}\left\{\frac{1}{R_a} + \frac{R_1 + R_t}{R_1 R_t}\right\} \tag{3-1}$$

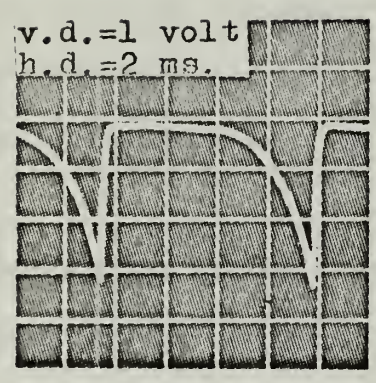
for a step function from zero to some finite value, and the time dependent relationship then becomes

$$E_c = \frac{e_{in}(R_1 R_t)(1 - e^{-\alpha t})}{R_a R_t + R_t R_1 + R_1 R_a} . \tag{3-2}$$

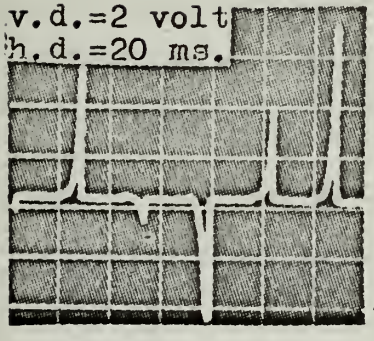
The similarity between this equation and equation (2-22b) is readily apparent, and with α periodically varying so that incoherency exists, the mode of operation as shown in Figure 2-5 is to be expected. The experimental circuit used is shown in Figure 3-4b with the plate supply generator switching between points a and b as represented on Figure 3-3b. In the actual circuit used for the following examples, R_1 is 10,000 ohms, R_a is 100,000 ohms and C is equal to 0.5 farads. Waveforms across C for small positive and negative d-c inputs are shown in Figures 3-5a and b where their similarity to the expected exponential rise is apparent. As the circuit was adjusted for more gain, induced hum became a serious problem and had to be amplitude and phase cancelled to prevent saturation. This is the purpose of the grid controls shown in Figure 3-4b. After this balance, the near random triggering by noise could be observed; an action typical of normal superregeneration without an input signal. Figure 3-5c is representative of such noise-triggered output, while Figures 3-5d and e



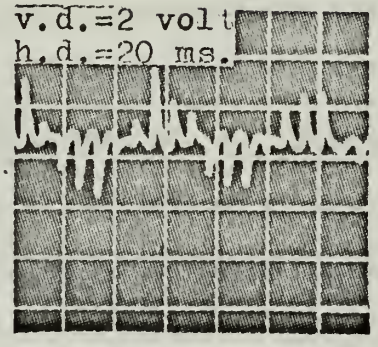
A



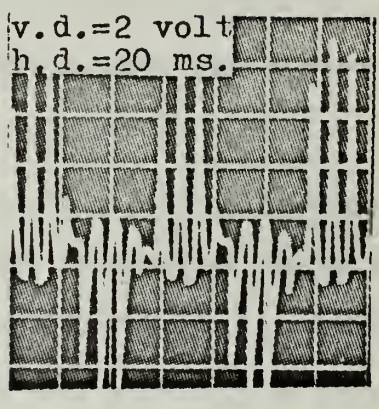
B



C



D



E

REPRESENTATIVE OSCILLOSCOPE PHOTOGRAPHS OF SELECTED MODES OF OPERATION OF THE FIRST ORDER SYSTEM

FIGURE 3-5

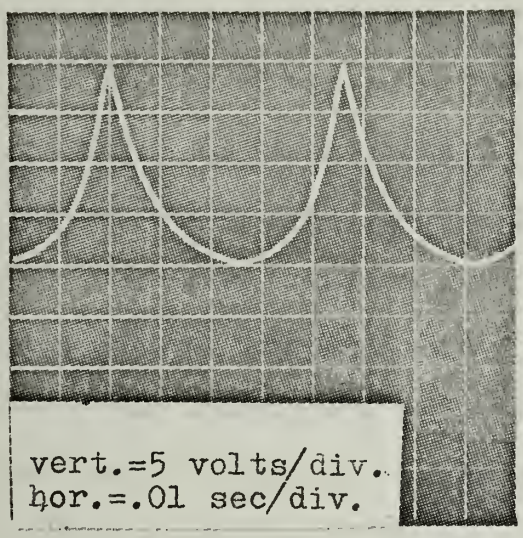




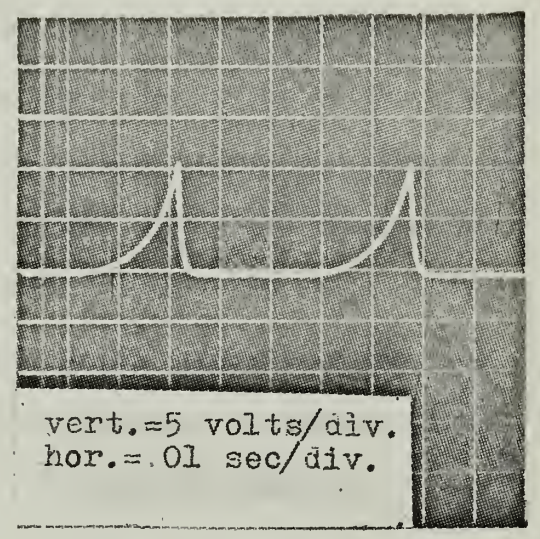
are the outputs from a 20 cps input signal at .05 and .20 volts respectively and a system quenching (switching) frequency of 200 cps. In general every behavior which has been traditionally associated with normal r-f superregeneration such as the influence of regenerative time or gain, the linear and nonlinear modes of operation and the random noise-pulses in the presence of no input signal and high gain adjustments, occurred in this degenerate (first order) unstable sampled system. This behavior is discussed in more detail in the following sections.

3.2 Linear vs NonLinear Operation

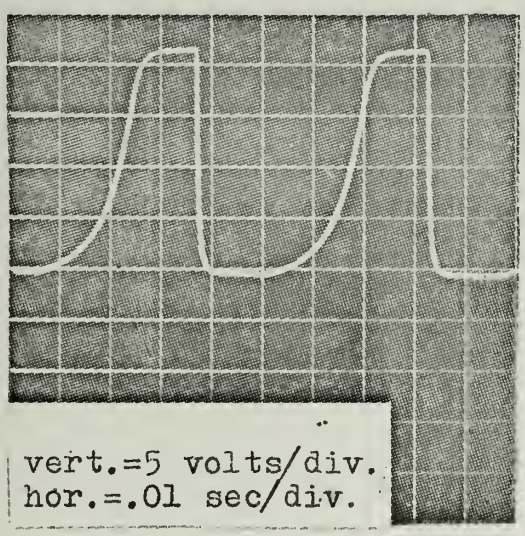
As empirically discussed in Appendix B and pictured in principle in Figure 3-3b, there is a region of linear negative resistance characteristic which developes gradually into a nonlinear region as the voltage amplitude across the negative resistance is increased. As the first experimental verification of system behavior of the circuit and schematic shown in Figure 3-4, the plate supply generator was adjusted so that square wave potentials were switching between points a and b as shown in Figure 3-3b, and a small minus d-c potential for e_{in} injected. Figure 3-6a represents E_c for this case with a 20 cps switching rate. The exponential shapes of both the rising and decreasing waveforms are as expected. In this particular case, there is also an asymmetric switching rate with turn on time less than turn off time. This was done to insure little coherency between wave trains. This coherency tendency, which is partially due to the finite decay time of the system during turn off was eliminated by the addition of a switched clamp across the dynatron. This is shown as a diode between the plate and cathode of the dynatron which will forward conduct when the switching generator goes to zero potential, but appear as an open circuit when the generator goes positive. Figure 3-6b shows the rapid decay



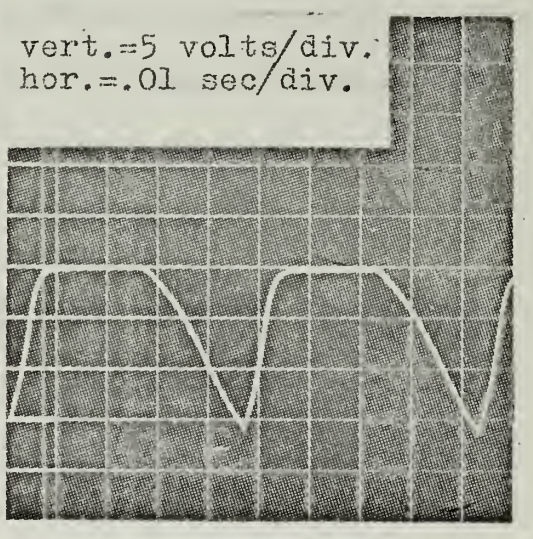
A



B



C



D

EXPERIMENTAL RESULTS REFLECTING LINEAR AND NONLINEAR OPERATION OF THE SAMPLING DYNATRON, FIRST ORDER SYSTEM

FIGURE 3-6







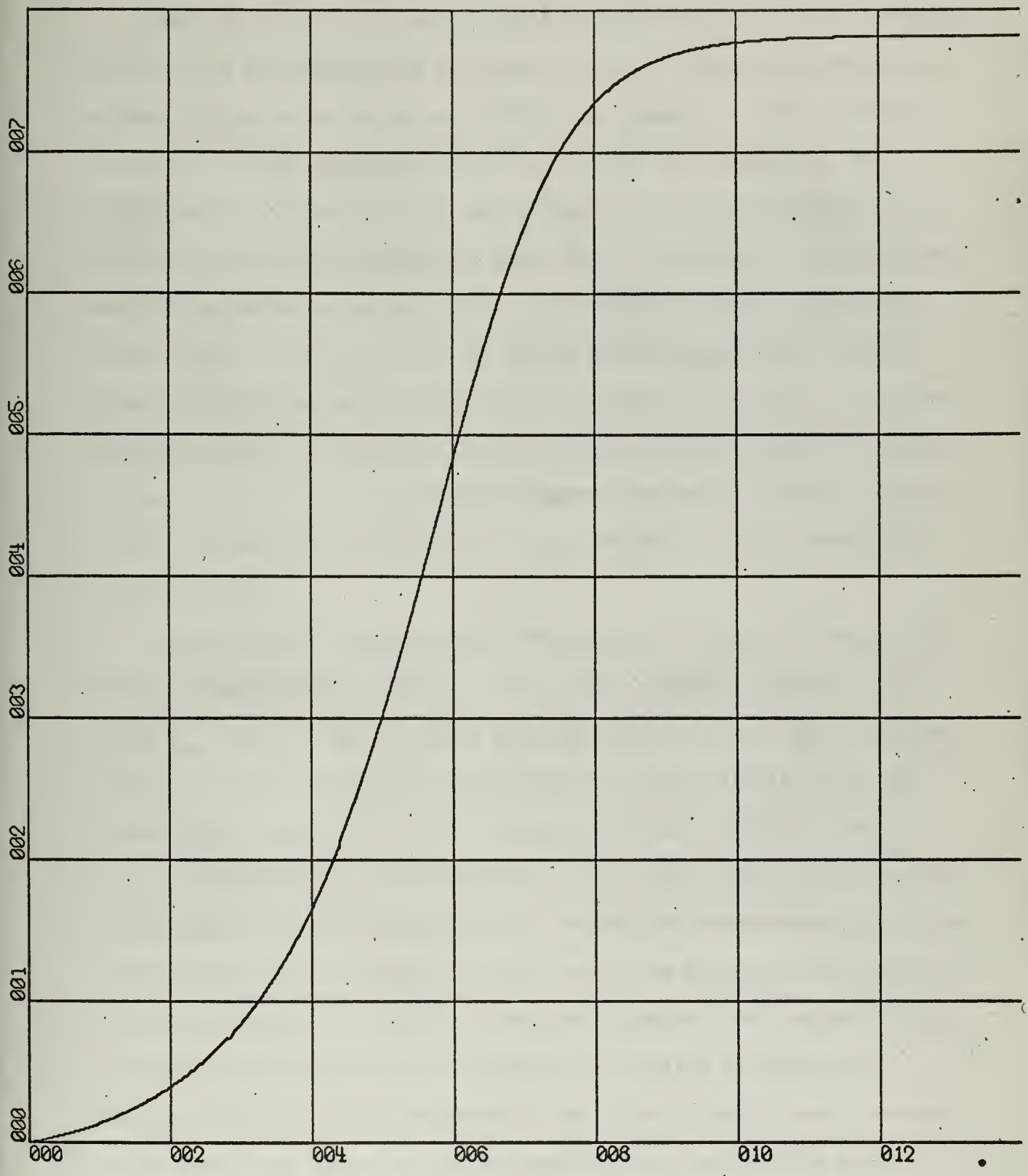
characteristics when the clamp was added, with all other parameters remaining the same. This minor addition which insures incoherent operation will be left connected in all future experimental work done in this chapter.

When the variable symmetric switching generator was now adjusted so that the time of turn on is increased, in this case by use of the symmetric control of the plate generator, the increased peak output and saturation effects of the system becomes apparent. Figure 3-6c shows these effects under operating conditions identical as before except for the increased turn on time. The nonlinearity of the device with respect to input polarity was demonstrated by repeating the experimental procedures which was done to obtain Figure 3-6b only now a positive e_{in} was used. This result is protrayed by Figure 3-6d and its different shape as compared to Figure 3-6b is apparent.

Finally, a digital computer solution to the nonlinear problem was done. This was accomplished by writing a series of equations that represented the circuit shown in Figure 3-4a for the regenerative mode. The basic equations and particular values of elements used was

$$
\begin{aligned}
&1)\ i_1 = -i_2 - i_3 + i_4 && C = 1 \text{ fd.} \\
&2)\ i_2 = .2q_1 && R_L = 5 \text{ ohms} \qquad (3\text{-}3) \\
&3)\ i_3 = -q_1(1 - q_1^2) && R_t = \frac{-1.}{1 - E_c^2} \text{ ohms} \\
&4)\ i_4 = .2(.05 - q_1) && R_A = 5 \text{ ohms} \\
&5)\ E_c = q_1 && e_{in} = .01 \text{ volts}
\end{aligned}
$$

Figure 3-7 is E_c for this set of conditions and the similarity to the experimental results shown in Figure 3-6c is apparent.



X-SCALE = 2.00E+00 UNITS/INCH.
Y-SCALE = 1.00E-01 UNITS/INCH.

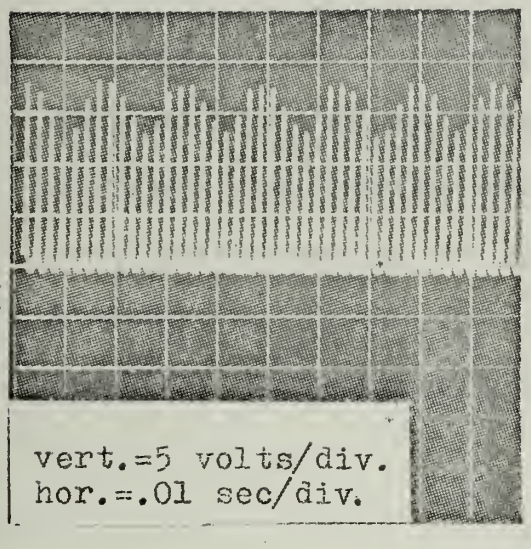
OUTPUT VS TIME (NONLINEAR SYSTEM)
RUN 1

FIGURE 3-7

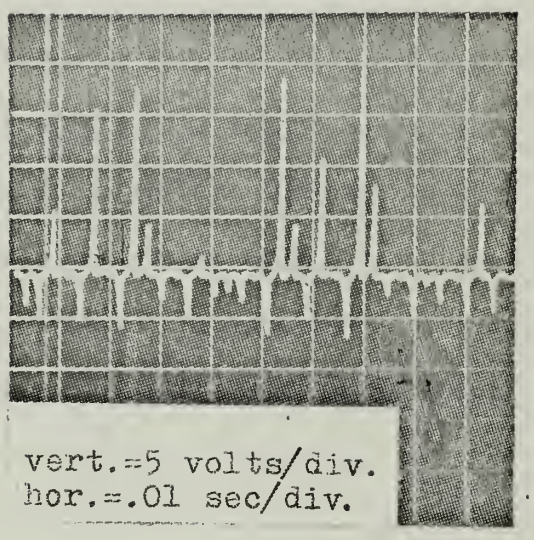
3.3 Sensitivity Tests

When the gain of the sampled system was increased by either increasing turn on time or reducing the load capacitance it became very difficult to adjust the system for no output voltage. An example is shown in Figure 3-8a for a 400 cps sampling rate and a .05 ufd. load capacitor. The ripple on top is due to circuit hum pickup on top of a negative d-c e_{in}, the system representing a gain of about 30 db. As the gain was increased, and the hum balancing controls used to minimize hum input, the random triggering by circuit noise of the system became apparent and could be observed both on an oscilloscope and aurally when E_c was used to drive an audio amplifier. A rushing or hissing sound could be heard, very similar to that which is heard in a standard superregenerative receiver. Figure 3-8b is representative of this near random behavior in the presence of no input signal.

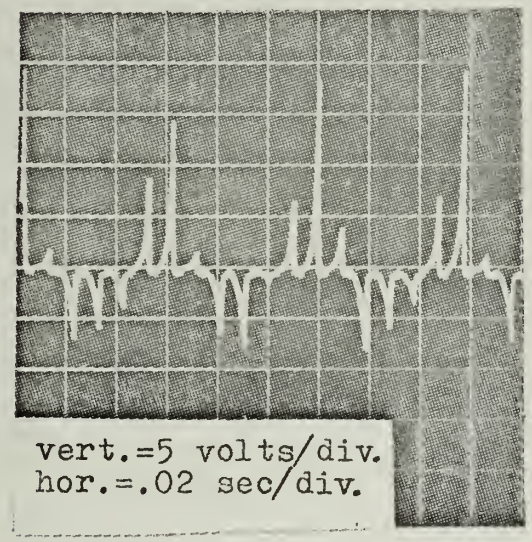
Two experimental verifications involving the behavior of the circuit when a sinusoidal input was used for e_{in} were performed. Figure 3-8c shows E_{out} for a 15 cps e_{in} and a sampling rate of 100 cps where care was taken to insure that with no input signal the random signal output was symmetrically disposed, ie., the turn on potential so adjusted that no current was across R_t at the beginning of the cycle. The envelope of the 15 cps signal is clearly represented. In addition the distortion in terms of peak output from the axis is clear, due to the nonlinear characteristics of the active device. Finally Figure 3-8d represents the output voltage when the grid of the dynatron was modulated, causing a modutated R_t in addition to the quenching phenomenon. The output clearly shows the modulation where here again the circuit gain was over 30 db. This mode of operation has certain desirable features in that by simply adjusting the



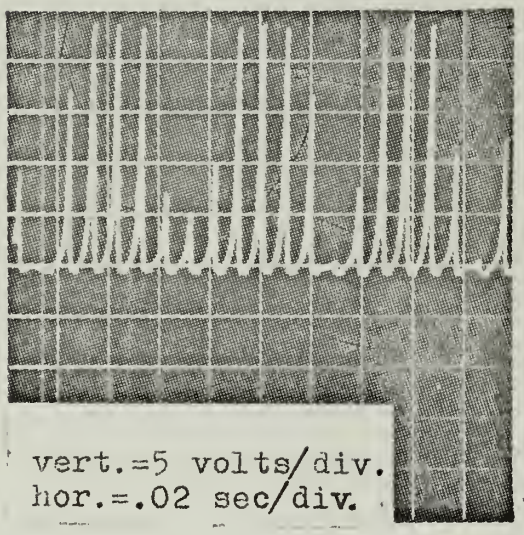
A



B



C ,



D

EXPERIMENTAL RESULTS REFLECTING THE FORM OF OUTPUT FOR DIFFERENT TYPES OF INPUT SOURCES, FIRST ORDER SYSTEM

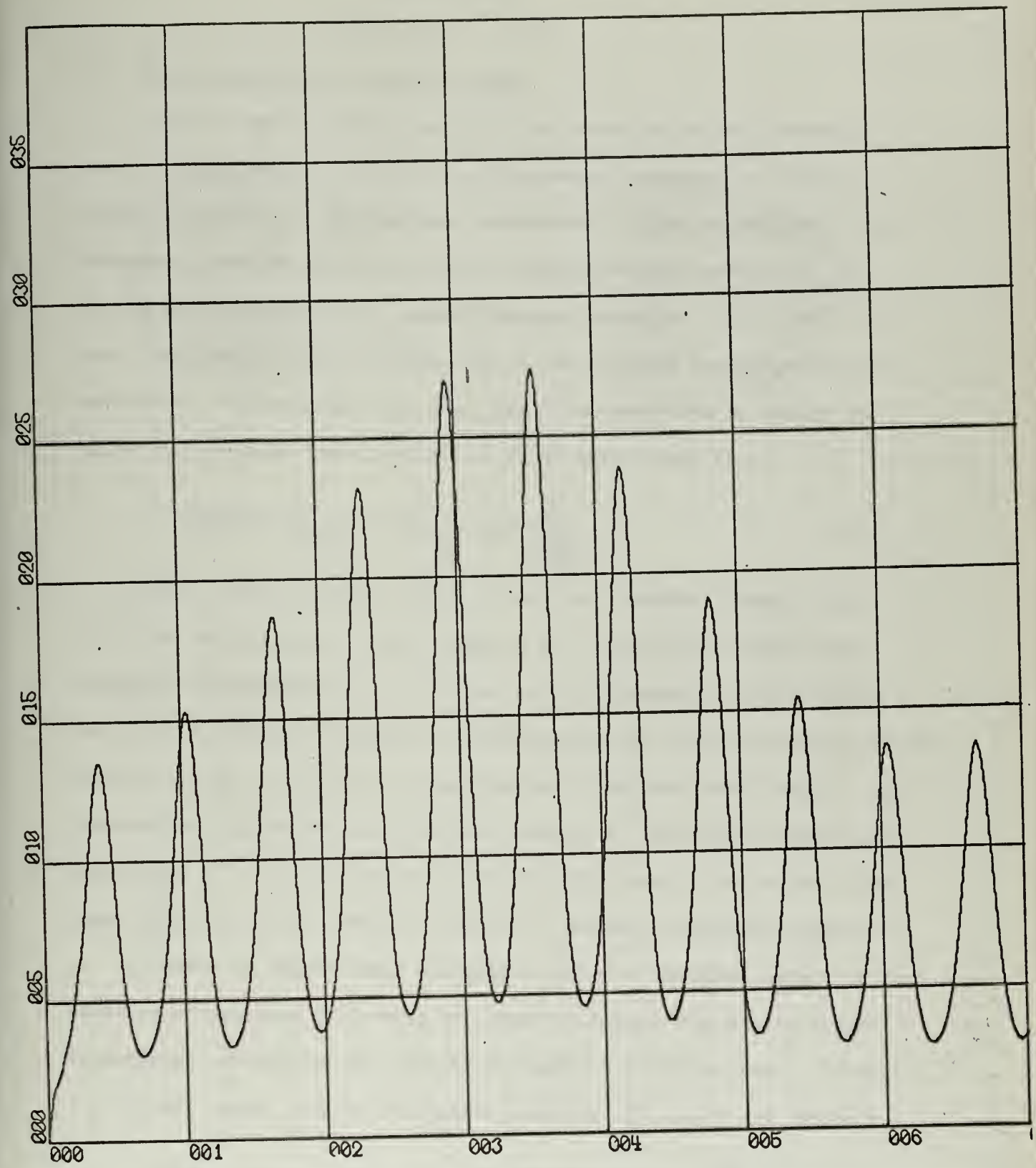
FIGURE 3-8





residual d-c in the circuit the form of modulated waveform can be changed. One advantage would be the ability to adjust the system to various levels of output by simply adjusting the d-c bias. In certain forms of radio transmitters this feature of clamped and/or unsymmetric output is desirable for maximum communication capability.

Finally, a digital computer simulation of the forementioned mode of operation with a variable resistance serving as the input source was performed. The equations used are similar in form to equation (3-3) except for the addtion of a low frequency modulation of R_t, and a high frequency sampling term (note equation (2-46a)). Figure 3-9 is the output of this simulation and its similarity to Figure 3-8d, is apparent.



X-SCALE = 1.00E+01 UNITS/INCH.
Y-SCALE = 5.00E-02 UNITS/INCH.

OUTPUT VS TIME (MODULATED RESISTANCE)
RUN 1

FIGURE 3-9

CHAPTER FOUR

Second Order System

4.1 Basic Second Order Considerations

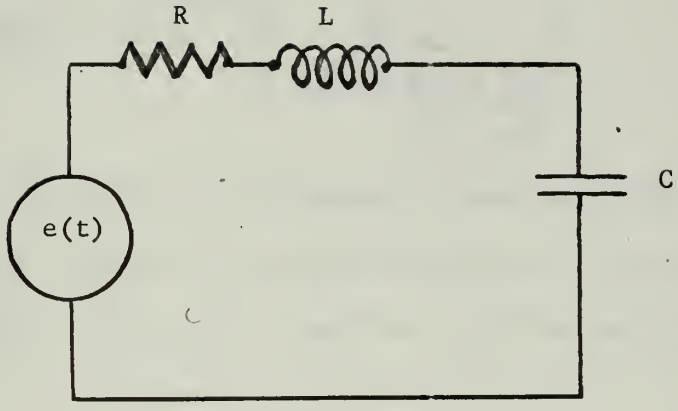
With the amplification possibilities exhibited by an electrical circuit described by a first order differential equation it would be proper to extend the mathematical development to the second order differential equation and its electrical equivalent, and observe its behavior when operated as an unstable sampled amplifier. As it will be seen, this leads to an understanding of the standard superregenerative amplifier. This mathematical study can be accomplished by adding one higher differential term to equation (2-1) which leads to

$$e(t) = a\,q + b\frac{dq}{dt} + c\frac{d^2q}{dt^2} \,. \qquad (4\text{-}1)$$

Unlike the first order system, there is no general formula that will give the solution to this equation for time varying coefficients though it is possible to use a series solution similar to that used in section 2.3. To gain insight into the behavior of the second order system, equation (4-1) will first be considered with constant coefficients. By considering e(t) as the input voltage source, a the series inverse capacitance, (C^{-1}), b the series resistance (R), and c the series inductance (L), the circuit shown in Figure 4-1 becomes a physical reality.

In order to allow a more convenient method of gaining insight to the behavior of equation (4-1) than by classical format, the use of transformational calculus on the circuit of Figure 4-1 will be used. An analysis of the circuit follows in Laplace form for $\frac{dq}{dt} = 0$, $t = 0$, reveals

$$\mathcal{L}[e(t)] = L[s^2Q(s)] + R[sQ(s)] + C^{-1}[Q(s)] \qquad (4\text{-}2a)$$



ELECTRICAL CIRCUIT EQUIVALENT FOR THE SECOND ORDER DIFFERENTIAL EQUATION

FIGURE 4-1



or

$$Q(s) = L^{-1}\left\{\frac{1}{s^2 + \frac{R}{L}s + \frac{1}{LC}}\right\}\mathcal{L}[e(t)], \qquad (4\text{-}2b)$$

and if e(t) is considered a step function as done in Chapter Two, then an understanding of the charge behavior as a function of the parameters can be obtained, similar to that done for the first order system, and equation (4-2b) becomes

$$E(s) = Q(s)C^{-1} = L^{-1}C^{-1}\left\{\frac{E_{IN}}{s\left(s^2 + \frac{R}{L}s + \frac{1}{LC}\right)}\right\}. \qquad (4\text{-}3)$$

Depending on the nature of the roots of equation (4-3), the solution to this equation will take on three different forms. They are

Case One $\left(\frac{1}{LC} - \frac{R^2}{4L^2} < 0\right)$. Equation (4-3) has as its solution

$$E_c = E_{IN}\left\{1 + \frac{\alpha e^{-\beta t} - \beta e^{-\alpha t}}{\beta - \alpha}\right\}, \qquad (4\text{-}4a)$$

where α , β are real roots to the equation $s^2 + \frac{RS}{L} + \frac{1}{LC}$. With α , β negative, a result which will happen if R is negative, equation (4-4a) as before can be approximated by

$$E_c \doteq E_{IN}\left\{\frac{\alpha e^{-\beta t} - \beta e^{-\alpha t}}{\beta - \alpha}\right\}, \qquad (4\text{-}4b)$$

when sufficient time has elapsed. This system is conceptually similar to the conventional overdamped RLC system except for the negative roots.

Case Two $(\frac{1}{LC} - \frac{R^2}{4L^2} = 0)$. Equation 4-3 has as its solution

$$E_c = E_{IN}\left\{1 - (1+\alpha t)e^{-\alpha t}\right\}, \qquad (4\text{-}5a)$$

where α is the real root to the equation $S^2 + \frac{RS}{L} + \frac{1}{LC}$. As in case one, when α is considered negative and sufficient time has elapsed then equation (4-5a) becomes

$$E_c \doteq E_{IN}\left\{-\alpha t e^{-\alpha t}\right\}. \qquad (4\text{-}5b)$$

This system is now conceptually similar to the conventional critically damped RLC system except for the negative root.

Case Three $(\frac{1}{LC} - \frac{R^2}{4L^2} > 0)$. Equation 4-3 now has as its solution

$$E_c = E_{IN}\left\{1 + \frac{e^{-\frac{Rt}{2L}}}{\sqrt{LC}\,\beta}\sin(\beta t - \psi)\right\}, \qquad (4\text{-}6a)$$

$$\psi = \tan^{-1}\frac{\beta}{\alpha}, \quad \beta = \sqrt{\frac{1}{LC} - \frac{R^2}{4L^2}}$$

where again for a regenerative system after sufficient time has past can be written as

$$E_c \doteq \frac{E_{IN}}{\sqrt{LC}\,\beta} e^{-\frac{Rt}{2L}} \sin(\beta t - \psi). \qquad (4\text{-}6b)$$

This system which is conceptually related to the underdamped RLC System except for the nature of the roots is one that will be studied in more detail as it has the potential to overcome the basic constraints on the mode

of operation and type of negative resistance device as mentioned in Chapter Two.

The similarity of the exponential behavior of these three forms of the solutions to the first order system reveals the possibility of a system gain under a sampled situation as discussed in Chapter Two. Representative behavior of the second order system for these three different cases are shown as Figures 4-2, 4-3, and 4-4 respectively. The particular equation solved was

$$1 = \frac{d^2q}{dt^2} - \frac{dq}{dt} + qC^{-1}, \quad E_c = qC^{-1} \tag{4-7}$$

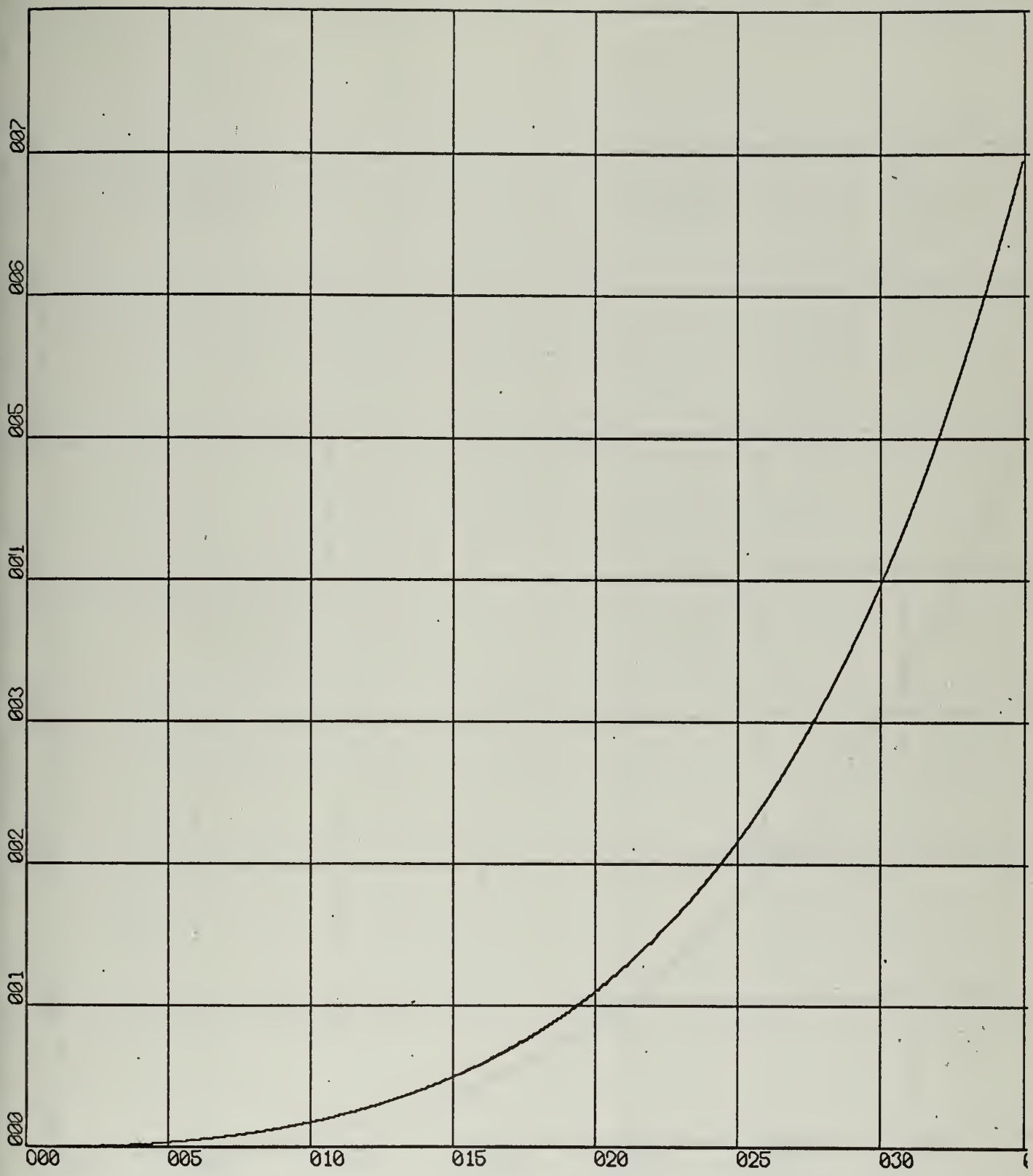
where C is 40 farads for case one (Figure 4-2), 4. farads for case two (Figure 4-3) and 0.4 farads for case three (Figure 4-4).

Finally as was done for the first order system, it is possible to modulate the exponential factor, such as through R, and influence the output. With this form of modulation the second order system, which normally is required to operate at r-f frequencies with conventional negative resistance devices, can be used for a-f amplification and, unlike the first order system, require no special device. This is discussed in more detail in the latter part of this chapter.

4.2 Frequency Dependency of the Second Order System.

With amplification possible under the conditions of sampled unstability for the second order system, the frequency sensitivity of such a system will be investigated. With an input now considered as $E\cos\omega t$, equation 4-2 becomes

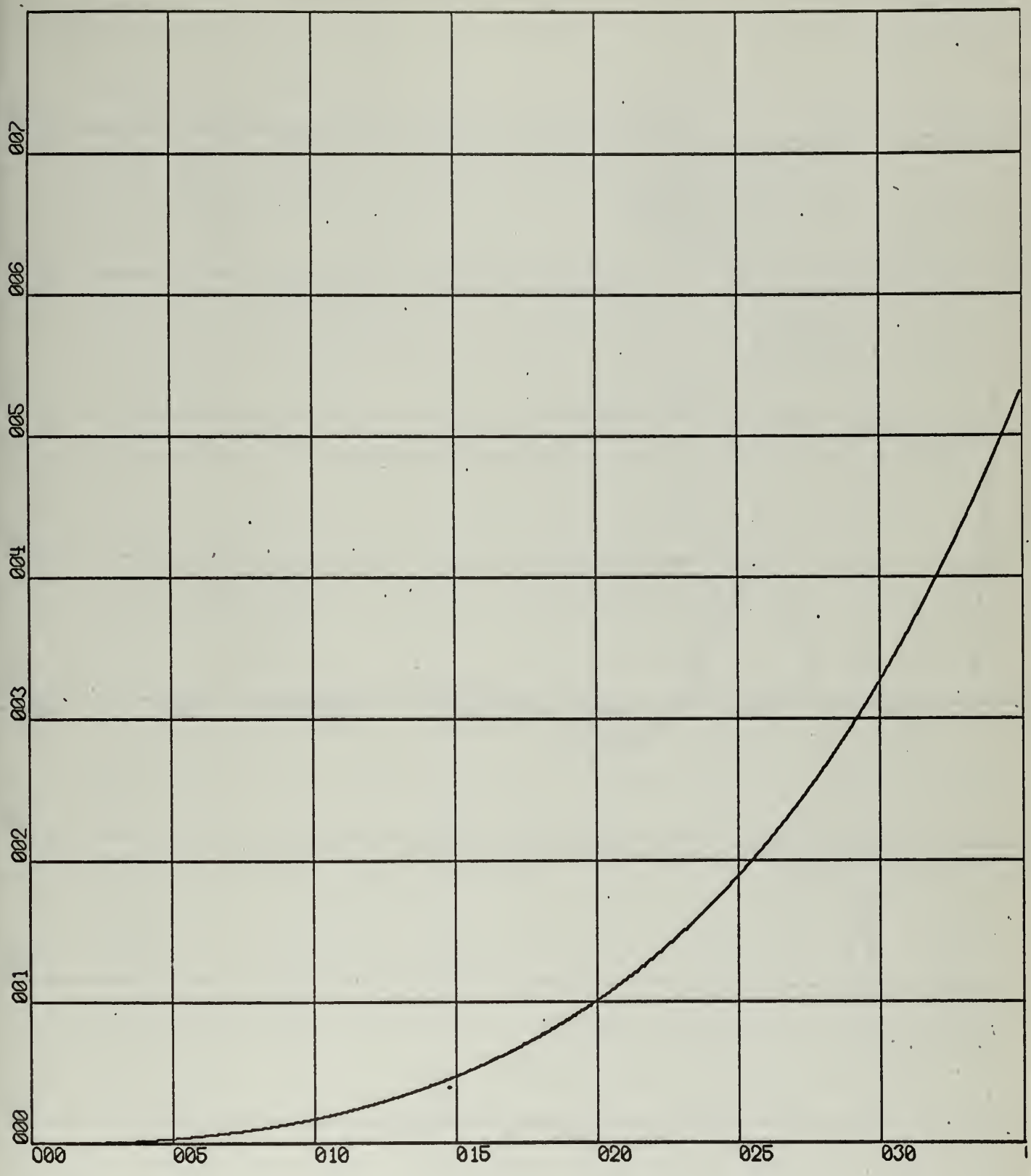
$$E_c(s) = \frac{Q(s)}{C} = \frac{E}{LC}\left\{\frac{s}{s^2+\omega^2} \otimes \frac{1}{s^2+\frac{Rs}{L}+\frac{1}{LC}}\right\}, \tag{4-8}$$



X-SCALE = 5.00E-01 UNITS/INCH.
Y-SCALE = 1.00E-01 UNITS/INCH.

OUTPUT VS TIME (OVERDAMPED SYSTEM)
RUN 1

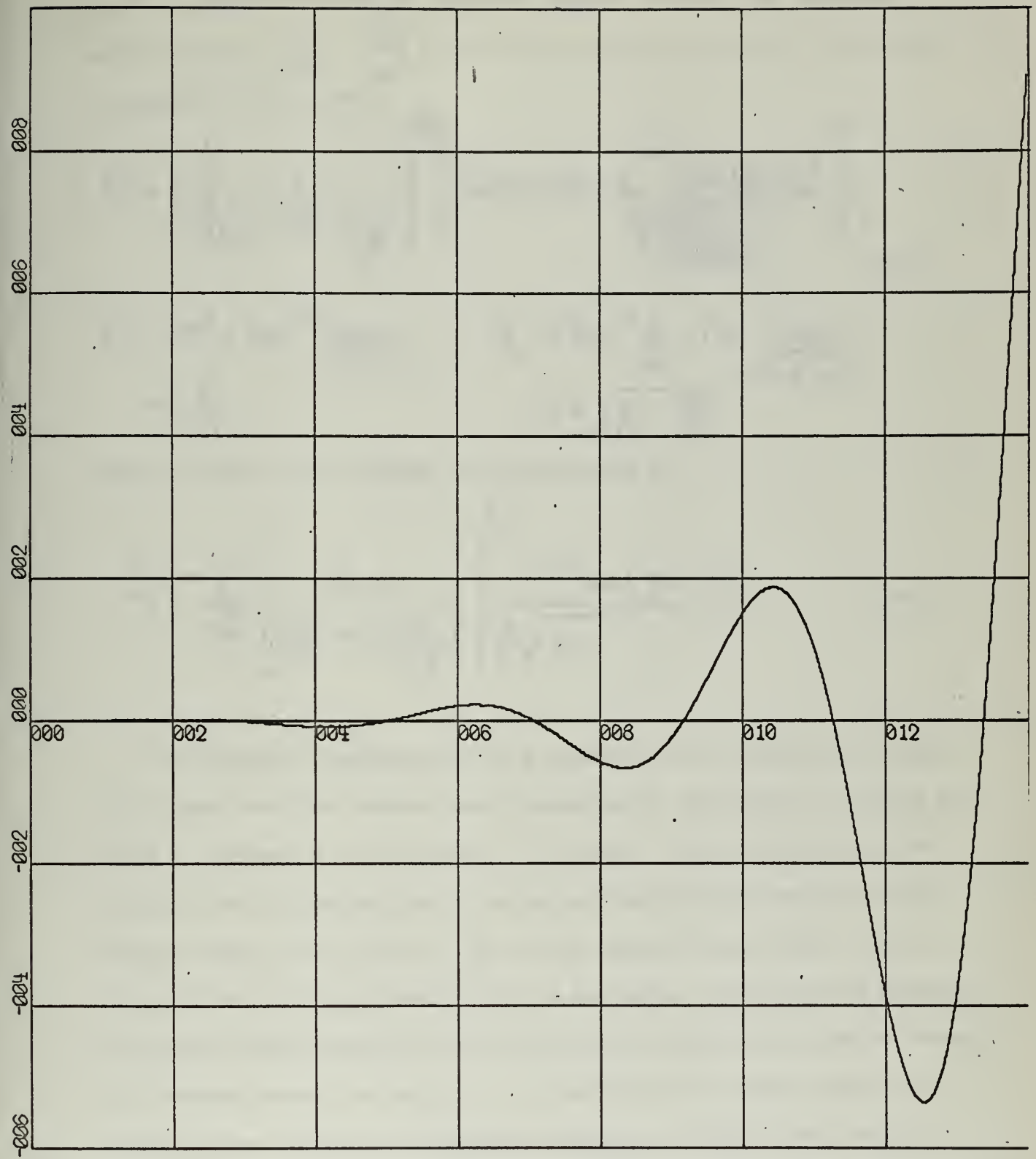
FIGURE 4-2



X-SCALE = 5.00E-01 UNITS/INCH.
Y-SCALE = 1.00E+00 UNITS/INCH.

OUTPUT VS TIME (CRITICALLY DAMPED)
RUN 1

FIGURE 4-3



X-SCALE = 2.00E+00 UNITS/INCH.
Y-SCALE = 2.00E+02 UNITS/INCH.

OUTPUT VS TIME (UNDERDAMPED SYSTEM)
RUN 1

FIGURE 4-4

where an appreciation of the system's response reveals that the parameter condition ($\frac{1}{LC} - \frac{R^2}{4L^2} > 0$) is of particular interest. The inverse of equation (4-8) becomes

$$E_c = \frac{E}{LC}\left[\frac{1}{\left(\frac{1}{LC}-\omega^2\right)^2 + \frac{R^2\omega^2}{L^2}}\right]^{1/2}\left[\sin(\omega t+\psi_1) + \frac{e^{-\alpha t}\sin(\beta t+\psi_2)}{\beta\sqrt{LC}}\right], \qquad (4\text{-}9a)$$

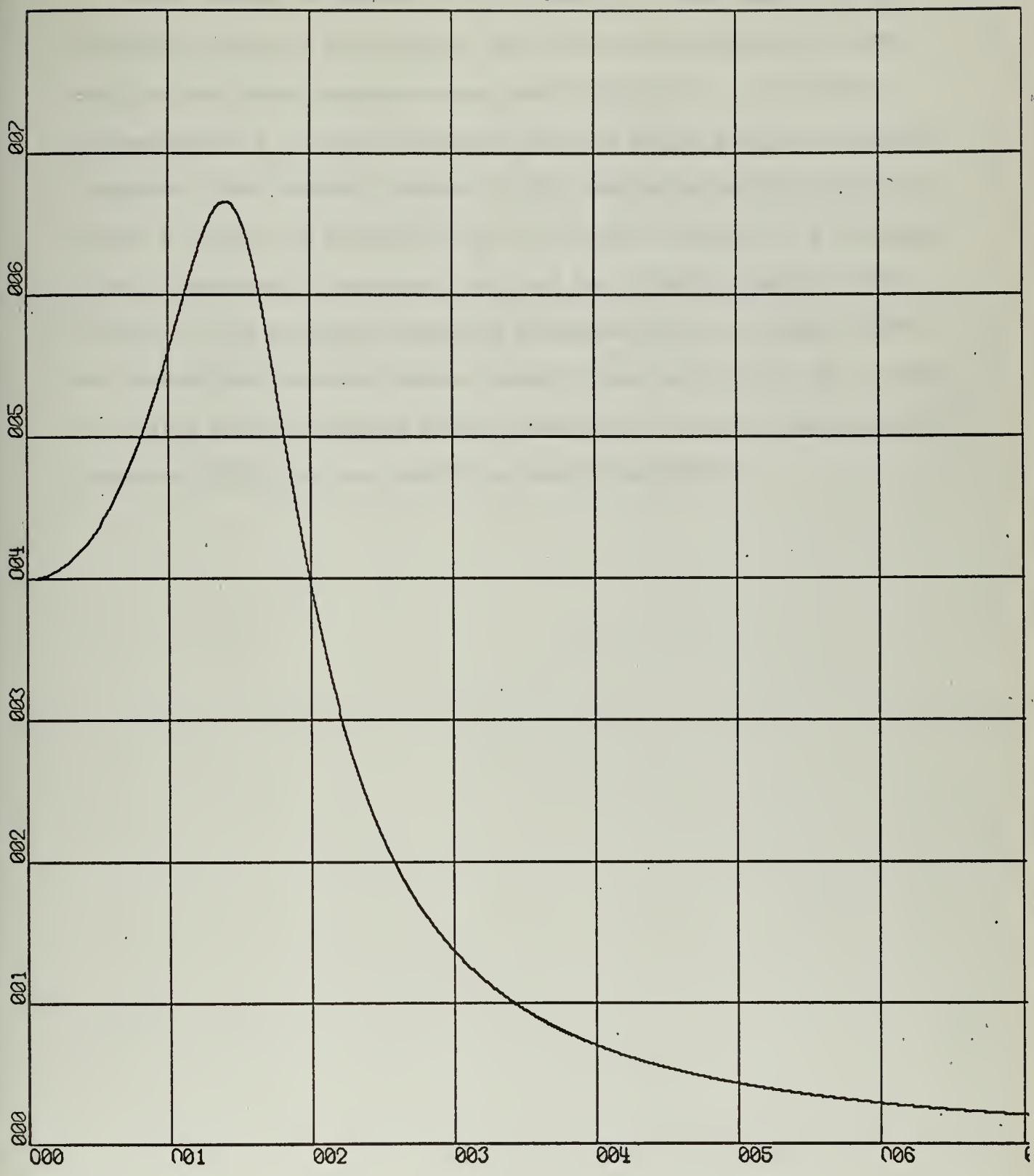
$$\psi_1 = 90^\circ - \tan^{-1}\frac{2\alpha\omega}{\alpha^2+\beta^2-\omega^2}, \quad \psi_2 = \tan^{-1}\frac{\beta}{\alpha} - \tan^{-1}\frac{-2\alpha\beta}{\alpha^2-\beta^2+\omega^2}$$

$$\alpha = \frac{R}{2L} \qquad \beta = \sqrt{\frac{1}{LC} - \frac{R^2}{4L^2}}$$

where as before with $\alpha t \ll 0$, can be expressed as

$$E_c = \frac{E}{LC}\left[\frac{1}{\left(\frac{1}{LC}-\omega^2\right) + \frac{R^2\omega^2}{L^2}}\right]^{1/2}\frac{e^{-\alpha t}\sin(\beta t+\psi)}{\beta\sqrt{LC}}. \qquad (4\text{-}9b)$$

The frequency dependency of this equation can be considered the portion within the first bracket and is graphically represented in Figure 4-5 for C = .4 farad, R = - 1.0 ohm, L = 1.0 henry. The characteristic selectivity curve associated with the series tuned circuit can be now observed, where in this case the "Q" of the system is quite low. What is of significance is its behavior as C is decreased, the difference between the system's amplification factor at d-c and at some point close to resonance becomes greater and greater. As the "Q" of the system becomes considerably over ten and the resonance frequency is raised, the system's gain at resonance is many times greater than at d-c and the swamping effect of the d-c permutation during the switching cycle as mentioned for the first order system can become nonexistent.

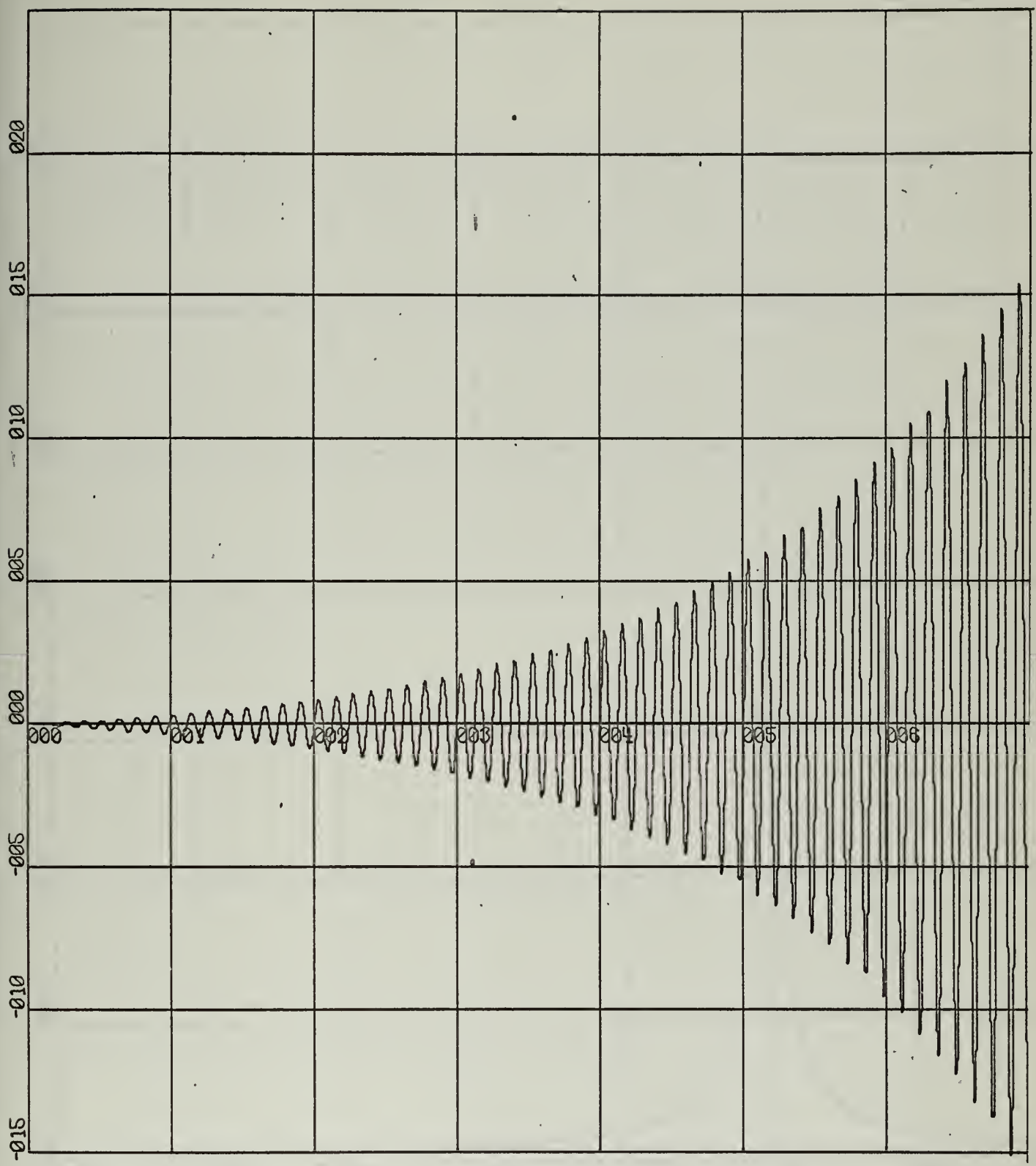


X-SCALE = 1.00E+00 UNITS/INCH.
Y-SCALE = 1.00E-01 UNITS/INCH.

NORMALIZED OUTPUT VS OMEGA (UNDERDAMPED)
RUN 1

FIGURE 4-5

As a further verification of this feature, if the capacity of the previously mentioned case becomes .0004 farad or one thousandth of that used for the system response demonstrated by Figure 4-5, one obtains a representative E_c vs time response as shown in Figure 4-6 for an input at resonance. The frequency response of this particular system is shown in Figure 4-7 where the sublimation of the d-c input compared to a frequency close to resonance is apparent. The need for a special negative device similar to that previously mentioned in Chapter Two is no longer needed and conventional feedback systems, tunnel diodes and the like can be used. It is this mode of operation which is exploited in normal superregeneration, where very high gains are possible at radio frequencies.

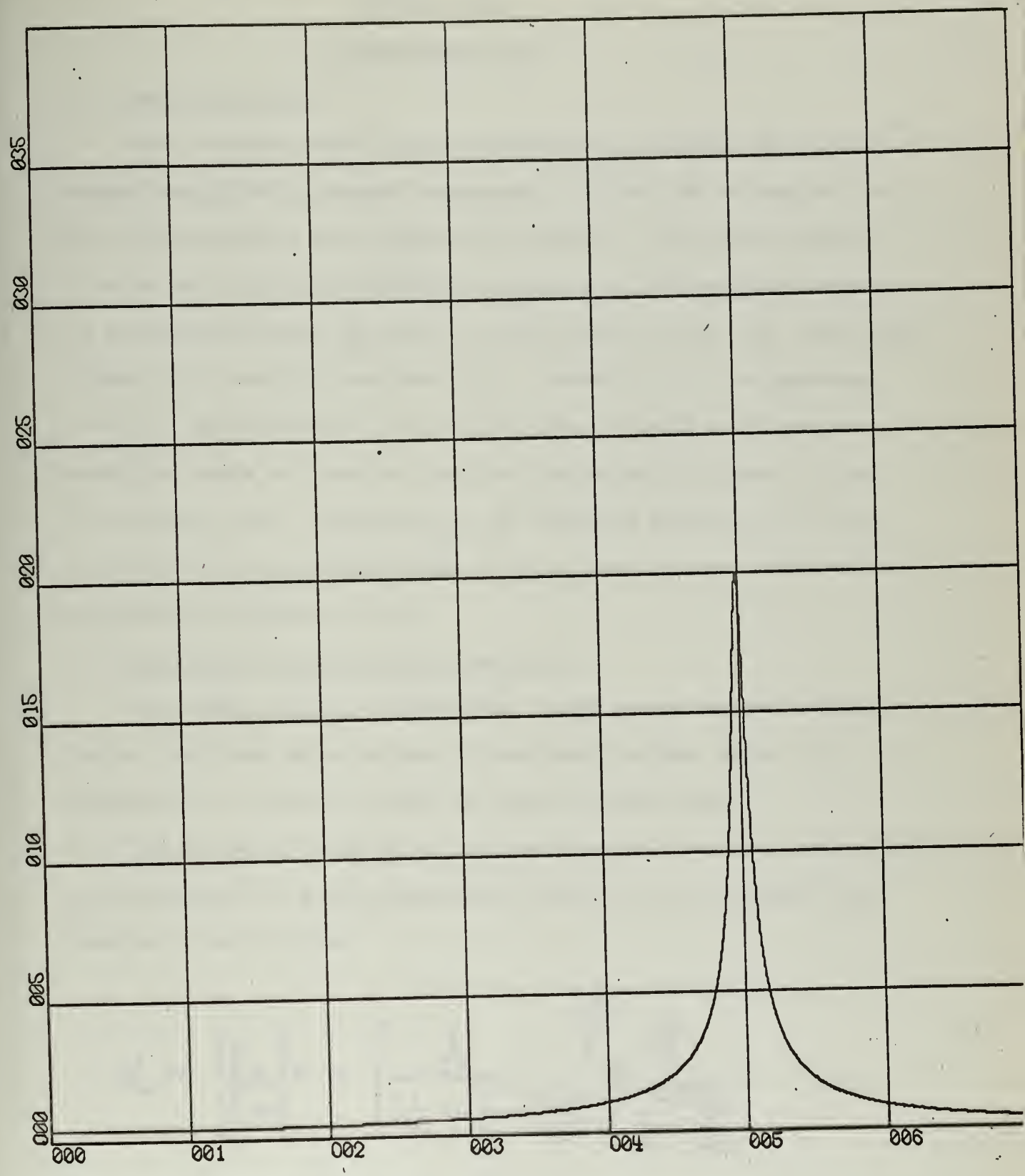


X-SCALE = 1.00E+00 UNITS/INCH.
Y-SCALE = 5.00E+02 UNITS/INCH.

OUTPUT VS TIME (UNDERDAMPED SYSTEM)

RUN 1

FIGURE 4-6



X-SCALE = 1.00E+01 UNITS/INCH.
Y-SCALE = 5.00E-03 UNITS/INCH.

NORMALIZED OUTPUT VS OMEGA

RUN 1

FIGURE 4-7



CHAPTER FIVE

Superregeneration

5.1 General Operation

With the second order system operating as an unstable periodically sampled amplifier at resonant frequencies well into the r-f region, one has the conventional Superregenerative amplifier. This form of amplification was originally patented by Armstrong (1) and has been analyzed in different ways over the years by such authors as Frink (9), Ataka (10), Riebman (11), Shaw (12) and Chang (13). Despite all of the advantages which the superregenerator has, such as being a stable very high gain amplifier, there are specific classical limitations which have limited its universal use. The majority of the remaining portions of this dissertation will be oriented towards analyzing some of these deficiencies and possible solutions of them.

5.2 Selectivity Vs Gain For The Linear Mode

The voltage gain of a second order system can be defined as the ratio of the peak output voltage to peak input voltage, where it is assumed that the output is under the control of the input.

This argument is similar to that used for the first order system and the voltage gain of a superregenerative amplifier can be obtained from Equation (4-9b) as being

$$K_v = \frac{|E_c|_p}{|E(t)|_p} = \left[\frac{\frac{1}{LC}}{\left(\frac{1}{LC}-\omega^2\right)^2 + \frac{R^2\omega^2}{L^2}}\right]^{1/2} \frac{e^{-\frac{R_I}{2L}}}{LC\sqrt{\frac{1}{LC}-\frac{R^2}{4L^2}}}, \qquad (5\text{-}1)$$

which is approximately for $\left(\frac{1}{LC} - \frac{R^2}{4L^2} >> 0\right)$.

$$K_V \doteq \frac{1}{LC}\left[\frac{1}{\left(\frac{1}{LC}-\omega^2\right)+4\alpha^2\omega^2}\right]e^{-\alpha\tau}, \quad \alpha=\frac{R}{2L}. \qquad (5\text{-}2)$$

The maximum gain that can be realized at resonance is approximately

$$K_{V_{MAX}} \doteq \frac{e^{-\alpha t}}{CR\omega_0}, \quad \omega_0^2=\frac{1}{LC}, \qquad (5\text{-}3)$$

and with Q defined as $\frac{\omega_0 L}{R}$ for a series system, equation (5-3) can be written as

$$K_{V_{MAX}} = Q e^{-\frac{\omega_0 t}{2Q}}. \qquad (5\text{-}4)$$

This expression reveals the dependency of maximum gain on the Q, L, C, sampling time and the resonant frequency of operation ω_0. If the input r-f frequency is amplitude modulated, it is normally required that the sampling frequency be over twice that of the highest modulated frequency to be recovered. With the linear system under the foremention restrictions, the maximum gain possible for a given ω_0 and a-m modulation frequency can be defined in terms of an optimun Q (therefore selectivity). Assuming a variable resistance characteristic that requires very little time to insure coherent operation and realizing by sampling theory that the switching period can be no longer than

$$t = \frac{1}{2f_m} \qquad (5\text{-}5)$$

where f_m is the highest modulating frequency under consideration,

equation (5-4) becomes

$$K_{V_{max}} \doteq Q e^{-\frac{\omega_o}{4Qf_m}} . \qquad (5\text{-}6)$$

To maximize this equation with respect to Q, the $\partial K/\partial Q$ is set to zero or

$$0 = \frac{1}{LC}\left[\frac{e^{-\frac{\omega_o}{4Qf_m}}}{\omega_o^2} + \frac{e^{-\frac{\omega_o}{4Qf_m}}}{4\omega_o f_m Q}\right] \qquad (5\text{-}7a)$$

or

$$|Q| = \frac{\pi f_o}{2 f_m} \text{, Q negative for } \alpha \text{ negative.} \qquad (5\text{-}7b)$$

This restriction has in addition another restriction that has to be adhered to, that is, the normal requirement that the static r-f bandwidth be sufficient to allow the sidebands to be present. To evaluate the bandwidth of the Q as defined in equation (5-7) and its effect on the sideband of an a-m signal, it can be shown that it is approximately π times too large if only a three db attenuation is to be allowed for the highest modulating frequency. This restriction now requires that Q should be approximately

$$|Q| \doteq \frac{f_o}{2 f_m} \quad \text{or} \quad \frac{\omega_o}{4\pi f_m} , \qquad (5\text{-}8)$$

and if this is substituted into equation (5-4), the maximum gain becomes

$$K_{V_{max}} \doteq \frac{\omega_o e^{+\omega_m \tau}}{4\pi f_m} , \qquad (5\text{-}9)$$

or utilyzing equation (5-5) can be written as

$$K_{V_{max}} \doteq \frac{f_o e^{+\pi}}{2 f_m} . \qquad (5\text{-}10)$$

This expression reveals the basic voltage gain limitation of a linear system for a given f_m and f_o with the output taken across the capacitor. This limitation is coupled with the fact that the system has a basic single tuned-circuit response that often does not give sufficient skirt selectivity for many communication systems.

To ascertain if there is a solution to this gain limitation, it was speculated that there might be some advantage to have a time-varying negative resistance during the regenerative cycle. Specifically, if a system was operated for a reasonably long time under the conditions where the maximum r-f selectivity commensurate with modulating frequency requirements were met, then allowed to become very regenerative ie., a rapidly increasing exponential term, possibly the gain limitation might be overcome. Phenomenologically, the system would be first operating at maximum desired selectivity but in an unstable operating mode, then allowed to become a very high gain system with its initial conditions being the output conditions of the high selective mode. Conceptually, a similar result could occur if the resistance was continuously increasing in instability instead of just suddenly changing value.

To verify this operating mode the selectivity curve of a linear system

defined mathematically by the following equation was computed by digital computer methods. This system is the same as used for Figure 4-7.

$$\cos\omega t = \frac{q}{.0604} - \frac{dq}{dt} + \frac{d^2q}{dt^2} \qquad (5\text{-}11)$$

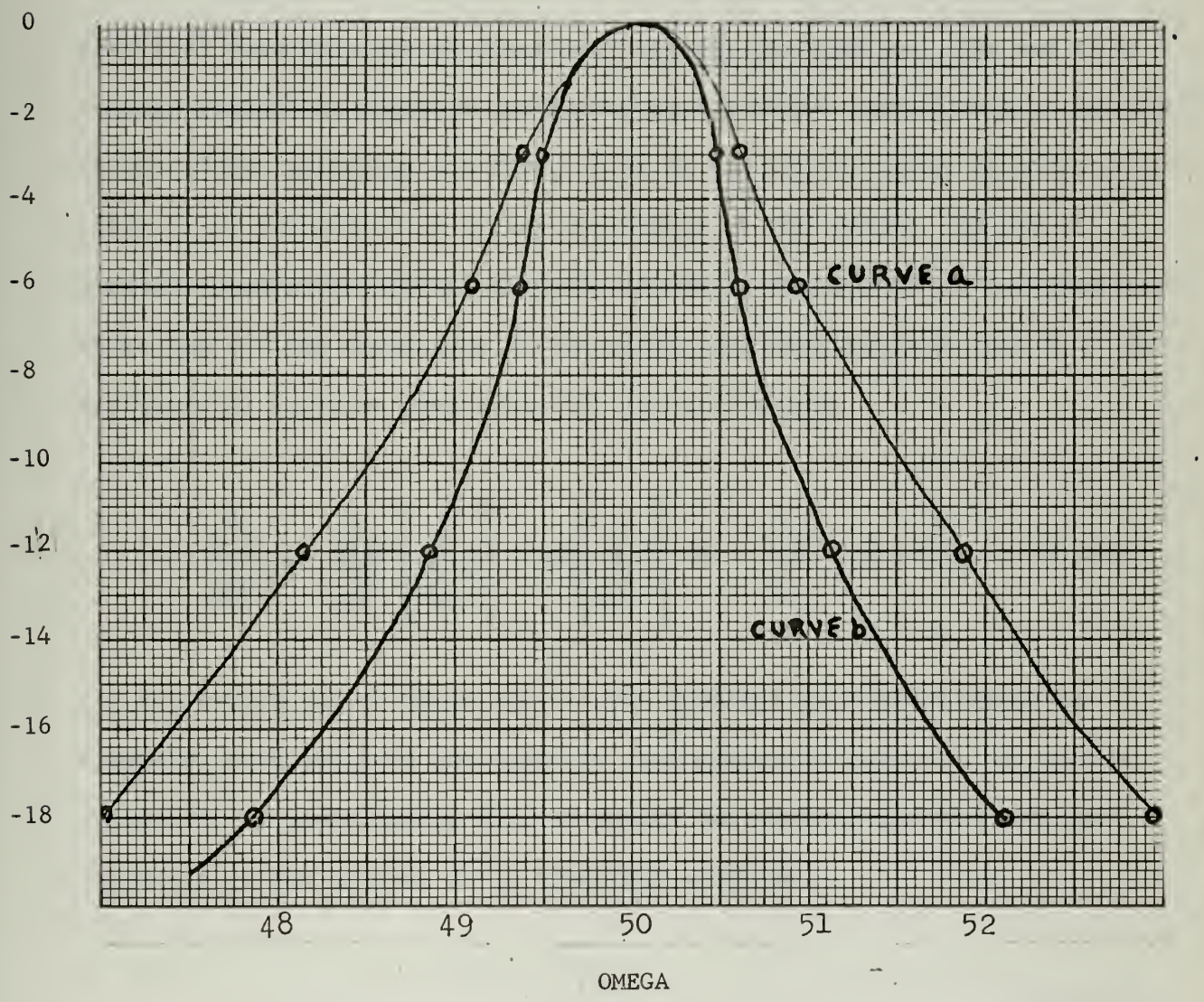
A regenerative time of 8 seconds was used and by plotting the peak output voltage for several different frequencies, curve a of Figure 5-1 was obtained. Next, the computer solution to the equation (5-12) was done in a similar fashion and is plotted as curve b in Figure 5-1.

$$\cos\omega t = \frac{q}{.0004} - .21t\frac{dq}{dt} + \frac{d^2q}{dt^2} \qquad (5\text{-}12)$$

It is noticed that this equation has a linearly increasing negative resistance and has had its parameters so chosen as to have the same gain and resonant frequency as the system described by equation (5-11), after eight seconds regenerative time. The increased selectivity of this time varying case over the linear case for identical gains and sampling time is another way of arriving at the potential of using a time varying regenerative cycle. The use of time controlled regeneration has not apparently been exploited in the past for superregeneration and should be considered. Experimental verification of this effect is done in Chapter Six. In addition the time varying selectivity curve no longer has the characteristics of an universal resonance curve. This fact has been appreciated and reported by Bradley (14) and Hazeltine etc. (15).

5.3 Parallel RLC System

Though the evaluation of a series RLC system has allowed a systematic



SELECTIVITY VS LINEARITY
FOR SECOND ORDER SYSTEM

FIGURE 5-1

evaluation of the potential advantages of superregeneration, it becomes analytically and operationally more advantageous to evaluate its parallel dual, that is a resistance, inductance and capacitance in parallel. One of the reasons for this is that it is nearly impossible to physically realize an inductance without its effective parallel capacity, therefore complicating the system analysis in a series RLC system along with the practical consideration of electronic circuit realization. The use of a voltage controlled negative resistance device adapts itself well to parallel tuned circuit operation and Figure 5-2a is the circuit under consideration where R_1 is the effective series resistance of the system. By use of Norton's equivalent circuit Figure 5-2a can be transformed into Figure 5-2b where now all the resistance of the system has been absorbed into R_t. The differential equation governing this circuit becomes

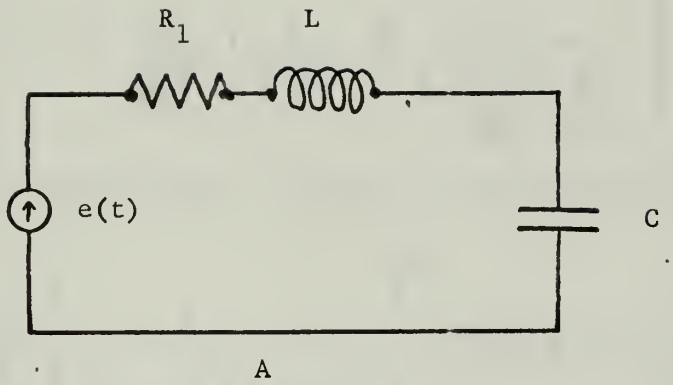
$$\frac{d^2e}{dt^2} + \frac{de}{dt}\left[\frac{1}{R_tC}\right] + e\left[\frac{1}{LC}\right] = \frac{L'(t)}{C}, \quad e = E_c \qquad (5\text{-}13)$$

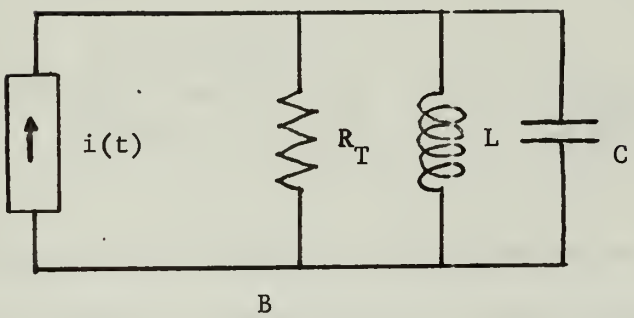
for any finite period where R(t) is the combined paralleled resistive elements, both positive and negative, and piecewise constant. E_c can be solved for by appreciating that it equals the current source times the impedence of the system, or in transform notation

$$E_c(s) = Z(s)\, I(s) \ , \qquad (5\text{-}14a)$$

where for $e(t) = E \sin \omega t$ transforms into

$$\mathcal{L}[I] = \mathcal{L}\left[\frac{E}{R_t} \sin \omega t\right] = \frac{E}{R_t}\left(\frac{\omega}{s^2+\omega^2}\right) \qquad (5\text{-}14b)$$





SECOND ORDER SYSTEM EQUIVALENTS

FIGURE 5-2



and

$$\mathcal{L}[Z] = \frac{sL}{1 + \frac{sL}{R_t} + s^2 LC} \tag{5-14c}$$

therefore

$$E_c(s) = \frac{E\omega}{R_t C}\left[\frac{1}{s^2+\omega^2} \circledast \frac{s}{s^2 + \frac{s}{R_T C} + \frac{1}{LC}}\right] \tag{5-14d}$$

whose Laplace inverse becomes, assuming no initial conditions,

$$E_c = \frac{E\omega}{R_t C}\left[\frac{1}{\left(\frac{1}{LC}-\omega^2\right)^2 + 4\alpha^2\omega^2}\right]^{1/2}\left[\sin(\omega\tau+\psi_1) + \frac{e^{-\alpha\tau}}{\beta\sqrt{LC}}\sin(\beta t+\psi_2)\right]$$

$$\psi_1 = -\tan^{-1}\frac{2\alpha\omega}{\alpha^2+\beta^2-\omega^2} + 90^\circ \quad , \quad \psi_2 = \tan^{-1}\frac{\beta}{-\alpha} - \tan^{-1}\frac{-2\alpha\beta}{\alpha^2-\beta^2+\omega^2} \tag{5-15}$$

$$\beta = \sqrt{\frac{1}{LC} - \alpha^2} \quad , \quad \alpha = \frac{1}{2R_T C} \; .$$

The similarity of the equation to equation (4-9b) is apparent, the major difference being the definition of α which now involves capacitance instead of inductance. As before, only the second portion of equation (5-15) is of consequence when $\alpha t \ll 0$. The conceptual amplification and selectivity features of this system are the same as for the series RLC system.

5.4 Non Linear Second Order Operation

Like the first order system, the nonlinear behavior of the second

order warrants investigation. The general nonlinear model to be assumed will be the same one as chosen for the first order system, that is a voltage controlled resistive device and with a general I vs E behavior as shown in Figure 3-3a. If the system is biased in the negative resistance portion of the transfer curve, it is intutitively reasonable to expect a containment of the envelope of the oscillations to some saturation value, the envelope similar to that obtained in the development of the first order nonlinear system. The particular analytical approach which gives direct insight to this behavior is one that is similar to the Kryloff and Bogoluoloff (KB) method (16) (17) which will allow the evaluation of the envelope of the contained oscillations for the general equation

$$\frac{d^2x}{dt^2} + uf\left(x, \frac{dx}{dt}\right) + \omega^2 x = 0 \qquad (5\text{-}16)$$

for the condition that u is well behaved. Under the transformation that

$$x = E_c = e \qquad (5\text{-}17a)$$

$$uf\left(x, \frac{dx}{dt}\right) = \left[\frac{1}{C R_T(e)}\right] \frac{de}{dt} \qquad (5\text{-}17b)$$

$$\omega^2 = \frac{1}{LC} \qquad (5\text{-}17c)$$

equation (5-16) becomes the complementary equation to equation (5-13), appreciating that when equation (5-17b) is written as

$$\frac{de}{dt}\left[\frac{1}{C R_T(e)}\right] = \frac{1}{C}\left[K + Me^2\right]\frac{de}{dt} \qquad (5\text{-}18)$$

that the quantity $1/K+Me^2$ would be the effective parallel resistance and is a reasonable model for a voltage controlled device when K is negative

and $-1 < M/K < 0$. The KB approximation argues that the solution to equation (5-16) is

$$e = a\sin(\omega t + \phi), \tag{5-19a}$$

$$\frac{de}{dt} = \omega a \cos(\omega t + \phi) \tag{5-19b}$$

when $u = 0$, where a and ϕ are determined by initial conditions. Now a solution to equation (5-16) is desired that preserves the form of equations (5-19a and b) but now with a and ϕ functions of time, therefore a solution to equation (5-16) is of the form

$$e = a(t)\sin(\omega t + \phi(t)) . \tag{5-20}$$

If this is differentiated, it becomes

$$\frac{de}{dt} = a\omega\cos(\omega t+\phi) + \frac{da}{dt}\sin(\omega t+\phi) + a\frac{d\phi}{dt}\cos(\omega t+\phi). \tag{5-21}$$

But for equation (5-21) to retain the form of equation (5-19b), the last two terms must be equal to zero or

$$\frac{da}{dt}\sin(\omega t+\phi) = -a\frac{d\phi}{dt}\cos(\omega t+\phi) \tag{5-22}$$

and differentiating, equation (5-19) again results in

$$\frac{d^2e}{dt^2} = -\omega^2 a\sin(\omega t+\phi) + \omega\frac{da}{dt}\cos(\omega t+\phi) - \omega a\phi\sin(\omega t+\phi). \tag{5-23}$$

This equation when substituted into equation (5-16) with the notation $\theta = \omega t + \phi$ gives

$$w\frac{da}{dt}\cos\theta = -wa\frac{d\phi}{dt}\sin\theta = u f\left[a\sin\theta, wa\cos\theta\right]. \quad (5\text{-}24)$$

Now equations (5-22) and (5-24) can be written as

$$\frac{da}{dt}\sin\theta + a\frac{d\phi}{dt}\cos\theta = 0 \ , \quad (5\text{-}25a)$$

$$\frac{da}{dt}\cos\theta - a\frac{d\phi}{dt}\sin\theta = -\frac{u}{w} f\left[a\sin\theta, wa\cos\theta\right], \quad (5\text{-}25b)$$

which when solved for da/dt and dØ/dt becomes

$$\frac{da}{dt} = -\frac{u}{w} f\left[a\sin\theta, wa\cos\theta\right]\cos\theta, \quad (5\text{-}26a)$$

$$\frac{d\phi}{dt} = \frac{u}{wa} f\left[a\sin\theta, wa\cos\theta\right]\sin\theta. \quad (5\text{-}26b)$$

Now if the degree of nonlinearity is slight, a(t), Ø(t) are <u>slowly</u> varying functions of time and in time $2\pi/w$, $\theta \doteq wt + \phi$ will increase by approximately 2π , and <u>a</u> and ϕ not changed appreciably. For conventional superregenerators, this has proven a valid approximation. If the right hand parts of equation (5-26) are replaced by the <u>average</u> values over a range and <u>a</u> is considered constant over the period, then equations (5-26a, b) become

$$\frac{da}{dt} \doteq \frac{-u}{2\pi w}\int_0^{2\pi} f(a\sin\theta, wa\cos\theta)\cos\theta \, d\theta \quad (5\text{-}27a)$$

$$\frac{d\phi}{dt} \doteq \frac{u}{2\pi wa} \int_0^{2\pi} f(a\sin\theta, wa\cos\theta)\sin\theta\, d\theta. \qquad (5\text{-}27b)$$

Since it is a(t) that is of particular interest here it will be calculated for the model assumed for $uf(x, \frac{dx}{dt})$ which was

$$\frac{K}{C}\frac{de}{dt} + \frac{M}{C}e^2\frac{de}{dt}, \qquad (5\text{-}28)$$

where $uf(x, \frac{dx}{dt}) = uf(a\sin\theta, wa\cos\theta)$ and results in $uf(x, \frac{dx}{dt})$ being equal to

$$\frac{K}{C}wa\cos\theta + \frac{M}{C}wa^3\cos\theta\sin^2\theta \qquad (5\text{-}29)$$

and therefore

$$\frac{da}{dt} = \frac{-1}{2\pi wC}\left[+K\int_0^{2\pi} wa\cos^2\theta\, d\theta + M\int_0^{2\pi} wa^3\sin\theta\cos^2\theta\, d\theta\right] \qquad (5\text{-}30)$$

which when integrated becomes

$$\frac{da}{dt} = \frac{-a}{2C}\left[K + \frac{Ma^2}{4}\right]. \qquad (5\text{-}31)$$

Now when equation (5-31) is integrated, it becomes

$$\frac{1}{2K} \ln \frac{a^2}{K+\frac{Ma^2}{4}} = -2Ct + \text{constant} \tag{5-32a}$$

or

$$\ln \left[\frac{a^2}{K+\frac{Ma^2}{4}} \right] = -4KCt + \text{constant} \tag{5-32b}$$

or

$$\frac{a^2}{K+\frac{Ma^2}{4}} = k e^{-4KCt}, \quad k \text{ a constant}, \tag{5-32c}$$

where again it is remembered that K is negative and M is positive and $|K| > |L|$. If now it is stipulated that $a = a_o$ when $t = 0$ for an initial condition, equation (5-32c) becomes

$$\frac{a^2}{K+\frac{Ma^2}{4}} = \frac{a_o^2}{K+\frac{Ma_o^2}{4}} e^{-4KCt} \tag{5-33}$$

when $t \to \infty$ the right hand side of the equation approaches infinity, which is met by the left side of the equation when

$$K = \frac{Ma^2}{4} \tag{5-34a}$$

or

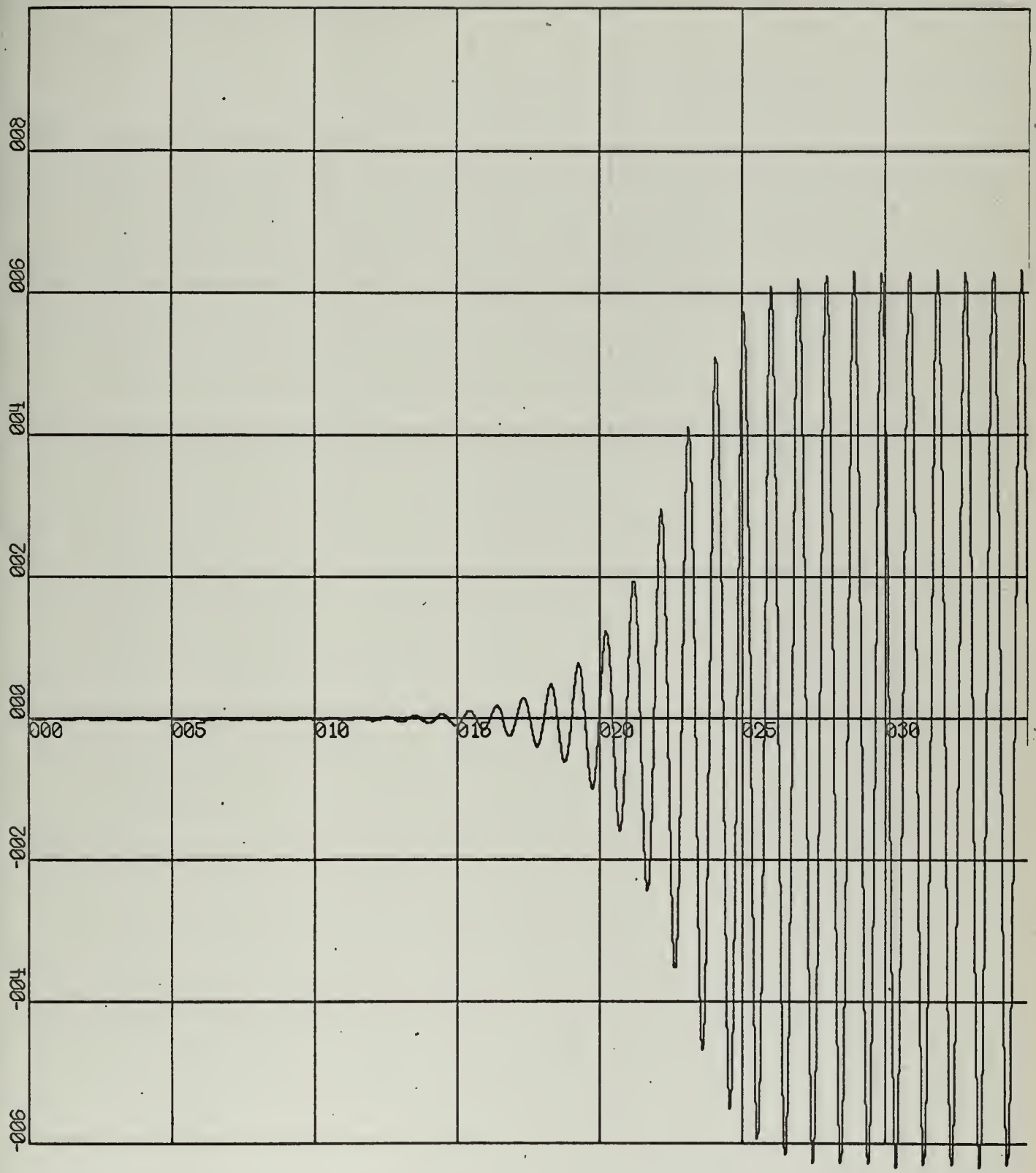
$$a = 2\sqrt{\frac{|K|}{|M|}} \tag{5-34b}$$

where now the term a(t) of equation (5-16) never exceeds the value shown

in equation (5-34a). It is noted that as the order of nonlinearity is decreased, that is, the ratio of $|K/M|$ is larger, the maximum peak value is also increased as would be expected by physical reasoning. To appreciate the fact that this form of analytical approach is appropriate, Figure 5-3 is a plot of a(t) sin(6.5t) for values of K = - 1, M = 0.1, C = 1, farad, utiliyzing equation (5-31), where the trignometric term sin(6.5t) was used as a modulating factor so that comparison with Figure 5-4 could be done. Figure 5-4 is a computer solution to equation (5-13) with similar parameters and a input source value so chosen to have the envelope essentially agree with that represented by Figure 5-3. The agreement of their envelopes justifies the KB approximation and the envelope similarity to that experimentally demonstrated by the first order system (Figure 3-6c) validates the resistive model.

5.5 Conventional Superregeneration With Modulated Resistance.

If a conventional linear superregenerative amplifier is allowed to operate under high gain conditions, the noise of the system will trigger the system so that random pulses of oscillations will occur, similar to that shown in Figure 3-5c for the first order system except it contains a high frequency oscillation. Following the argument as mentioned in Section 2-1 and experimentally demonstrated for the first order system in Figure 3-8d, it is reasonable to expect that if the resistance of the system was modulated at a frequency much lower than the sampling frequency, it is expected that this low frequency permutation would show up as a modulation on the output of the triggered pulses. This gives rise to the possibility of amplification of a-f frequencies without the need of a special negative resistance device, overcoming a limitation of the first order system. This mode of operation will be demonstrated in Chapter Six.

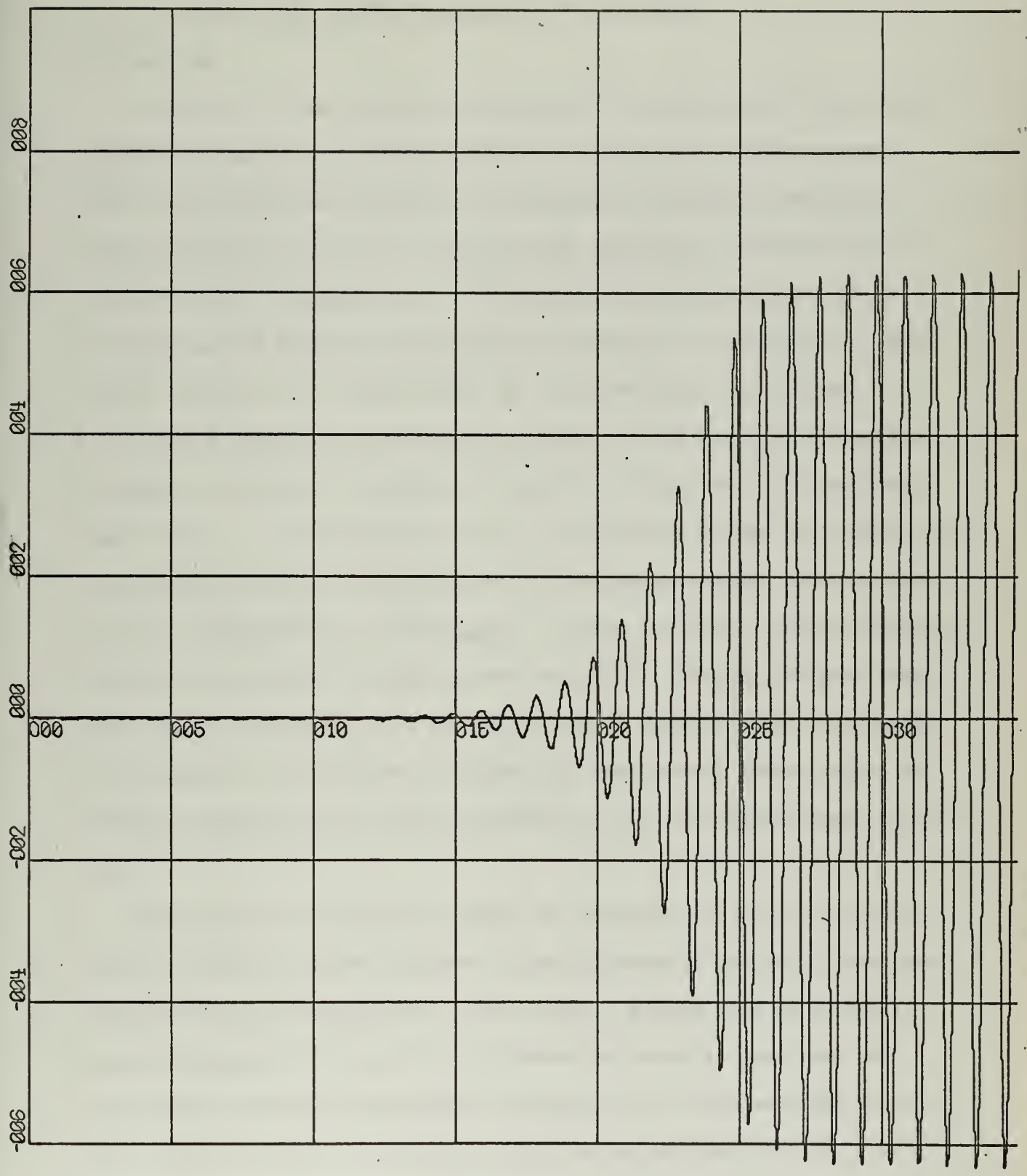


X-SCALE = 5.00E+00 UNITS/INCH.
Y-SCALE = 2.00E+00 UNITS/INCH.

ALPHA VS TIME (NONLINEAR)

RUN 1

FIGURE 5-3



X-SCALE = 5.00E+00 UNITS/INCH.
Y-SCALE = 2.00E+00 UNITS/INCH.

VOLTAGE VS TIME (NONLINEAR)

RUN 1

FIGURE 5-4

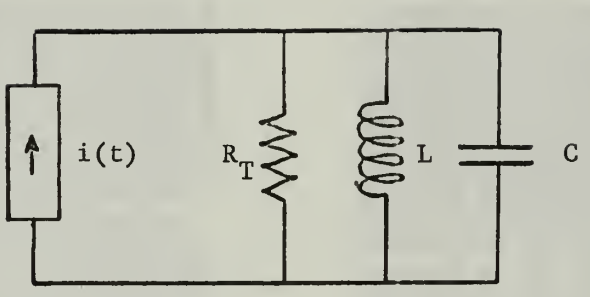
CHAPTER SIX

Second Order System Experimental Verification

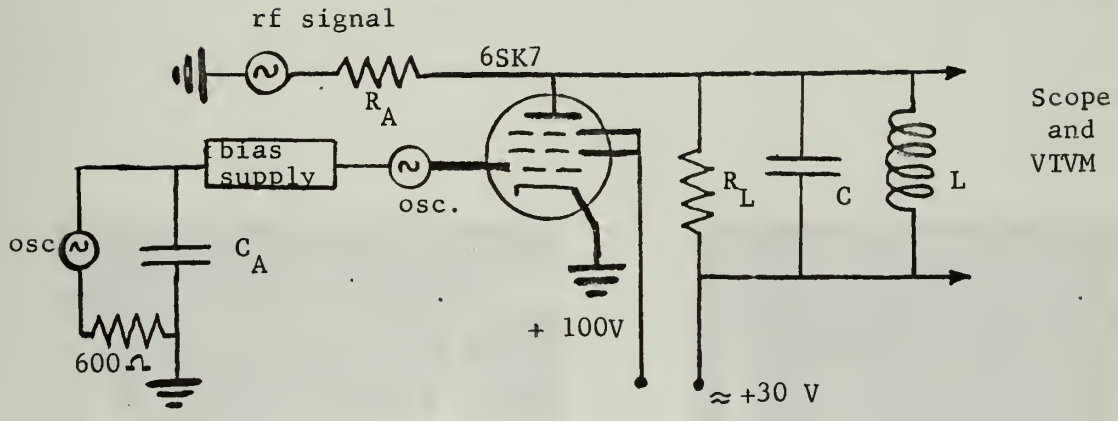
6.1 General

In order to allow controlled experimental verification of the superregeneration amplifier, the basic dynatron configuration used for the first order system was used with the addition of a parallel inductor, where equation (5-13) is the representative expression. Figure 6-1a is a typical electrical equivalent of the expression while Figure 6-1b is the experimental setup for evaluating the behavior of this circuit. With typical values of R_1 = 10,000 ohms, Ra = 100,000 ohms, C = 500 pfd. L = 1. mh, a switching (quenching) oscillator at 250 cps with a capacitor C_A across its output, an oscillator at 30 cps for use as a low frequency signal input, a dc bias supply, and a r-f oscillator to use for selectivity measurements; all the derived analytical considerations for the last chapter can be experimentally investigated. Unlike the first order experimental conditions, the periodic sampling here is done by changing the grid bias, therefore the effective value of the dynatron's dynamic plate resistance. This change was made in order to allow the experimental demonstration of improved gain/selectivity characteristics for the time varied regenerative cycle.

Experimental evaluation was begun by observing the behavior of the output voltage (E_c) under different superregenerative operating conditions with system noise serving as an input source. Figure 6-2a is an oscilloscope photograph of E_c vs time for about one cycle of quenching frequency, where the near exponential rise and decay of the envelope is evident. The input level was adjusted here for nonsaturation of the system and therefore comes under the definition of a linear mode. This same



A

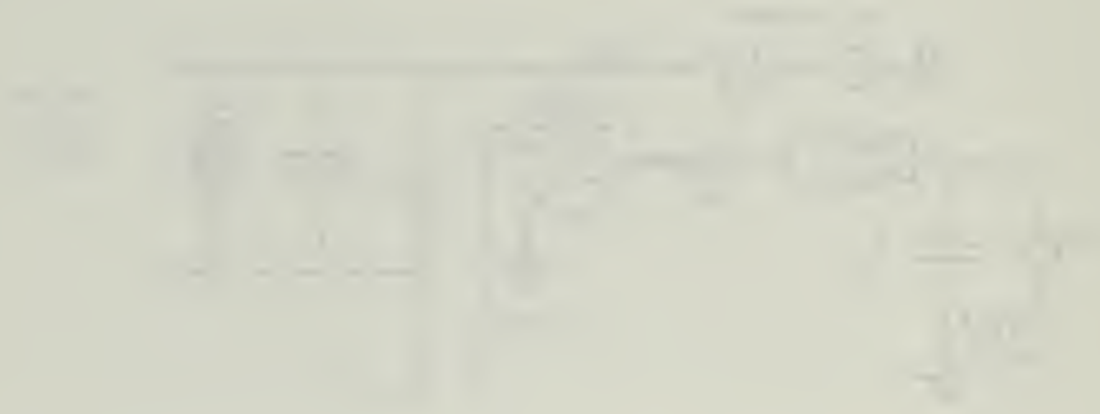


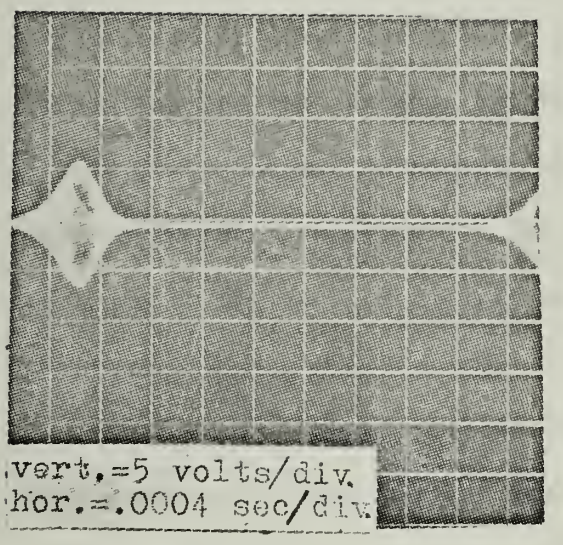
B

SECOND ORDER SYSTEM CIRCUITRY

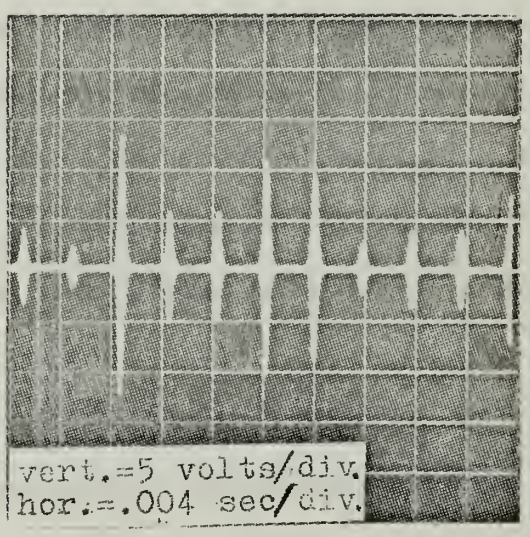
FIGURE 6-1



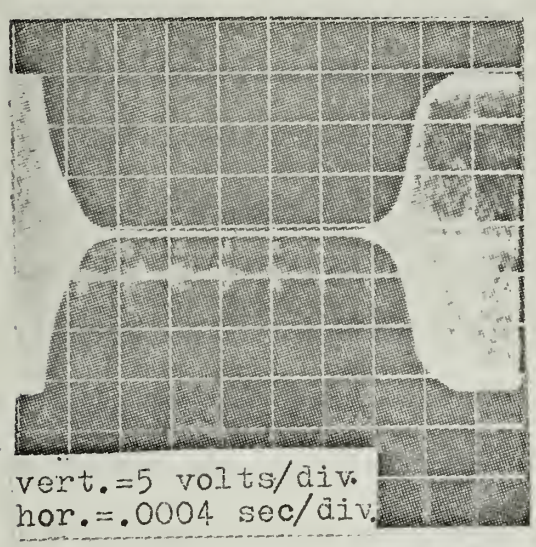




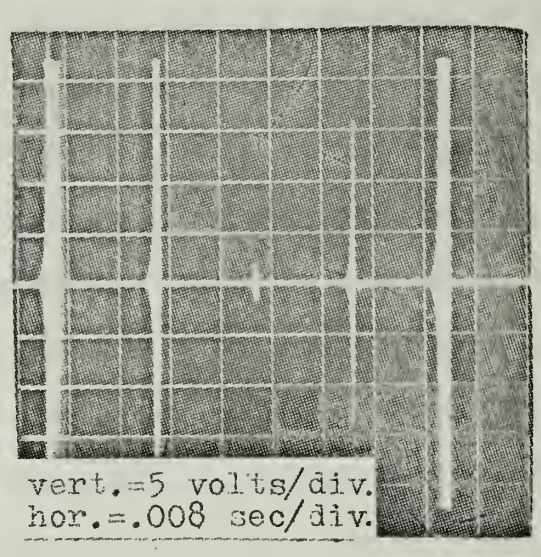
A



B



C



D

TYPICAL ENVELOPE WAVEFORMS FOR LINEAR AND NONLINEAR MODES, SECOND ORDER SYSTEM

FIGURE 6-2

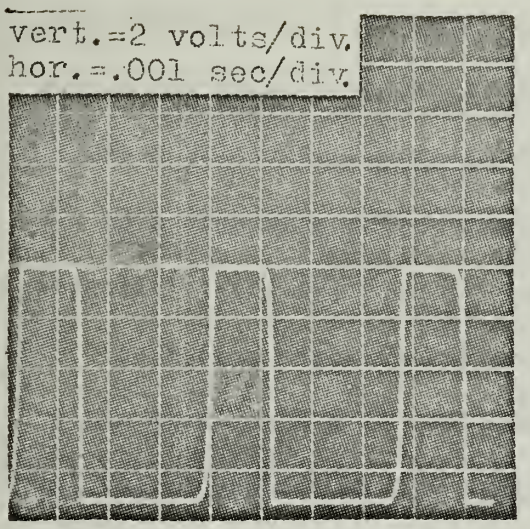




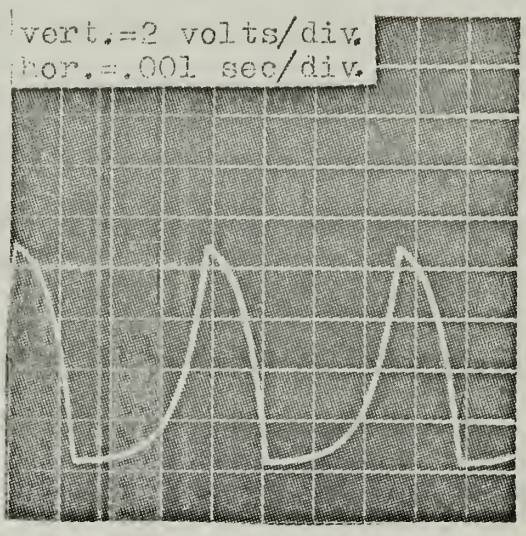


operating condition with the time scale slowed down by a factor of ten is shown in Figure 6-2b where the random heights caused by noise triggering is apparent, Figure 6-2c is similar to Figure 6-2a except the time of the regenerative cycle was increased until saturation occurred. Finally Figure 6-2d is representative of the system adjusted so that the random triggering has the envelope heights sometimes saturated and sometimes at a very low value and is typical of the mode of operation of many operational superregenerative receivers. The contained rf oscillations do not show here due to the lack of definition of the oscilloscope and the time scale chosen.

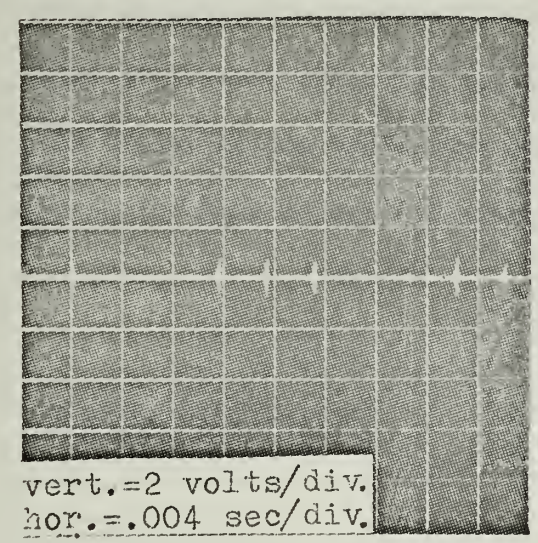
Next to be investigated was the selectivity vs gain characteristics as a function of time varying resistive parameters in the regenerative cycle, analytically discussed and computer verified in Chapter Five. The experimental procedure was to obtain a selectivity curve for both the linear and time varying regenerative cycles, maintaining identical resonant frequency gains. By appreciating the fact that the negative resistance of the dynatron increases with increase grid bias, it can be seen that if the time constant across the quenching square wave oscillator is increased considerably and the fixed bias adjusted so the resonance frequency gain remains the same, an experimental condition exists which conceptually agrees with that discussed in Section 5-2. Figure 6-3a shows a few cycles of grid voltage for the linear mode where the generator is switching between about a negative nine volts and zero volts. Figure 6-3b is this grid voltage now for the time varying case where C_a has been increased from .07 to .7 ufd, the .07 ufd capacitor was necessary for the near linear case to prevent ringing of the tuned circuit. For the parameters chosen, the effective period of regeneration is approximately the same except for the time variation. Though it was difficult to accurately calculate the resistive values



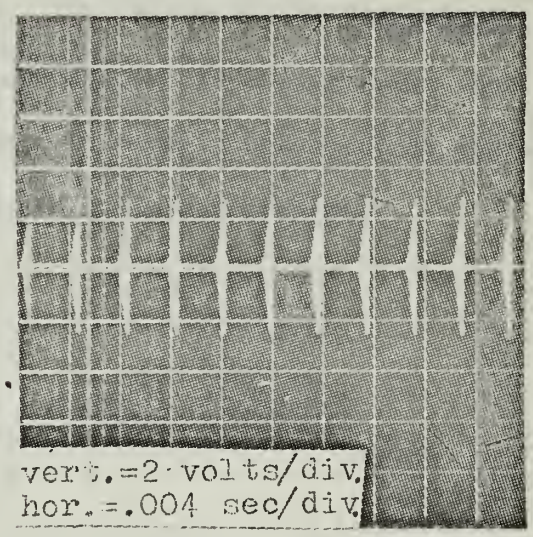
A



B



C



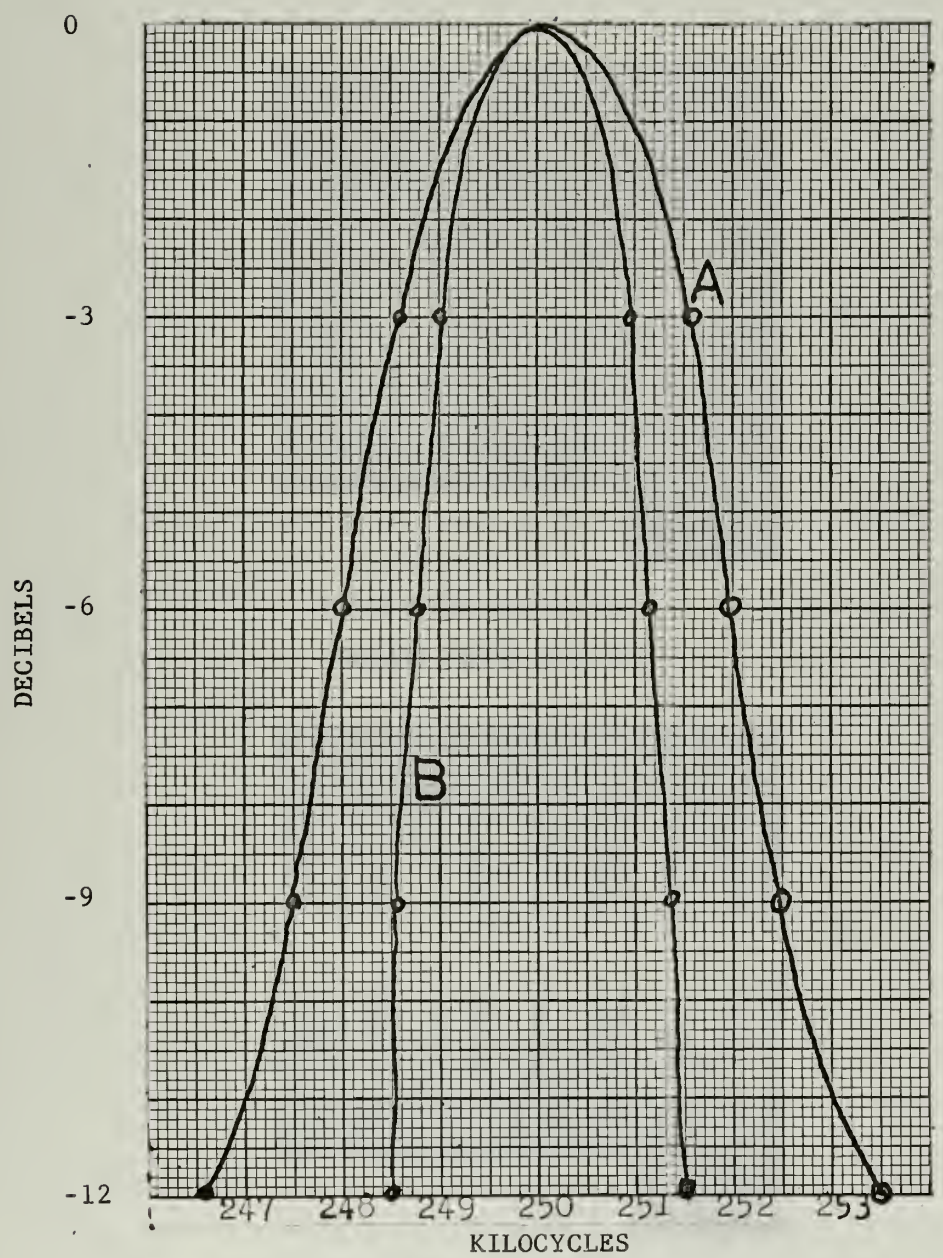
D

GRID AND PLATE WAVEFORMS OBSERVED
DURING SELECTIVITY MEASUREMENTS

FIGURE 6-3

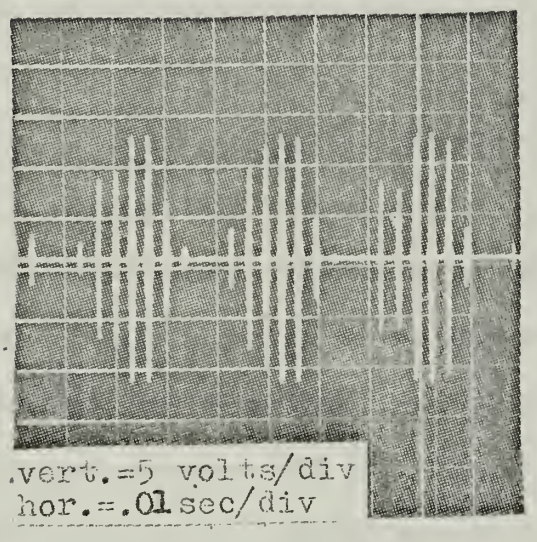
for this case, by plotting the two resulting selectivity curves, the pronounced change in selectivity could be observed and the qualitative effects observed. Since a peak reading meter was used for relative measurements, monitoring of the waveforms during the measurements, was done to insure no saturation occurred. Figure 6-3c is representative of how the pulse trains look for an input signal off resonance while Figure 6-3d is representative for a resonance condition. Finally Figure 6-4 is a composite of the two resulting selectivity curves, the increased selectivity for the time varying case (curve b) being quite apparent.

As a final experimental evaluation, a .1 volt, 30 cps input signal to the dynatron's grid was observed with Figure 6-5a showing the resulting modulation on the output with about a 30 db voltage gain being demonstrated. A similar result was had when a carbon microphone was placed in series with R_1 and tone modulated. Typical of the type of oscilloscope presentation for linear superregeneration without the presence of signal is shown in Figure 6-5b where the trace period allows many pulses to be observed in sequence. The randomness of the output, similar to that shown for the first order system, is apparent and when the output of the system was demodulated and aurally observed the characteristics hiss associated with superregeneration was present.



FREQUENCY RESPONSE CURVES FOR LINEAR AND TIME VARYING REGENERATIVE CYCLE, SECOND ORDER SYSTEM

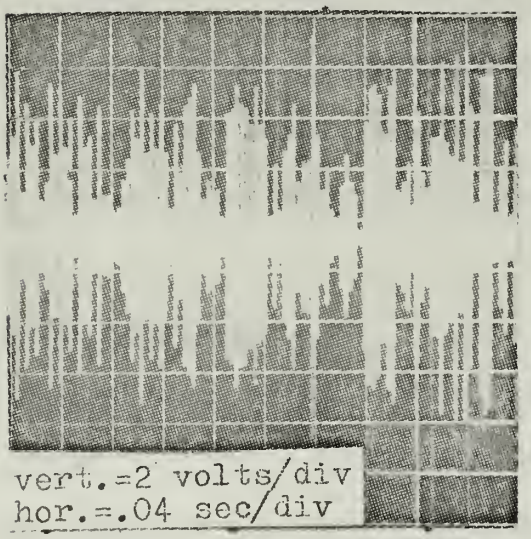
FIGURE 6-4



A

RESISTANCE MODULATED

SECOND ORDER SYSTEM



B

RANDOMNESS OF OUTPUT FOR

LINEAR SUPERREGENERATOR

FIGURE 6-5

CHAPTER SEVEN

Superregenerative Noise

7.1 General

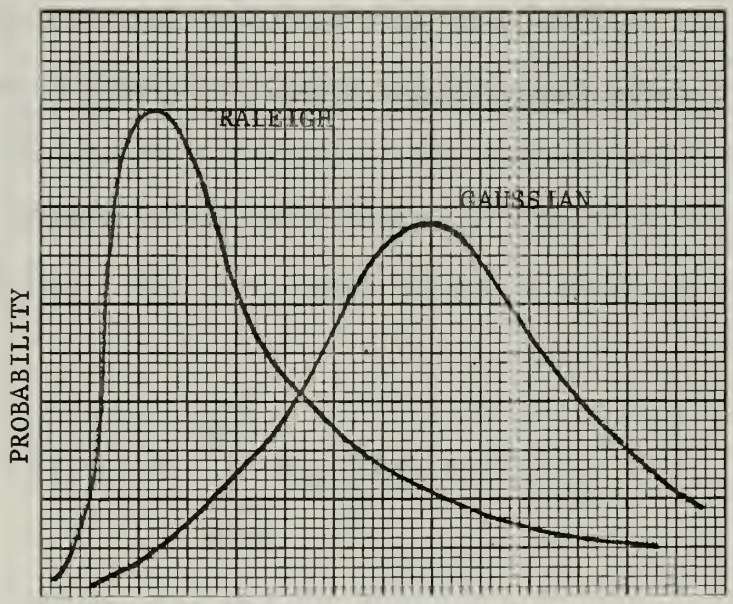
When a linear superregenerative amplifier is allowed to be triggered spontaneously by noise during the period of negative conductance, a randomness of heights of the pulse train occurs. It is this fluctuation that determines the character of the hiss in a superregenerative amplifier, therefore an analysis of its statistical nature will give insight into the noise spectrum and possible methods that could allow for a solution to one of the main disadvantages of commercial superregeneration: - the presence of an objectional hiss-like noise when no input signal is present. The commercial desirability of such a device is evident by the many techniques which have been patented (18) (19) (20) but apparently none were found commercially exploitable. Normal squelch control systems such as the reliance on a change of some parameter voltage with the presence of an input signal have apparently proven unsatisfactory for amplitude modulated r-f signals due to circuit complexity and unreliability. The one form that was commercially produced, which did happen to use the superregenerative hiss as a form of control signal, also proved quite complex in form (20).

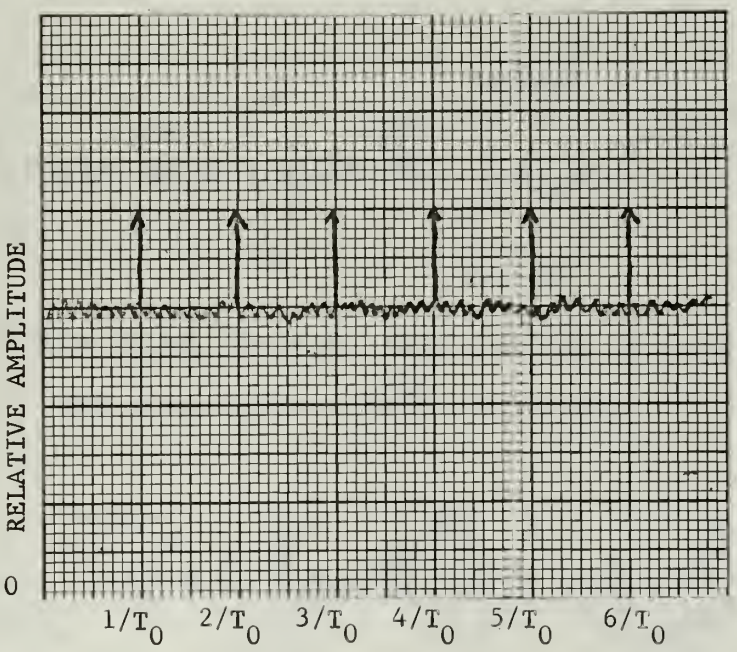
7.2 Theoretical Considerations.

In the mathematical model of the superregenerative amplifier developed in Chapter Five, there was shown a current source (Figure 5-2b). The output of this current generator will now be considered as noise energy and analyzed. This noise energy, which has as its origin such devices as shot effect, partition effect, flicker effect and thermal effect, can be considered white noise Gaussian distributed and stationary up to a frequency

dependent on the transit time of the device and is an instrument of current control (here the space charge configured vacuum tube). Though it is true that some of the above mentioned noise sources have some frequency dependency, at conventional superregenerative operating frequencies they are quite broadband in response. The discussion of these noise models has been throughly discussed and evaluated by such authors as Davenport and Root (21), Lawson and Uhlenbeck (22), Rice (23), and Schwartz (24). A typical value of the rms voltage of modern devices will be in the order of microvolts. Previously, the development of the gain and selectivity models was done assuming driving signals that were large compared to the active element's noises. This was done in order to get an understanding of the fundamental mechanisms involved in amplification. In this section, the physical problem is to decide on the statistical variations of the heights of the individual pulses under the influence of noise energy, where as before, the assumption will be that the history and influence of the noise source before the time of the oscillatory state will not appreciably influence the operation of the excitation of the exponential build up that will take place.

The probability distribution of the envelope heights of such noise through a narrow band filter has been discussed by Rice (25) and Middleton (26), who have shown that it to be Raleigh distributed for random noise input, becoming Gaussian in distribution with decreasing variance as a superimposed sinusoidal input level is increased. The fact that the system is sampling at a high repetition frequency should not affect this basic distribution effect though of course in the frequency domain it will add harmonically related components. Figure 7-1a graphically represents these two distributions. This speculation on the distribution behavior will be experimentally verified in the next chapter where the distribution of the





PROBABILITY DISTRIBUTION AND FREQUENCY SPECTRUM OF NOISE FOR THE SUPERREGENERATIVE AMPLIFIER

FIGURE 7-1

noise pulses will be evaluated for two different levels of input signal.

7.3 The Power Spectrum Of The Characteristic Hiss.

The last section discussed the amplitude distribution of the envelope of the superregenerative pulse train. In this section, the development of the frequency spectrum, resulting from this envelope fluctations will be done in a manner similar to Lawson and Uhlenbeck (27). It was speculated that pure random noise activation of the radio frequency pulse trains with incoherency between pulses would result in a Rayleigh distributed, stationary set of pulses. The time domain of such a series of pulses can be stated as

$$h(t) = \sum_{M=0}^{\infty} a_m f(t - n T_o) \,, \tag{7-1}$$

where T_o is the quench period, a_m the amplitude of the nth pulse which is Rayleigh (or any other) distributed. From the Fourier Transform F(f) equals

$$F(f) = \int_{-\infty}^{\infty} h(t) e^{-j\omega t} dt = \int_{-\infty}^{\infty} f(\tau) e^{-j\omega\tau} dt \sum_{n=-N}^{n=+N} a_n e^{-j\omega N T_o} \tag{7-2}$$

and when N becomes large, there are approximately 2N pulses involved in the summation. The power spectrum $\overline{G(f)}$ now becomes

$$\lim_{N\to\infty} \frac{2}{2NT_o} \overline{|F(f)|^2} = \frac{2}{T_o} \left\{ \left| \int_{-\infty}^{\infty} f(\tau) e^{-j\omega t} dt \right|^2 \right\} \left\{ \left[\overline{a^2} - (\bar{a})^2 \right] \frac{+(\bar{a})^2}{2N+1} \left| \sum_{-N}^{N} e^{-j\omega N T_o} \right|^2 \right\}_{N\to\infty} \tag{7-3}$$

which again can be simplified to:

$$\frac{2}{T_o}\left\{\left|\int_{-\infty}^{\infty} f(t)e^{-j\omega\tau}dt\right|^2\right\}\left\{\left[\bar{a}^2-(\bar{a})^2\right]+\frac{(\bar{a})^2}{T_o}\sum_{n=0}^{\infty}\left\{\delta\left(f-\frac{n}{T_o}\right)\right\}\right\}, \quad \delta \text{ a Dirac function} \tag{7-4}$$

which is a composite of a series of Dirac functions at n/T_o plus a continuous spectrum determined in total intensity by

$$\left[\bar{a}^2-(\bar{a})^2\right], \tag{7-5}$$

both terms having the envelope multiplication factor of

$$\left[\int_{-\infty}^{\infty} f(t)\,e^{-j\omega\tau}dt\right]^2 \tag{7-6}$$

which is just the power spectrum of one pulse train. As signal is added to the system, the distribution tends towards a Gaussian distribution with the variance decreasing as signal input is increased thereby reducing the noise in the system.

The linearity detected audio portion of such an envelope will give a series of outputs of nf_o spacing where f_o is the quench frequency to which has been added a broad band noise limited in frequency only by the original limitations and the bandwidth of the amplifier. For the investigation of this noise in the audio spectrum, considered here to be the band of frequencies below fifty kilocycles when the radio frequency tuned circuit is in the megacycles, the bandwidth of the unit will normally be broad enough to offer no limitation to the noise output in the forementioned region.

Figure (7-1b) is the expected spectrum of the superregenerator for the above conditions.

For the vast majority of superregenerative circuits the quenching frequency is made sufficiently high to either be filtered out or be above human hearing, the remaining broadband noise (within bandwidth limitations of the tuned circuit during regeneration)appears as a hiss similar to a rapidly rolling snare drum, a feature used by at least one electronic organ manufacturer. With an incoming signal, the hiss will disappear with no basic change to its audio frequency structure.

CHAPTER EIGHT

Experimental Verification Of Noise Behavior

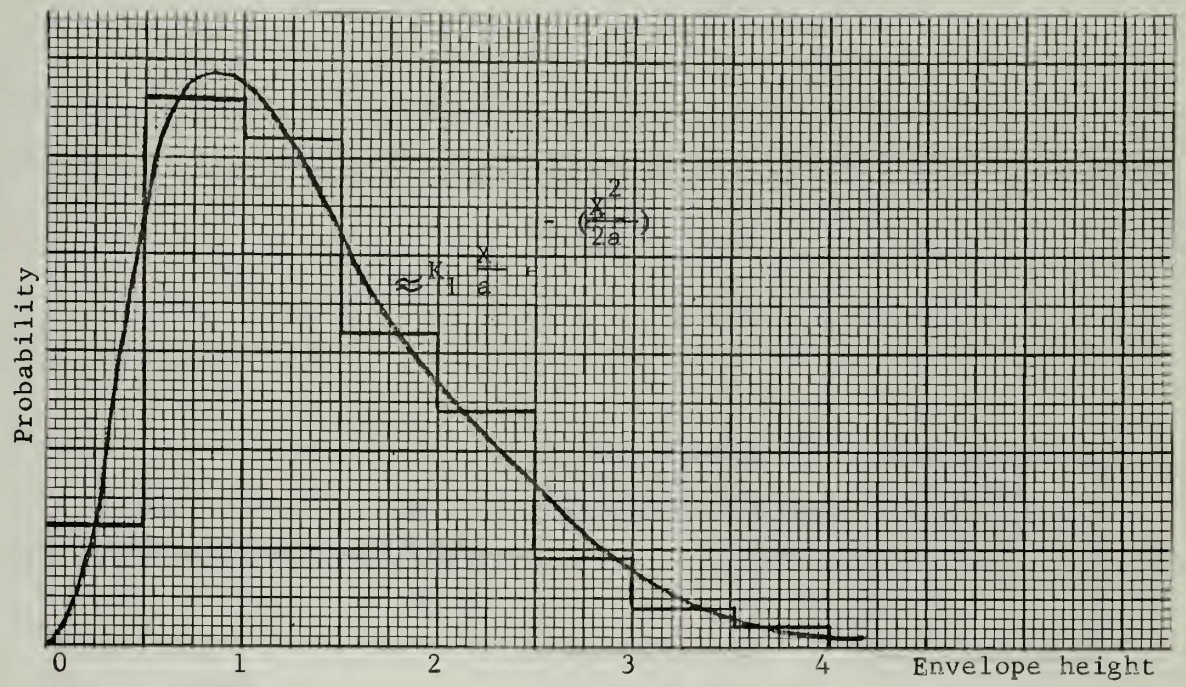
8.1 General

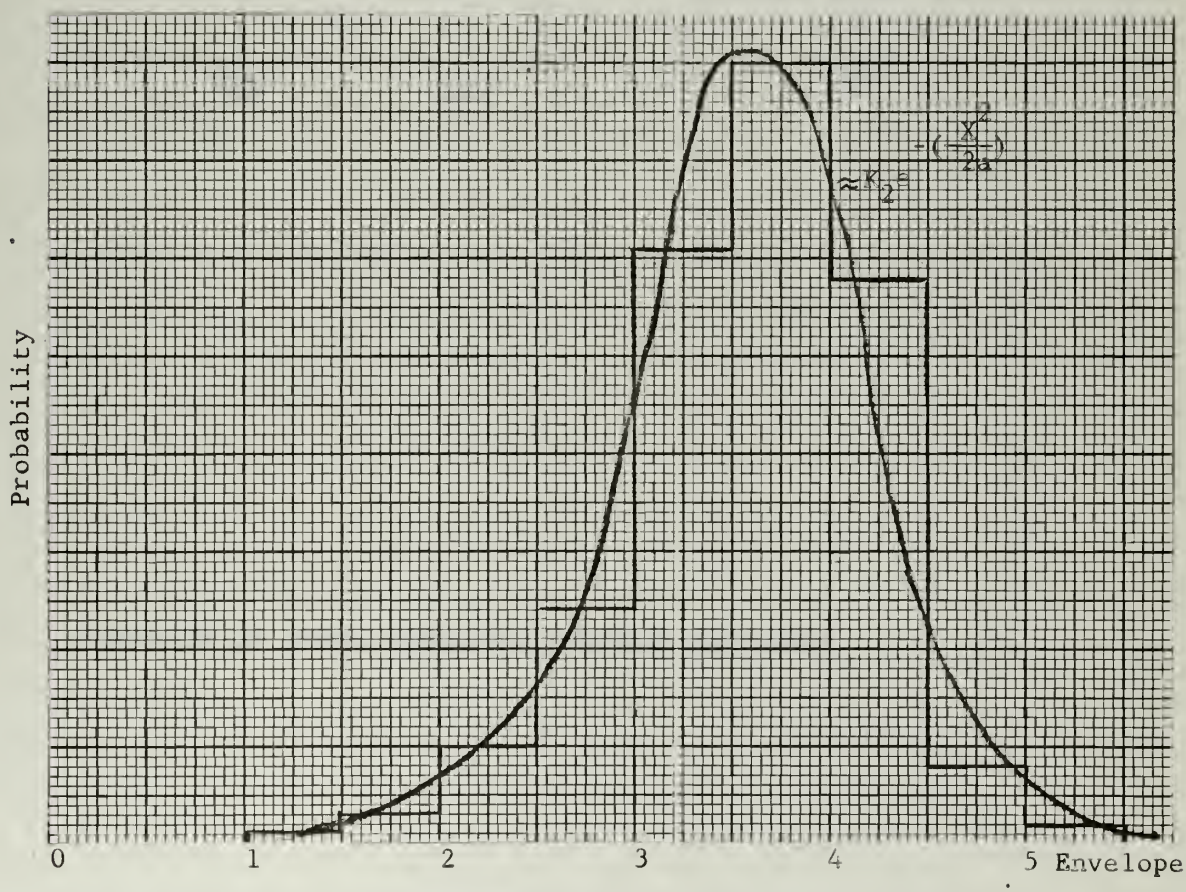
The experimental verification of the nature of the characteristic hiss as discussed in the last chapter was done in two parts; the first being the verification of the envelope height probability distribution, the second being the direct determination of the noise frequency spectrum. Both parts used the operation of the basic superregenerative circuit at a r-f frequency of one megacycle and a quenching frequency of 10 kcs. Unintentional hum injection into the system was a major problem in measurements due to the effect that a sine wave injection would have on the distribution of the peaks of the pulses. Hum reduction was performed by using a phase and amplitude balancing system similar to that used by the first order system on the circuit shown in Figure 6-1b. The actual adjustment of hum reduction was done by observing the hum modulation on the waveforms as they appeared on the oscilloscope and verified by listening to the rectified output.

With the system adjusted for incoherent operation and in the linear mode, a time domain picture similar to that of Figure 6-5b was obtained. By recording at random the heights of hundreds of these pulses, an indication of the population could be had. This data, taken randomly off an oscilloscope screen, was placed into cells of .1 vertical divisions. Analysis of the data revealed that the best the observer could do was regroup the data into cells of 0.5 vertical divisions. This was found necessary when it became apparent that resolution limitations existed due to the deficiencies of the oscilloscope along with the natural tendency of the observer to favor certain cells. Other factors complicating data

collection were the change of system gain, caused by power line fluctations, and environment influences. The long term gain changes were partially stabilized by measuring the integrated rms value of the noise output and adjusting the circuit parameters to bring them to a norm before a reading was taken. Such gain stabilization problems for the linear mode are discussed in Hall (2). Figure 8-1a is a graphical presentation of the experimental histogram of 491 samples with a smooth curve drawn through the middle of the amplitude bins. The similarity of the shape of this curve to that shown in Figure 7-1a for a Raleigh distribution is apparent. Finally the same data taking procedure was done for the system with a r-f input signal but with the input level so adjusted that the hiss level was only partially suppressed. Figure 8-1b is a plot of this data and its similarity to that shown in Figure 7-1a for Gaussian distribution is apparent.

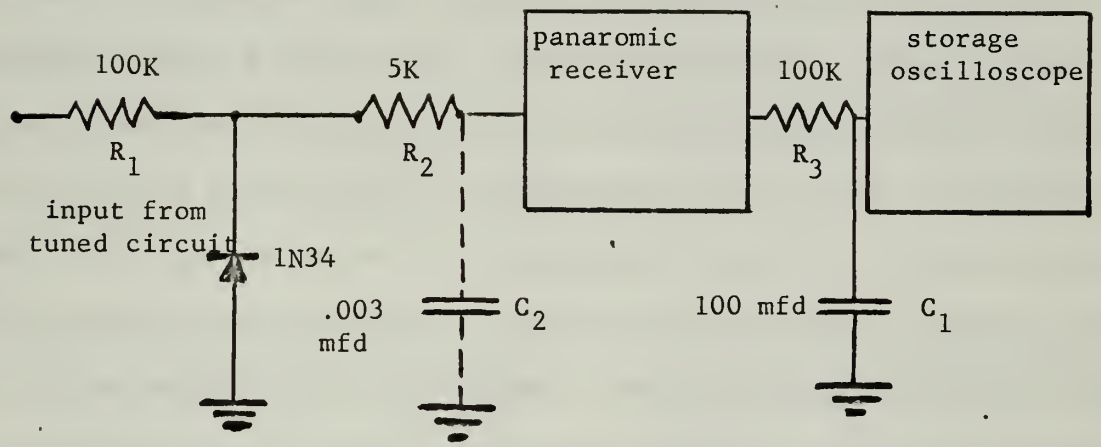
The experimental verification of the audio spectrum was done by taking the output of the superregenerator, putting it through a reasonably linear detector and feeding the demodulated signal into a sweep frequency narrow band receiver capable of tuning from 100 cps to 50 kcs. The output of this unit was fed into a lossy integrator and then into a storage type oscilloscope for retention. The horizontal sweep of the oscilloscope and the frequency of the receiver were varied in unison so that a plot of the relative amplitude vs frequency could be had. Figure 8-2 pictorially shows the setup, with the filter composed of R_2 and C_2 used only for checking the validity of the experimental setup. It was found that great care had to be taken as not to overload the input of the receiver by the high level quench frequencies. Even with the limitations mentioned it was possible to make qualified tests on the nature of the frequency spectrum of the rectified





DISTRIBUTIONS OF THE PULSE WAVEFORMS OF A SUPERREGENERATOR

FIGURE 8-1

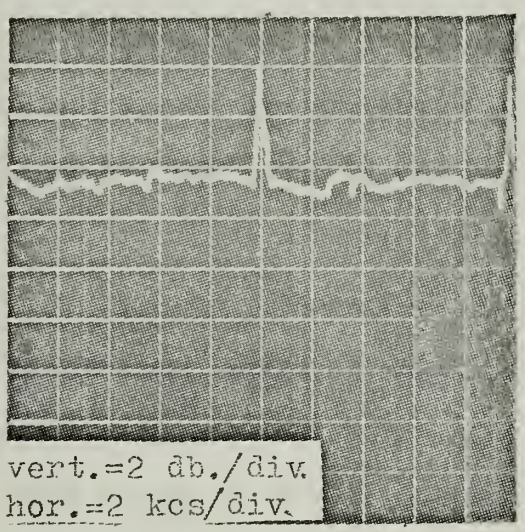


SCHEMATIC OF AUDIO FREQUENCY SPECTRUM ANALYZER

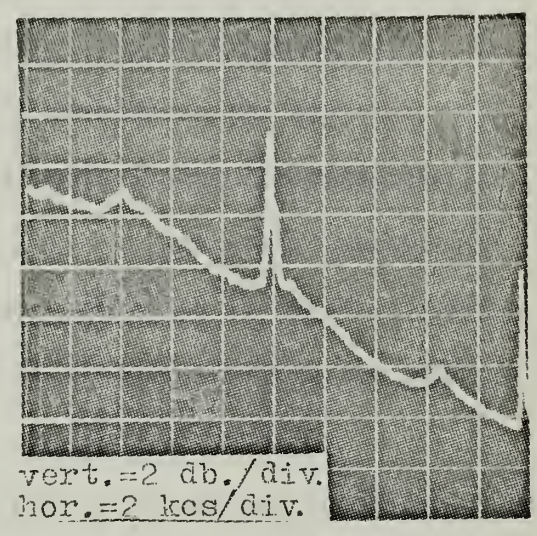
FIGURE 8-2



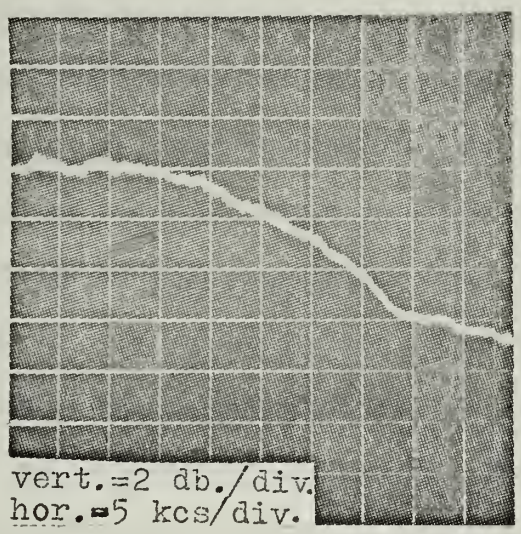
output. This verification in part involved observing the output of the analyzer without C_2 connected, essentially making the unit flat to fifty kilocycles. The result is shown in Figure 8-3a where the horizontal division correspond to two kilocycles intervals from zero to 20 kilocycles. The vertical divisions correspond to about two decibels over a fifteen decibel range. The pips shown are the quench frequency and harmonics with a ten kilocycles fundamental. Within plus or minus one decibels, the output is essentially flat to twenty kilocycles, which was within the bandwidth of the system. To verify this result, C_2 was connected and under identical conditions as forementioned, the frequency spectrum was again evaluated. Figure 8-3b is such a representation with C_2 being so adjusted so that a three decibels loss at ten kilocycles and seven decibels loss at twenty kilocycle would exist. The photograph clearly shows the expected trends. The choice of a ten kilocycle turnover was done to let in enough of the quench frequency so that if the quench frequency was distorting the input its effect would still be present. This potential distorting factor would probably have shown as a broad band output due to overload distortion in the receiver. Since this broading of response did not occur, the frequency spectrum shown in Figure 8-3a can be assumed to be representative of the superregeneration. Figure 8-3c is a similar study as done for Figure 8-3a only with the panoramic receiver tuned over a fifty kilocycle range so that the influence of the tuned circuit selectivity could be observed, and the decrease of level at the higher frequencies is as expected. The lack of ten kilocycle markers was avoided here by bypassing tuning the sweep frequency receiver at these marker frequencies. Finally the sweep frequency receiver was left constant for two minutes at five kilocycles with the output now representing the variation of noise output over this time. Figure 8-3d represents this, and an integrated stability of one



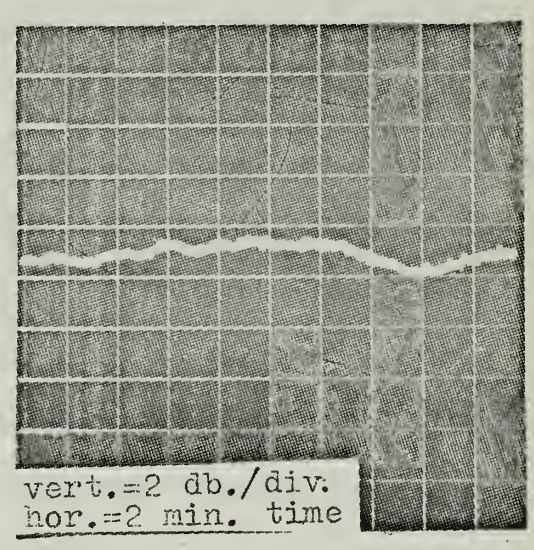
A



B



C



D

REPRESENTATIONS OF THE OUTPUT OF THE SPECTRUM ANALYZER

FIGURE 8-3









decibel was obtained. Since this is the same time used for the previous sweep times, the results of the proviously obtained results can be given the approximate confidence of one decibel over the sweep range.

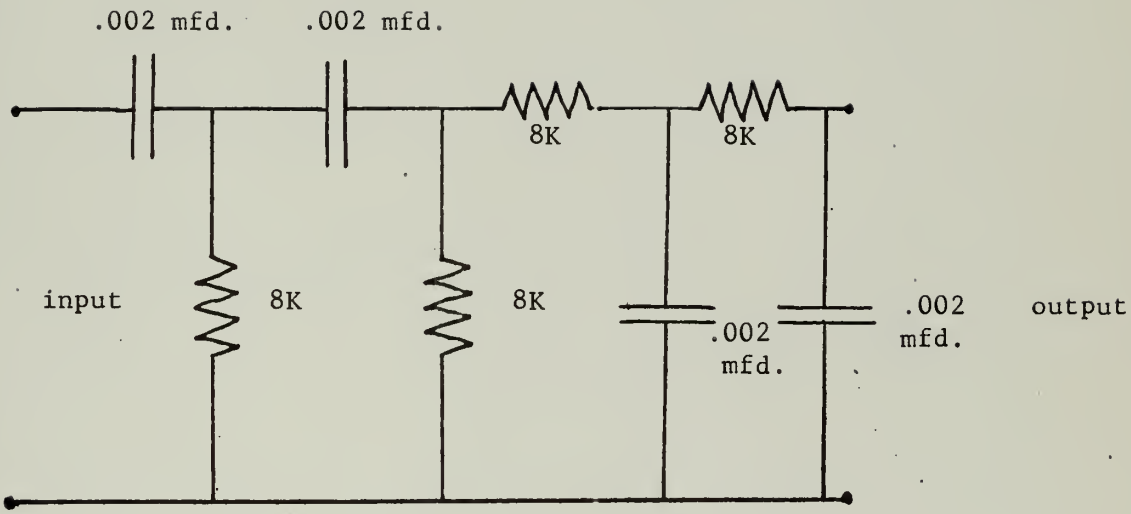
8.2 The Procurement Of Control Voltage From A Superregenerator Amplifier/ Detector In The Presence Of An A-M Signal.

As originally stated in the introduction, one of the motivations for this study was the possibility of using the results on the behavior of hiss (and the lack of it in the presence of signal) for the operation of a squelch circuit in a superregenerator. This section will describe one method which takes advantage of the knowledge obtained in the last section in designing an operational device to use as a control signal for squelch operation.

Even though the demodulated audio output of an a-m can be of the same magnitude as the noise output, the voice modulation frequencies are contained between 300-3000 cps nominally while the noise will have its energy distributed throughout the spectrum. What is desired is a device which would let as large as possible band of noise energy into a control amplifier/ rectifier but which would discriminate against the detected audio. A simple one stage RC high pass filter could do this but the rejection below the turnover frequency would not normally be sufficient to keep out enough of the voice frequencies from the control amplifier to prevent it from affecting it. Two cascaded RC stages with a 5000 cps turnover frequency was found to give sufficient rejection to the a-m signal preventing it from activating the control amplifier while still allowing sufficient noise energy through. If such a filter is fed directly from the superregenerator detector's output before attenuation at the medium high frequencies (10 kilocycles) takes place due to shunting effects of capacity, a noise output dependent only on the higher frequency band, but still substantial in voltage magnitude, will

be developed. If now this signal is amplified and then rectified and the d-c output used to switch on and off a gate to the output stage, or any other stage, the circuit could be adjusted so that the controlled device or element is activated by the change in noise voltage thus making it independent of the modulation present. As a squelch, the reduction of hiss can be used to close the gate to an audio stage and let the signal through.

All of the above discussion did not take into account the quench frequency and its effect on the control amplifier. If the quench frequency is high enough so that it cannot get through the interstage coupling circuits, the quench frequency is of no consequence. Unfortunately, often the quench frequency is in the near audio range, such as around 50 kcs, and can possibly feed into the noise amplifier and continously override the noise voltage changes. The problem then becomes, that of developing a band-pass filter which will prevent both the audio and quench frequency from activating the noise amplifier. This can be done many ways but if enough bandwidth is available, say from five to fifteen kilocycles, such a higher frequency quench signal can be filtered easily by shunting the coupling stages with capacity or by adding additional filters of the low pass type. Such a complete filter is shown in Figure 8-4 which is imperfect but simple in form and quite reliable. This particular type of filter was used commercially (28) and found quite adequate. Actually the output of the filter was fed into a class B transistor amplifier which allowed the combining of a switch amplifier and rectifier device. It is the output of this amplifier which can serve as a control voltage for a gate. As a further enhancement, a capacitor was placed at the output of the class B amplifier which served as an integrator causing the system to be less sensitive to impulse noise or peaks of modulation, though the capacitor cannot



BANDPASS FILTER FOR SQUELCH CONTROL SIGNAL

FIGURE 8-4



be too large or initial passages of modulation will be lost.

Even with the success of the system discussed above, Appendix C will be devoted to still another scheme of control-comparable in results and requiring fewer components operating on an entirely different principle. The author is particularly grateful to Professor R. Murray of the Electronics Department of the US Naval Postgraduate School for his assistance on the experimental work of this Chapter and Appendix C.

APPENDIX A

DIGITAL COMPUTER SOLUTIONS

A.1 General

All computer solutions of this dissertation were performed on the CDC 1604 Computer using a common program for all calculations. The vast majority of these computations involved the solution of a differential equation written in state space although a few times it was used as a convenient means of graphing data. The basic program used is a library routine known as INTEG1 at the U.S. Naval Postgraduate School. The next section is a reprint of the instructions governing this program, while the last section is a listing of the subroutines used for the graphic presentations of this dissertation.

A.2 INTEG1

The following 8 pages are reprints of INTEG1.

A. IDENTIFICATION:

TITLE: Runge-Kutta Solution of Ordinary Differential Equations with Built-in Input and Output Routines.

CO-OP ID: D2-NPS-INTEG1 (FORTRAN 60)

CATEGORY: Numerical Solution of Ordinary Differential Equations

PROGRAMMER: J.R. Ward

DATE: October 1963

REVISED: June 1964

B. PURPOSE:

This subroutine is intended to provide a simple but moderately flexible means for the solution of ordinary differential equations. Input, and both print and graph output routines are built in. The integration step size of the fourth-order Runge-Kutta numerical integration can be changed at will by appropriate data input and/or programming.

C. USAGE:

1. General:

This subroutine is intended for use when all that is required is the solution of ordinary differential equations with pre-determined parameters. Although possible, it will seldom be desirable to build the subroutine into a more complex program.

2. Program Format:

The subroutine will normally be called from the FORTRAN Library tape by a program which is being compiled and executed under monitor control. In this case the calling program deck must be of the following form:

```
..JOB* SMITH J   BOX 777                    (Job Ident.)
       PROGRAM TRYIT                        (Arbitrary name)
       DIMENSION X(30), XDOT(30), C(15)     (Standard card)
       C(10) = 1.                               "      "
     1 CALL INTEG1(T,X,XDOT,C)                  "      "
                                            (Equations written in
                                            FORTRAN Language)
       GO TO 1                              (Standard card)
       END                                      "      "
       END                                      "      "
```

This deck must be followed by the usual blank card and the data cards, which will be described below.

A typical program, together with its output, is appended.

3. The Equation Statements:

The equations to be solved must be reduced to standard first order form:

$$\frac{dx_i}{dt} = f_i(x_1, x_2, \ldots x_n, t) \qquad i = 1, 2, \ldots n.$$

in which the independent variable must be designated by t, and the dependent variables by x_i. The number of such equations is designated by n, with $n \leq 30$. At this point these equations must be written in FORTRAN language. Additional unsubscripted variables may be used as convenience dictates, as may any of the standard library functions or subroutines. The order of the equation statements is usually unimportant. A typical set might read:

```
ERROR   = SINF (C(1)*T) - X(1)
XDOT(2) = ERROR + C(2)*XDOT(1)
XDOT(1) = X(2) - 0.1*X(1)
```

A set of constants, c_i, $i \leq 8$, is available so that parameters may be introduced through a data card. The constant c_{10} must <u>never</u> be used except as in 2., above, but c_{11}, c_{12} and c_{13} may be used as follows:

Normally, print-out will be initiated at every 20th step of the integration, and graph points will be generated at every 5th. However, either or both may be altered by statement(s) such as:

```
C(11) = 10.
```

and/or `C(12) = 1.`

The first of these would cause print-out to take place at every 10th integration step, while the second would cause the generation of graph points at every step. In a similar way, the integration step size, which is usually set on a data card, can be modified through the constant c_{13}. Note that no more than 4500 integration steps, 450 lines of print-out, or 900 graph points (per curve) can be generated in any one run.

Any legal FORTRAN statement or technique can be used in the calling program, provided that a transfer of control does not prevent the processing of all relevant statements during each step of numerical integration. An acceptable set of statements might be:

```
      IF(T-10.)3,2,2
2     C(1) = 0.
3     CONTINUE
```

which would cause c_1 to take the value specified on the data card for $t < 10$ and the value zero for $t \geq 10$. It must be noted that only the quantities x_i and t can be output. If some quantity other than one of the variables is to be output, it must be equated to one of the x_i such that $n < i \leq 30$. Thus:

```
      X(3)  = ERROR
      X(7)  = ERROR*ERROR
```

The above auxiliary statements must be placed with the equation statements, between the CALL INTEG1 and the GO TO 1 statements shown in the standard program format above.

4. The Data Cards:

   a. The first data card must contain the job identification. It will be reproduced on print-out and graphs. Use columns 1 thru 48.

   b. The second card contains the number of runs to be processed, with a maximum of 9. Use column 1. The run number is placed on all output, along with the above job identification.

   c. The third card contains the value of n. This must be right justified in columns 1 and 2.

   d. The fourth card introduces the initial and final values of t, TI and TF, together with the step size(s), DT. The integration can be processed in up to 3 segments, each with a different step size, thus:

$$TI \xrightarrow{DT1} TF1 \xrightarrow{DT2} TF2 \xrightarrow{DT3} TF$$

$$\text{or} \quad TI \xrightarrow{DT1} TF1 \xrightarrow{DT2} TF$$

$$\text{or} \quad TI \xrightarrow{DT1} TF$$

The corresponding values (with decimal points) are placed, in the above order, in columns 1 thru 10, 11 thru 20, etc.

e. The values (with decimal points) of the constants c_1 thru c_8 are placed, in that order, in columns 1 thru 10, 11 thru 20, etc. on the 5th card. Blanks may be used for either zero or unused constants.

f. The sixth (and, if necessary, succeeding card(s)) contain the values of the initial conditions, $(x_1)_0$ thru $(x_n)_0$, in that order. The format is the same as in e.

g. The next card controls print-out. A blank card will suppress this output. Otherwise, up to 8 quantities chosen are specified by entries in columns 1 thru 10, 11 thru 20, etc. In each group of 10 columns, the first 8 contain the chosen column heading, and the last two contain the subscript, right justified, of the variable to be printed under the heading. Each column heading must contain at least one character. The subscript zero (or blank) is used to specify the independent variable, t.

h. The last card controls the graph output. A blank card will suppress this output. Otherwise, up to 4 curves can be graphed. The specifications for each curve are placed in columns 1 thru 20, 21 thru 40, etc. The first 16 columns in each group of 20 contains the graph title, the 17th and 18th contain the subscript, right justified, of the Y ordinate, while the X ordinate is similarly placed in the 19th and 20th columns. Two options exist. Either, up to 4 separate, single-curve graphs may be output, or, up to 4 curves on a single graph. The rules are:

   (i) For single curve graphs, each graph required must be given a title of at least one character.

   (ii) For multiple curve graphs there must be only one title (the first) of at least one character. The X ordinate must be the same for all curves.

   The graph X- and Y- scales are set automatically. Note that the scales are the same for all curves on a multi-curve graph, and that the scales are chosen so that all curves lie within the bounds of the graph.

5. Multiple Runs:

   If several solutions of the same equations are required, it is necessary to specify the number of runs on the data card described in 4a., above, and to supply a data deck for each run. For each run after the first, only the cards described in 4d. through 4h. are required. Note that with the exception of the data described in 4a. thru 4c., no information is retained by the subroutine between runs. It must always be completely re-specified for each successive run.

6. Space Required: Approximately 13,000 decimal (includes DRAW)

7. Temporary Storage Required: None.

8. Error Print-outs:

   The subroutine's error stops are preceded by self-explanatory print-outs. An incorrect program or data card may, of course, generate an error print-out from the basic FORTRAN Compiler or input routine.

9. Error Returns: None.

10. Error Stops: See 8. above

11. Tape Mountings: Logical Tape #8 will receive binary graph output.

12. Output Format:

    All job identification, together with the run number and a record of all input data, is automatically output for each run. The output specifications for the solution are described in 4g. and h. above.

13. Selective Jump and Stop Settings: None.

14. Timing:

    Variable; depends upon the number and complexity of the equations and on the choice of integration step size(s).

15. Accuracy:

    This has a complex dependency on the actual equations undergoing solution. It may be controlled through the choice of integration step size(s).

16. Cautions to Users:

    a. If the calling program (containing the equations to be solved) is listed as output from the 1604, this listing, together with the input data record, should be carefully checked for errors, since these completely define the program as accepted by the computer.

b. Too large a step size can result in unacceptable integration errors and even instability of the integration process. The only (moderately) safe test is to run a problem with at least two different step sizes and then to compare the two (or more) results.

17. Equipment Configuration:
CDC 1604 with FORTRAN 60 compiler and library. The subroutine uses subroutine GRAPH2 to prepare the binary output for off-line plotting on the CDC 160 with Calcomp Plotter. The 160 uses the USNPGS GRAFPLOT Program.

D. METHOD:

The integration is performed by the standard fourth-order Runge-Kutta method of numerical integration.

```
..JOB*WARD J R     BOX 244
      PROGRAM TYPICAL
      DIMENSION X(30), XDOT(30), C(15)
      C(10) = 1.
    1 CALL INTEG1 (T, X, XDOT, C)
      ERROR = 1.0 - X(1)
      XDOT(2) = C(1)*(ERROR - C(2)*X(2)) - 15.0*X(2)
      XDOT(1) = X(2)
      X(3) = ERROR
      C(11) = 50.
      GO TO 1
      END
      END

 WARD J R   BOX 244 TEST   10/30.
2
02
    0.0     |  0.0005   |  0.9      |           |           |           |
  300.0     |  0.1      |           |           |           |           |
    0.0     |  0.0      |           |           |           |           |
  TIME  00  | OUTPUT 01 | VELOCITY02|  ERROR   03         |           |
OUTPUT VS.  | TIME 0100 | ERROR VS. | TIME    0300| ERROR VS. | OUTPUT0301
    0.0     |  0.0005   |  0.9      |           |           |           |
  300.0     |  0.1      |           |           |           |           |
    0.0     |  0.0      |           |           |           |           |
OUT,ERR VS. | TIME0300  |           |           0100        |           |
```

Input Listing.

Columns of 10 are shown for the data.

```
      PROGRAM TYPICAL
      DIMENSION X(30), XDOT(30), C(15)
      C(10) = 1.
1     CALL INTEG1 (T, X, XDOT, C)
      ERROR = 1.0 - X(1)
      XDOT(2) = C(1)*(ERROR - C(2)*X(2)) - 15.0*X(2)
      XDOT(1) = X(2)
      X(3) = ERROR
      C(11) = 50.
      GO TO 1
      END
      END
```

A.3 Subroutines.

The following 23 pages lists the subroutines used in this dissertation, following the general instructions and concerns as mentioned in the previous section.

```
..JOB0388F, HARRIS J R 61HD BOX48
      PROGRAM COMPUTE  1
      DIMENSION X(30),XDOT(30),C(15)
      C(10)=1.
    1 CALL INTEG1 (T,X,XDOT,C)
      X(1)=1.-EXPF(T-5.)
      C(11)=50.
      GO TO 1
      END
      END

         VOLTAGE GAIN VS ALPHA*TIME
1

.0          .004       7.


TIME     00A         01B         02
  FIGURE 2-2     0100
```

```
..JOB0388F, HARRIS J R 61HD BOX48
      PROGRAM COMPUTE  1
      DIMENSION X(30),XDOT(30),C(15)
      C(10)=1.
    1 CALL INTEG1 (T,X,XDOT,C)
      X(1)=1.-EXPF(T-5.)
      X(2)=.5*(1.-2.*EXPF(T-5.)+EXPF(2.*(T-5.)))
      X(3)=-X(1)
      X(4)=-X(2)-X(3)
      C(11)=50.
      GO TO 1
      END
      END

         POWER RECEIVED VS ALPHA*TIME
1

.0         .004       7.


TIME    00A        01B        02
  FIGURE 2-3    0200                0300                0400
```

```
..JOB0388F, HARRIS J·R 61HD BOX48
      PROGRAM COMPUTE  1
      DIMENSION X(30),XDOT(30),C(15)
      C(10)=1.
    1 CALL INTEG1 (T,X,XDOT,C)
      X(1)=(1.-2.*EXPF(T-4.)+EXPF(2.*(T-4.)))/(2. -2.*EXPF(T-4.))
      C(11)=50.
      GO TO 1
      END
      END

           POWER GAIN VS ALPHA*TIME
1

.0      .004       7.


TIME    00A        01B        02
  FIGURE 2-4    0100
```

```
..JOB0388F, HARRIS J R 61HD BOX48
      PROGRAM COMPUTE  1
      DIMENSION X(30),XDOT(30),C(15)
      C(10)=1.
    1 CALL INTEG1 (T,X,XDOT,C)
      X(1)=SINF(ATANF(1./T))/SQRTF(1.+T*T)
      C(11)=50.
      GO TO 1
      END
      END

         NORMALIZED OUTPUT VS OMEGA
1

.0         .002       8.


TIME     00A        01B      02
 FIGURE 2-6      0100
```

```
..JOB0388F, HARRIS J R 61HD BOX48
      PROGRAM COMPUTE  1
      DIMENSION X(30),XDOT(30),C(15)
      C(10)=1.
    1 CALL INTEG1 (T,X,XDOT,C)
      X(1)=SINF(.3533*T+ATANF(-1.))
      X(2)=SINF(.3533*T+ATANF(-2.))
      X(3)=SINF(.3533*T+ATANF(-.5))
      C(11)=50.
      GO TO 1
      END
      END

     OUTPUT VOLTAGE VS INPUT PHASE ANGLE
1

.0         .002        8.


TIME    00A        01B        02
  FIGURE 2-7    0100          0200                0300
```

```
..JOB0388F, HARRIS J R 61HD BOX48
      PROGRAM COMPUTE  1
      DIMENSION X(30),XDOT(30),C(15)
      C(10)=1.
    1 CALL INTEG1 (T,X,XDOT,C)
      X(1)=SINF(        +ATANF(-1./T))
      X(2)=SINF(1.047   +ATANF(-1./T))
      X(3)=SINF(2.094   +ATANF(-1./T))
      C(11)=50.
      GO TO 1
      END
      END

   NORMALIZED OUTPUT VS OMEGA (PHASE VARIED)
1

.0         .002       8.


TIME     00A        01B        02
  FIGURE 2-8     0100                0200                0300
```

```
..JOB0388F, HARRIS J R 61HD BOX48
      PROGRAM COMPUTE  1
      DIMENSION X(30),XDOT(30),C(15)
      C(10)=1.
    1 CALL INTEG1 (T,X,XDOT,C)
      XDOT(1)=X(1)-1.
      C(11)=50.
      GO TO 1
      END
      END

            OUTPUT VOLTAGE VS TIME
1
 1
.0         .002       7.


TIME 00   A        01B
  FIGURE 2-12   0100
```

```
..JOB0388F, HARRIS J R 61HD BOX48
      PROGRAM COMPUTE  1
      DIMENSION X(30),XDOT(30),C(15)
      C(10)=1.
    1 CALL INTEG1 (T,X,XDOT,C)
      XDOT(1)=(COSF(.1*T)-X(1))*(1.+4.*COSF(T))
      C(11)=50.
      GO TO 1
      END
      END

     OUTPUT VOLTAGE VS TIME (INCOHERENT)
1
 1
.0      .02       80.


TIME 00   A       01B
  FIGURE 2-13   0100
```

```
..JOB0388F, HARRIS J R 61HD BOX48
      PROGRAM COMPUTE  1
      DIMENSION X(30),XDOT(30),C(15)
      C(10)=1.
    1 CALL INTEG1 (T,X,XDOT,C).
      XDOT(1)=(COSF(.1*T)-X(1))*(-.1+4.*COSF(T))
      C(11)=50.
      GO TO 1
      END
      END

       OUTPUT VOLTAGE VS TIME (COHERENT)
1.
 1
.0         .02        70.


TIME 00   A        01B
  FIGURE 2-14   0100
```

```
..JOB 388F, HARRIS J R 61HD BOX48
      PROGRAM COMPUTE  1
      DIMENSION X(30),XDOT(30),C(15)
      C(10)=1.
    1 CALL INTEG1 (T,X,XDOT,C)
      XDOT(1)=(-COSF(T+.034*T)-X(1))*(+1.+4.*COSF(T))
      C(11)=50.
      GO TO 1
      END
      END

        OUTPUT VOLTAGE VS INPUT PHASE
1
 1.
.0         .02        80.


TIME 00   A        01B
  FIGURE 2-15   0100
```

```
..JOB0388F, HARRIS J R 61HD BOX48
      PROGRAM COMPUTE  1
      DIMENSION X(30),XDOT(30),C(15)
      C(10)=1.
    1 CALL INTEG1 (T,X,XDOT,C)
      XDOT(1)=-XDOT(2)-XDOT(3)+XDOT(4)
      XDOT(2)=X(1)/C(1)
      XDOT(3)=-X(1)*(1.-X(1)*X(1))
      XDOT(4)=(.05-X(1))/C(2)
      X(5)=XDOT(1)
      X(6)=XDOT(2)
      X(7)=XDOT(3)
      X(8)=XDOT(4)
      C(11)=50.
      GO TO 1
      END
      END

      OUTPUT VS TIME (NONLINEAR SYSTEM)
1
 4
.0          .004        16.
5.          5.

TIME 00   A        01B        05C        06D        07E
  FIGURE 3-7    0100
```

```
..JOB0388F, HARRIS J R 61HD BOX48
      PROGRAM COMPUTE  1
      DIMENSION X(30),XDOT(30),C(15)
      C(10)=1.
    1 CALL INTEG1 (T,X,XDOT,C).
      XDOT(1)=-XDOT(2)-XDOT(3)+XDOT(4)
      XDOT(2)=X(1)/C(1)
      XDOT(3)=+X(1)*(1.-X(1)*X(1))*(.5+COSF(T)+.2*COSF(.1*T))
      XDOT(4)=(.25-X(1))/C(2)
      X(5)=XDOT(1)
      X(6)=XDOT(2)
      X(7)=XDOT(3)
      X(8)=XDOT(4)
      C(11)=50.
      GO TO 1
      END
      END

     OUTPUT VS TIME (MODULATED RESISTANCE)
1
 4
.0         .02        80.
50.        5.

TIME 00   A        01B        05C        06D        07E        08
  FIGURE 3-9    0100
```

```
..JOB0388F, HARRIS J R 61HD BOX48
      PROGRAM COMPUTE  1
      DIMENSION X(30),XDOT(30),C(15)
      C(10)=1.
    1 CALL INTEG1 (T,X,XDOT,C)
      XDOT(1)=+X(1)+X(2)
      XDOT(2)=-X(1)/40.+1.
      X(3)=X(1)/40.
      C(11)=50.
      GO TO 1
      END
      END

   .  OUTPUT VS TIME (OVERDAMPED SYSTEM)
1
 2
.0         .001       3.5


TIME 00   A        01B        05C        06D        07E        08
  FIGURE 4-2    0300
```

```
..JOB0388F, HARRIS J R 61HD BOX48
      PROGRAM COMPUTE  1
      DIMENSION X(30),XDOT(30),C(15)
      C(10)=1.
    1 CALL INTEG1 (T,X,XDOT,C)
      XDOT(1)=+X(1)+X(2)
      XDOT(2)=-X(1)/4. +1.
      X(3)=X(1)/4.
      C(11)=50.
      GO TO 1
      END
      END

      OUTPUT VS TIME (CRITICALLY DAMPED)
1
 2
.0         .001       3.5


TIME 00   A        01B        05C        06D        07E        08
  FIGURE 4-3     0300
```

```
..JOB0388F, HARRIS J R 61HD BOX48
      PROGRAM COMPUTE  1
      DIMENSION X(30),XDOT(30),C(15)
      C(10)=1.
    1 CALL INTEG1 (T,X,XDOT,C)
      XDOT(1)=+X(1)+X(2)
      XDOT(2)=-X(1)/.4 +1.
      X(3)=X(1)/.4
      C(11)=50.
      GO TO 1
      END
      END

      OUTPUT VS TIME (UNDERDAMPED SYSTEM)
1
 2
.0         .004       14.


TIME 00   A        01B        05C        06D        07E        08
  FIGURE 4-4    0300
```

```
..JOB0388F, HARRIS J R 61HD BOX48
      PROGRAM COMPUTE  1
      DIMENSION X(30),XDOT(30),C(15)
      C(10)=1.
    1 CALL INTEG1 (T,X,XDOT,C)
      XDOT(1)=-XDOT(2)-XDOT(3)+XDOT(4)
      XDOT(1)=+X(1)+X(2)
      XDOT(2)=-X(1)/.4 +COSF(10.*T)
      X(3)=X(1)/.4
      X(4)=1./SQRTF((2.5-T*T)*(2.5-T*T)+T*T)
      C(11)=50.
      GO TO 1
      END
      END

   NORMALIZED OUTPUT VS OMEGA (UNDERDAMPED)
1
 2
.0         .002       8.


TIME 00    A        01B        05C        06D        07E        08
  FIGURE 4-5     0400
```

```
..JOB0388F, HARRIS J R 61HD BOX48
      PROGRAM COMPUTE  1
      DIMENSION X(30),XDOT(30),C(15)
      C(10)=1.
    1 CALL INTEG1 (T,X,XDOT,C)
      XDOT(1)=+X(1)+X(2)
      XDOT(2)=-X(1)/.0004+COSF(50.*T)
      X(3)=X(1)/.0004
      X(4)=1./SQRTF((2500.-T*T)*(2500.-T*T)+T*T)
      C(11)=50.
      GO TO 1
      END
      END

      OUTPUT VS TIME (UNDERDAMPED SYSTEM)
1
 2
.0         .002       7.


TIME 00    A         01B         05C         06D         07E         08
  FIGURE 4-6     0300
```

```
..JOB0388F, HARRIS J P 61HD BOX48
      PROGRAM COMPUTE  1
      DIMENSION X(30),XDOT(30),C(15)
      C(10)=1.
    1 CALL INTEG1 (T,X,XDOT,C)
      XDOT(1)=+X(1)+X(2)
      XDOT(2)=-X(1)/.0004+COSF(50.*T)
      X(3)=X(1)/.0004
      X(4)=1./SQRTF((2500.-T*T)*(2500.-T*T)+T*T)
      C(11)=50.
      GO TO 1
      END
      END

            NORMALIZED OUTPUT VS OMEGA
1
 2.
.0         .02        80.

TIME 00   A        01B        05C        06D        07E        08
  FIGURE 4-7    0400
```

```
..JOB0388F, HARRIS J R 61HD BOX48
      PROGRAM COMPUTE  1
      DIMENSION X(30),XDOT(30),C(15)
      C(10)=1.
    1 CALL INTEG1 (T,X,XDOT,C)
      XDOT(1)=X(1)+X(2)
      XDOT(2)=-X(1)/.0004+COSF(2.*C(1)*T)
      X(3)=X(1)/.0004
      C(11)=50.
      GO TO 1
      END
      END

                VOLTAGE VS TIME
9     .
 2
.0        .002       8.
25.

TIME  00  A        01B        02C        03D        04E        05F
  FIGURE 5-1A   0300
```

```
..JOB0388F, HARRIS J R 61HD BOX48
      PROGRAM COMPUTE  1
      DIMENSION X(30),XDOT(30),C(15)
      C(10)=1.
    1 CALL INTEG1 (T,X,XDOT,C)
      XDOT(1)=X(1)*(.0+.210*T)+X(2)
      XDOT(2)=-X(1)/.0004+COSF(2.*C(1)*T)-.125*X(1)
      X(3)=X(1)/.0004
      C(11)=50.
      GO TO 1
      END
      END

                VOLTAGE VS TIME
9
 2
.0         .002       8.
25.

TIME  00  A        01B        02C        03D        04E        05F
  FIGURE 5-1B   0300
```

```
..JOB0388F,'HARRIS J R 61HD BOX48
      PROGRAM COMPUTE  1
      DIMENSION X(30),XDOT(30),C(15)
      C(10)=1.
    1 CALL INTEG1 (T,X,XDOT,C)
      XDOT(1)=X(1)*(.0+.210*T)+X(2)
      XDOT(2)=-X(1)/.0004+COSF(2.*C(1)*T)-.125*X(1)
      X(3)=X(1)/.0004
      C(11)=50.
      GO TO 1
      END
      END

                VOLTAGE VS TIME
9
 2
.0          .002       8.
25.

TIME  00  A        01B        02C        03D        04E        05F
  FIGURE 5-2     0300
```

```
..JOB0388F, HARRIS J.R 61HD BOX48
      PROGRAM COMPUTE  1
      DIMENSION X(30),XDOT(30),C(15)
      C(10)=1.
    1 CALL INTEG1 (T,X,XDOT,C)
      XDOT(1)=-.5*X(1)*(-1.+.025*X(1)*X(1))
      X(2)=X(1)*COSF(6.5*T)
      C(11)=50.
      GO TO 1
      END
      END

          ALPHA VS TIME (NONLINEAR)
1
 1
.0          .01         40.

.00005
TIME    00A         01B         02
  FIGURE 5-3    0200
```

```
..JOB0388F, HARRIS J R 61HD BOX48
      PROGRAM COMPUTE  1
      DIMENSION X(30),XDOT(30),C(15)
      C(10)=1.
    1 CALL INTEG1 (T,X,XDOT,C)
      XDOT(1)=X(2)+X(3)
      XDOT(2)=-40.*X(1)
      XDOT(3)=C(1)*COSF(50.*T)+XDOT(1)*(1.-.1*X(1)*X(1))
      C(11)=50.
      GO TO 1
      END
      END

         VOLTAGE VS TIME (NONLINEAR)
1
 3
.0         .01        40.
.1

TIME  00  A        01B        02C        03D        04E        05F
  FIGURE 5-4    0100
```

APPENDIX B

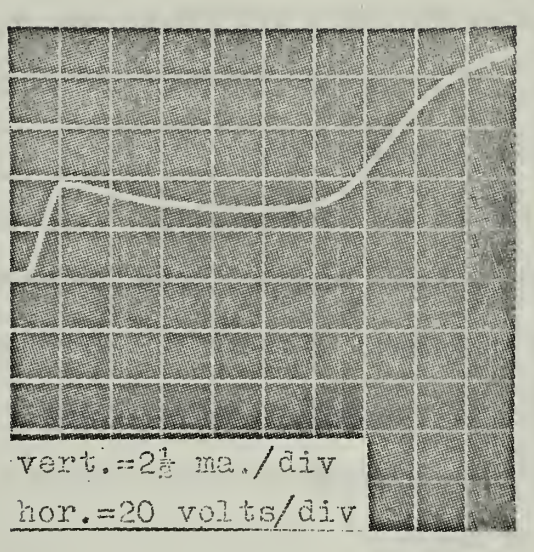
Dynatron Investigation

Experimental verification of the first order system was complicated until a device could be obtained which would allow for a rapid switching between an effective positive and negative resistance value without permutating the rest of the system. The topic of negative resistance devices has been well documentated by Herold (8) for all major active devices except for modern solid state devices, though his theoretical applications apply even here. In normal feedback amplifiers, used as negative resistance devices, there is required a change of dynamic state which would impose a large input to the unstable system swamping any low level input signal. An example of this would be the switching on of a feedback amplifier which would impose a change in collector or plate potential, a change which unfortunately can serve as a signal and of such magnitude as to swamp the influence of a weak input signal. This problem of a state change in the system does not normally affect a second order (standard RLC) system where the system does not have the ability to amplify a steady state signal. The method used to overcome this fundamental problem in the experimental study of the first order system was to evaluate certain two terminal devices, such as the dynatron, arc discharge and tunnel diode, hoping to find the desired transfer characteristics. The initial guidance was in the direction of the dynatron because of the peculiar behavior which occurs when secondary emission from the plate is used to obtain a negative resistance characteristic. This feature is not new, in fact it presented a problem in the development of the tetrode where care had to be taken in order to assure that the plate voltage did not go below that of the screen voltage, otherwise a curious "knee" occurred in the plate current causing

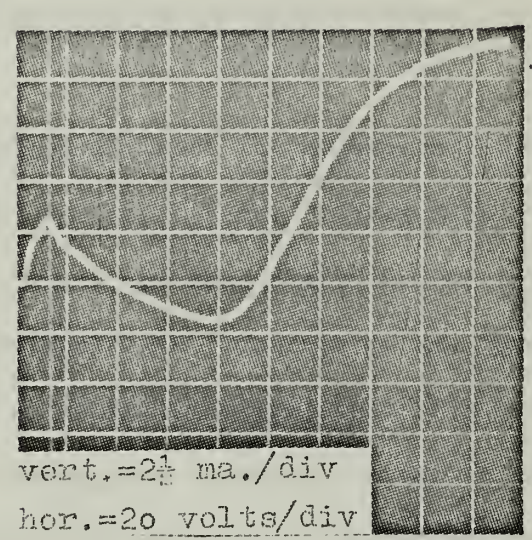
distortion and possible unstable operation. This was one of the reasons the pentode was developed; the suppressor grid biased such as to force the plate ejected electrons to be reattracted by the plate. Because of this, only certain pentodes, those with separate suppressor leads, and tetrodes were studied for their negative resistance characteristics.

It was found that many common pentodes when operated as tetrodes by connecting the screen and suppressor grids together and operated with the screen potential above the plate potential would give a negative resistance plate characteristic, ie., the dynatron. Figure B-1a is the plate current vs voltage of a typical 6SK7 type vacuum tube utilizing the circuit shown in Figure B-2. When the plate voltage is lower then the screen voltage, there can be a negative resistance characteristics but unfortunately it demands a finite current to flow in the load resistor, a current which demands a voltage across it that can swamp the influence of a weak input signal. This was the normal plate characteristic that was observed but fortunately not a universal one. Certain manufacturers of the 6SK7, 6SJ7 and other similar vacuum tubes have a plate characteristic as shown in Figure B-1b, demonstrating a reverse current capability. What is of particular interest is the possibility of switching between two plate voltages, either which require no load current, but differing in that one voltage has a positive resistive characteristic, and other a negative resistive characteristic. This is what was required for the switching mode of operation described in Chapter Two and performed in Chapter Three.

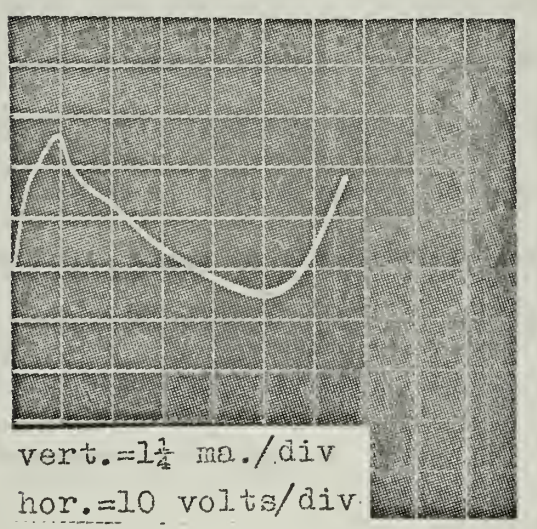
To further study the properties of the dynatron for these selected tubes the hysteresis behavior was investigated, thus giving insight to the frequency limitations of the special dynatron. Here, the plate supply



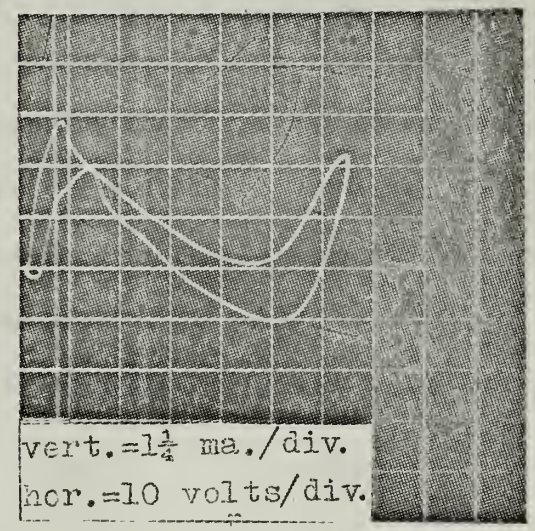
A



B



C



D

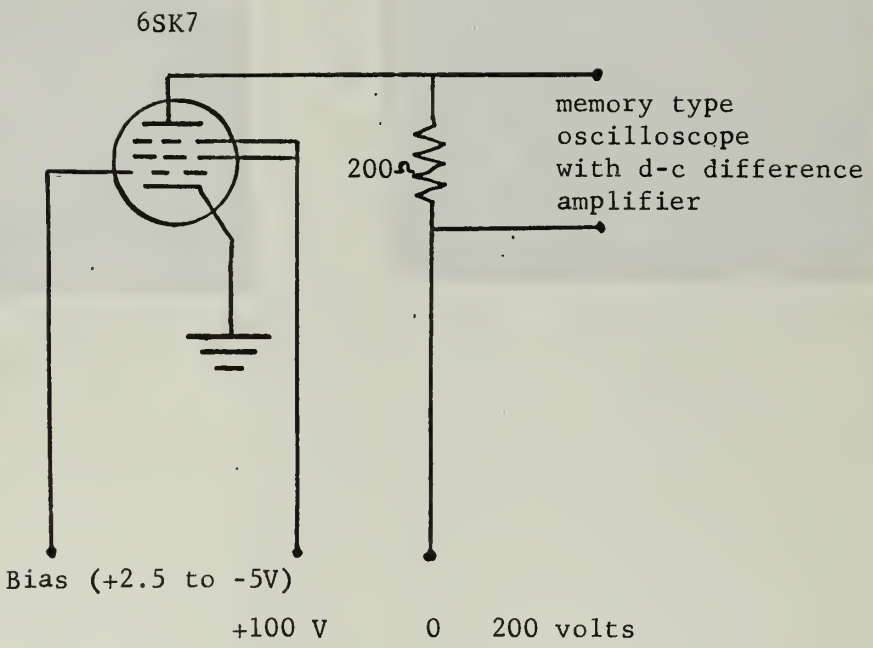
STATIC AND DYNAMIC PLATE CHARACTERISTICS OF THE
DYNATRON MODE OF OPERATION

FIGURE B-1



of Figure B-2 was replaced by an audio oscillator in series with a fixed positive potential, adjusted so that the plate voltage swung between zero and about 60 volts. This allowed for the dynamic switching behavior to be observed and photographed. Figure B-1c shows this for a 200 cps switching rate where a little hysteresis behavior is apparent while Figure B-1d shows the same except for a ten kcs switching rate which produces a rather pronounced hysteresis effect.

A further investigation of the dynatron was made in to observe what effect the grid voltage had on the plate characteristics. Figure B-3a shows a family of plate characteristics, where the zero plate current for each curve is shown as labeled on the vertical axis. The curves are for, reading from top to bottom, $+2\frac{1}{2}$, 0, $-2\frac{1}{2}$, -5 volts control grid bias. It is noticed that the negative resistance value, the slope of the curve, gets larger as the bias is increased in a negative direction. In addition, for biases less than zero, the plate voltage at which a zero plate current occurs is very close to the same value regardless of grid bias over a large range. This is shown in Figure B-3b where the four transfer curves are transposed so that a common origin occurs for all biases. Because of this fact the output of the sampled unstable amplifier can be modulated by varying the input voltage to the dynatron which will cause, to a first order approximation, only a change in the negative resistance value during the regenerative cycle.



SCHEMATIC FOR TESTING DYNAMIC AND STATIC
DYNATRON CHARACTERISTICS

FIGURE B-2



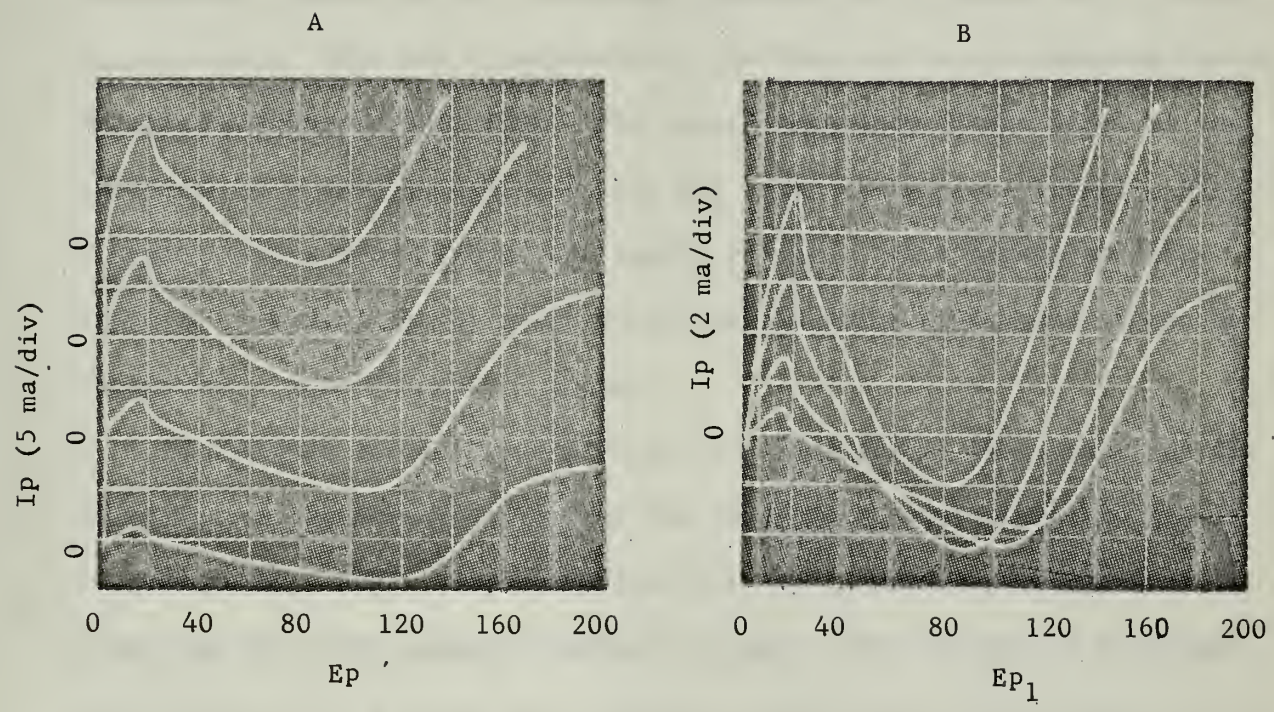


PLATE CHARACTERISTICS FOR THE DYNATRON WITH VARIOUS GRID BIAS

FIGURE B-3





APPENDIX C

A Second Method Of Squelch Control

As mentioned in section 8-2, this Appendix will delve into a second method of developing control voltage from a parameter change in a super-regenerative circuit. The form of parameter change considered here for a control signal is that of the quench frequency of a self quenching super-regenerator, where the self quenching frequency will change with incoming signal level. This was experimentally verified and is collaborated by the results of Younger etc., (29). The quench frequency output level at the collector of a self quenching system was found to be proportionally high - a typical value being 1/5 of the supply voltage. This signal and its shift in frequency serves respectively as the power source and parameter change for a squelch control signal.

If a high-Q series-tuned circuit is placed across the quench voltage developed at the detector's output and tuned to approximately the quench frequency, the output across the inductor or capacitor would approach Q times the effective quench frequency voltage. This voltage if rectified and filtered with a large time constant, could serve as the source of control voltage. Unfortunately, the quench frequency is often not a stable parameter thereby limiting the sharpness of the tuned circuit usable for voltage multiplication. Another limiting factor is the effect the series tuned circuit has on the superregenerator itself. Considerable pulling effects were observed when the series tuned circuit was placed at the quench frequency. These two considerations demanded that the series circuit be adjusted on the slope of the resonance curve, positioning it where the rate of change of output to input signal was still considerable. As the input signal increases, the quench frequency will increase as a function of the logarithm of the input amplitude (9), causing the quench frequency to rise to a different position on the resonant curve and changing its output voltage. This output voltage when rectified becomes the control signal to a

gate in the audio section of the receiver thereby allowing squelch operation.

Figure C-1 is a reprint of an actual commercial receiver utilizing this form of squelch control and was cited by patent 3,199,031 (3). In actual operation the squelch behavior of this receiver is such that signals which only quiet the noise by about 6 decibels will still reliabily open the gate of the audio section.

Aug. 3, 1965 J. R. HARRIS ETAL 3,199,031

GENERATION AND USE OF CONTROL SIGNAL IN SUPERREGENERATIVE RECEIVERS

Filed May 3, 1962

CIRCUIT OF SUPERREGENERATIVE RECEIVE WITH SQUELCH CONTROL

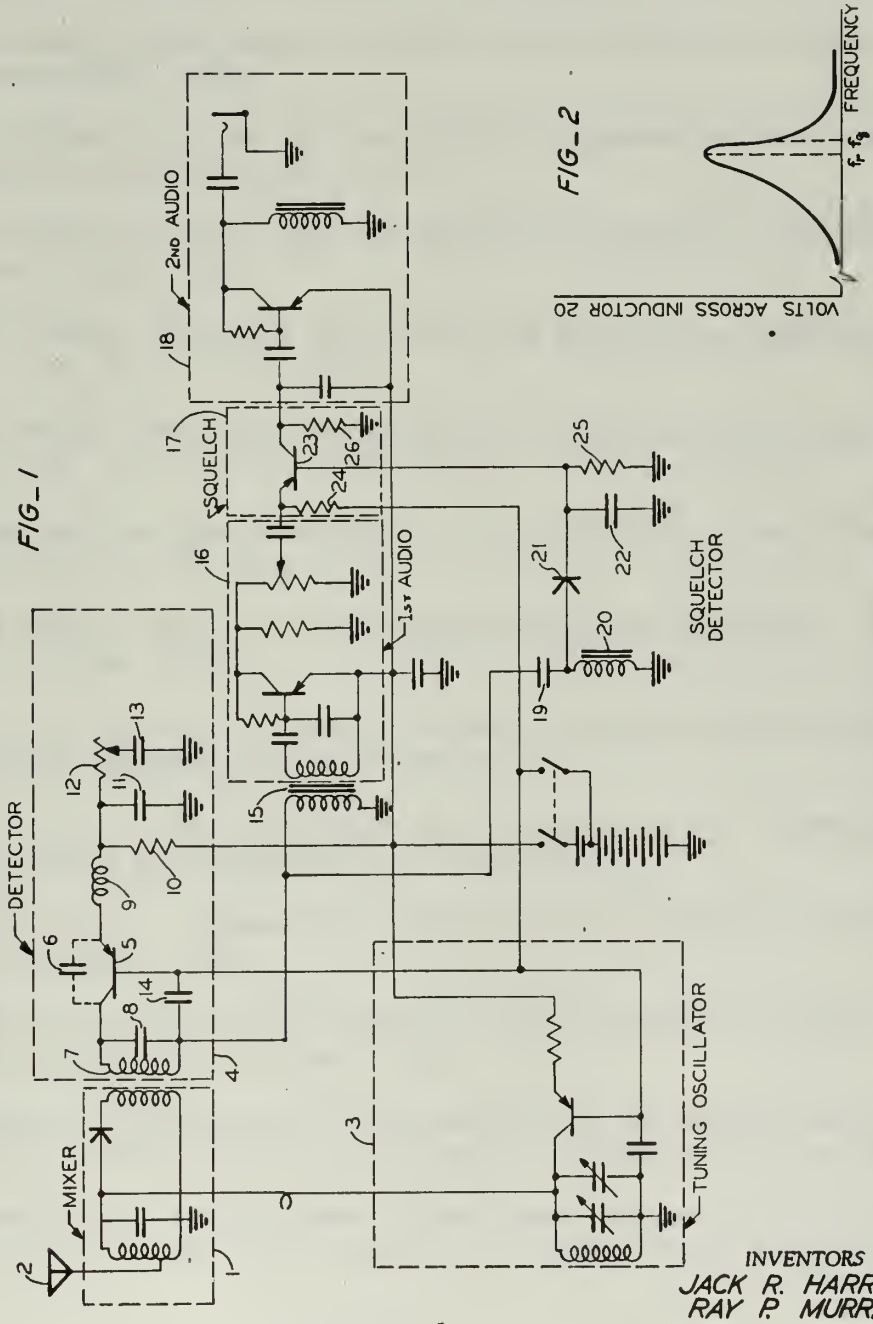


FIGURE C.1

F/G_1

F/G_2

INVENTORS
JACK R. HARRIS
RAY P. MURRAY

BY Paul M. Klein Jr.
ATTORNEY



BIBLIOGRAPHY

1. Edwin E. H. Armstrong, "Some Recent Developments Of Regenerative Circuit", Proc IRE, Vol. 10, August 1922.

2. Van Voorhes (editor), "Microwave Receivers", Radiation Laboratory Series, Chapter 20, McGraw Hill, 1948.

3. Harris and Murray, "Generation And Use Of Control Signal In Super-regenerative Receivers", U.S. Government Letters Patent, No. 3,199,031 issued 3 August 1965.

4. I.S. and E.S. Sokolnikoff, "Higher Mathematics For Engineers and Physicists", pp 284-5, McGraw Hill, 1941.

5. S.Goldman, "Transformation Calculus And Electrical Transients", Prentice-Hall, 1958.

6. L.A. Pipes, "Applied Mathematics For Engineers And Physicist", Chapter 21, McGraw-Hill, 1958.

7. V. Volterra, "Lecons sur les Equations Integrales", Gauthier-Villers, Paris, France, 1913.

8. E.W. Herold, "Negative Resistance And Devices For Obtaining It', Proc IRE, Vol. 23, Oct 1935.

9. F.W. Frink, "The Basic Principles Of Superregenerative Reception", Proc IRE, Vol. 26, Jan 1938.

10. H. Ataka, "On Superregeneration Of An Ultra-Short Wave Receiver", Proc IRE, Vol. 23, Aug 1935.

11. L. Riebman, "Theory Of The Superregenerative Amplifier", Proc IRE, Vol. 37, Jan 1949.

12. P. Bura, "Resonant Circuit With Periodically-Varying Parameters", WIRELESS ENGINEER, April and May 1952.

13. S.H. Chang, "Theoretical and Experimental Studies On Superregeneration", Phd. thesis Harvard University, Oct 1947.

14. W. E. Bradley, "Superregenerative Detection Theory", Electronics, Vol. 21, Sept 1948.

15. Hazeltine, Richman and Langhlin, "Superregenerator Design", Electronics, Vol. 21, Sept 1948.

16. Kryloff and Bogoliuboff, "Introduction To Non-Linear Mechanics", (a free translation by S. Lefschetz), Princeton University Press, 1947.

17. N. Minorsky, "Introduction To Non-Linear Mechanics", (originally restricted reports of U.S. Navy), J.W. Edwards, Ann Arbor, Michigan 1947.

18. H.A. Wheeler, "Superregenerative Receiver", U.S. Government Letters Patent, No. 2,414,992, Jan. 28, 1947.

19. R.A. Kirkman, "Radio Receiving System", U.S. Government Letters Patent, No. 2, 584,132, Feb. 5, 1952.

20. H. Wood et al, "Superregenerative Type Of Wave-Signal Translating System". U.S. Government Letters Patent, No. 2,617,020, Nov. 4, 1952.

21. Davenport and Root, "Random Signals and Noise", Cpts. 7 and 8, McGraw-Hill, 1958.

22. Lawson and Uhlenbeck, "Threshold Signals", Radiation Laboratory Series, Cpt. 4, Mc Graw-Hill ; 1950.

23. S.O. Rice, "Mathematical Analysis of Random Noise", Bell System Tech. J, Vol. 23, 1944.

24. M. Schartz, "Information Transmission, Modulation And Noise", McGraw-Hill, 1959.

25. S.O. Rice, "Mathematical Analysis Of Random Noise", Bell System Tech. J., Vol. 24, 1945.

26. D. Middleton, "Introduction To Statistical Communication Theory", C'pt. 9, McGraw-Hill, 1960.

27. Lawson and Uhlenbeck, "Threshold Signals", Radiation Laboratory Series, Cpt. 3, McGraw-Hill, 1950.

28. The Partner Receiver, produced by Monterey Electronics Products, Monterey, California.

29. Younger et al, "Superregenerative Operation Of Parametric Amplifiers", 1959 IRE WesCon, Part One (antenna, microwave theory).

The following additional material relates to the general theme of this dissertation.

30. H.P. Kalmus, "Some Notes On Superregeneration With Emphasis On Its Possibilities For FM", Proc IRE Vol. 32, Oct 1944.

31. J. Burgess, "New Concepts In Detecting Weak Electromagnetic Signal", Electronics, Sept. 15, 1961.

32. R.K. Keenan, Proc. IEEE (correspondence), Vol. 52, p. 1060; Sept., 1964.

33. Jordan and Elco, PROC IRE (correspondence), Vol. 48, p. 1902; Nov. 1960.

This document has been approved for public release and sale; its distribution is unlimited.
Mannebach 12/16/69

[redacted]

[redacted]

thesH2894
Studies of periodically quenched regener
3 2768 001 01922 7
DUDLEY KNOX LIBRARY